

## ABSTRACT

Title of Document: MONITORING LEVELS OF DISSOLVED METHANE AND METALS IN MARYLAND STREAMS OVERLYING THE MARCELLUS SHALE PRIOR TO HYDRAULIC FRACTURING

Caroline G. Coulter, Master of Science, 2015

Directed By: Associate Professor Johan Schijf, Marine Estuarine Environmental Sciences

In western Maryland above the Marcellus Shale, 25 streams were monitored for baseline concentrations of dissolved  $\text{CH}_4$ ,  $\text{Sr}^{2+}$ , and  $\text{Ba}^{2+}$ , constituents that may be affected by fracking activity. Migrated shale  $\text{CH}_4$  may intrude streams, and  $\text{Sr}^{2+}$  and  $\text{Ba}^{2+}$  may be introduced by fracking fluid leakages or spills. Stream constituents were also measured in Maryland's coastal plain for reference. In western Maryland,  $\text{CH}_4$  concentrations are significantly variable yet in agreement with concentrations reported for other North American pristine rivers. Measurements of  $\delta^{13}\text{C}-\text{CH}_4$  suggest  $\text{CH}_4$  is primarily biogenic. Dissolved  $\text{Sr}^{2+}$  and  $\text{Ba}^{2+}$  are spatially and temporally variable, although Sr/Ba ratios are relatively stable at most sites, indicating these may be useful fracking fluid tracers. Major ions  $\text{Na}^+$ ,  $\text{K}^+$ ,  $\text{Mg}^{2+}$ ,  $\text{Ca}^{2+}$ ,  $\text{Cl}^-$ ,  $\text{SO}_4^{2-}$  and  $\text{HCO}_3^-$  were measured. These were elevated relative to  $\text{Sr}^{2+}$  and  $\text{Ba}^{2+}$  and are not suitable fracking fluid tracers. Major ions were highly variable, indicative of variable bedrock geology in western MD.

MONITORING LEVELS OF DISSOLVED METHANE AND METALS IN  
MARYLAND STREAMS OVERLYING THE MARCELLUS SHALE PRIOR TO  
HYDRAULIC FRACTURING

By

Caroline G. Coulter

Thesis submitted to the Faculty of the Graduate School of the  
University of Maryland, College Park, in partial fulfillment  
of the requirements for the degree of  
Master of Science  
2015

Advisory Committee:  
Associate Professor Johan Schijf, Chair  
Professor Keith Eshleman  
Assistant Research Professor Hali Kilbourne  
Assistant Professor Laura Lapham

© Copyright by  
Caroline G. Coulter  
2015

## Acknowledgements

First I acknowledge my major advisor Dr. Johan Schijf as well as Dr. Laura Lapham, both of whom provided much guidance, help, and patience in this process.

Acknowledgement is also given to committee members Dr. Hali Kilbourne and Dr. Keith Eshleman for their guidance and their enthusiasm for my project. I also thank Dr. Andrew Heyes who contributed financial support as well as insight during my time as a student.

Acknowledgement is given to Maryland Department of Natural Resources for supporting this work and allowing access to sites. Thanks to the IRMS lab of Dr. Jeff Chanton at Florida State University, including Claire Langford who oversaw sample analysis. Thanks are owed to former students and Faculty Research Assistants in the Schijf and Lapham labs who provided advice and assistance in both lab and field activities: Emily Christenson, Kathleen Marshall, Dr. Cedric Magen, Katherine Hoffman, and Joshua Condon.

Thanks are in order for the many CBL friends who provided encouragement and laughs, in particular my office mates and house mates: Lauren Gelesh, Yuan Yuan Xu, Alex Atkinson, Christina Goethel, Kathleen Marshall, Jenna Luek, MengJie Zhang, and Rachel Clark. Finally, thanks to my family members in Arkansas for their continuous love and support.

## Table of Contents

Acknowledgements.....	ii
List of Tables .....	v
List of Figures.....	vii
Chapter 1: Hydraulic fracturing in the U.S. and its impact on the environment .....	1
1.1 Introduction.....	1
1.2 Oil and natural gas production.....	4
1.2.1 Origins of oil and natural gas.....	4
1.2.2 Drilling of conventional oil and gas reservoirs.....	5
1.2.3 Drilling of unconventional oil and gas reservoirs.....	6
1.3 Environmental challenges related to fracking.....	9
1.3.1 Range of environmental impacts .....	9
1.3.2 Impacts of fracking fluids on water resources .....	11
1.3.3 Methane release associated with fracking.....	14
1.4 Environmental management in the Marcellus Shale region of Maryland .....	17
1.5 Study of dissolved methane and metals in Maryland surface waters .....	20
Chapter 2: Baseline monitoring of dissolved metals in western Maryland streams ...	26
2.1 Introduction.....	26
2.1.1 Hydraulic fracturing fluids as sources of water contamination .....	26
2.1.2 Characteristics of fracking fluids and wastes.....	27
2.1.3 Fates of fracking fluids in surface and groundwater.....	28
2.1.4 Use of metals as fracking fluid tracers.....	32
2.1.5 Monitoring of Sr <sup>2+</sup> and Ba <sup>2+</sup> in western and southern MD streams.....	35
2.1.6 Characterizing waters by major ion composition .....	37
2.2 Materials and methods .....	40
2.2.1 Sampling sites .....	40
2.2.2 Field sampling.....	46
2.2.3 Analysis of Sr <sup>2+</sup> and Ba <sup>2+</sup> .....	47
2.2.4 Analysis of major cations.....	48
2.2.5 Analysis of major anions .....	49
2.2.6 Analysis of Acid Neutralizing Capacity .....	51
2.2.7 Analysis of Dissolved Organic Carbon.....	52
2.3 Results.....	53
2.3.1 Dissolved Sr <sup>2+</sup> and Ba <sup>2+</sup> concentrations .....	53
2.3.2 Major ion concentrations .....	59
2.4 Discussion.....	61
2.4.1 Charge balance in western MD streams.....	61
2.4.2 Major ions as tracers of fracking fluids .....	63
2.4.3 Sr <sup>2+</sup> and Ba <sup>2+</sup> as tracers of fracking fluids .....	71
2.4.4 Sr and Ba solubility and its effect on tracer use.....	76
2.4.5 Implications and Conclusions.....	81

Chapter 3: Monitoring of dissolved methane in western Maryland streams .....	84
3.1 Introduction.....	84
3.1.1 Sources of methane in natural waters .....	84
3.1.2 Methane in groundwater .....	85
3.1.3 Methane in surface waters .....	87
3.1.4 The isotopic composition of carbon in dissolved CH <sub>4</sub> .....	89
3.1.5 Methane behavior in relation to fracking.....	90
3.1.6 Monitoring baseline dissolved CH <sub>4</sub> in western and southern MD streams .....	94
3.2 Materials and methods.....	98
3.2.1 Field sampling methods.....	98
3.2.2 Analysis of CH <sub>4</sub> partial pressure in the headspace .....	101
3.2.3 Theory.....	102
3.2.4 Calculation of stream CH <sub>4</sub> saturation .....	103
3.2.5 Analysis of δ <sup>13</sup> C-CH <sub>4</sub> .....	104
3.3 Results.....	106
3.3.1 Temporal Variability.....	106
3.3.2 Spatial variability.....	107
3.3.3 Carbon isotopic composition of CH <sub>4</sub> .....	113
3.4 Discussion.....	116
3.4.1 Temporal variability of stream CH <sub>4</sub> .....	117
3.4.2 Spatial variability of stream CH <sub>4</sub> .....	119
3.4.3 Carbon Isotope Measurements.....	128
3.4.4 Monitoring Implications and Conclusions.....	134
 Chapter 4: Conclusions.....	 138
4.1 Use of Sr <sup>2+</sup> , Ba <sup>2+</sup> , and major ions as fracking fluid tracers.....	138
4.2 Use of dissolved CH <sub>4</sub> for tracing fracking contamination .....	140
4.3 Further implications for fracking regions .....	142
 Appendices.....	 145
Appendix A.....	145
Appendix B.....	156
 Bibliography .....	 160

## List of Tables

**Table 2.1** Names and locations of sampling sites in western MD for the Feb 2012–Feb 2013 and Apr 2013–Apr 2014 sets and sampling sites in Calvert County from the Summer 2014 set. Site name SPRS represents the Savage River Pumping Station and Reservoir represents the Piney Creek Reservoir. WTP Intake and WTP Finished represent the intake of the Frostburg City water treatment plant and the treated water from the plant, respectively. Sites in the Apr 2013–Apr 2014 set are named according to catchment, where CASS indicates the Casselman River catchment, GEOR the Georges Creek catchment, PRUN the Potomac River Upper North Branch catchment, SAVA the Savage River catchment, and YOUG the Youghiogheny River catchment. Sites in this set are numbered based on stream order, with numbers in the 100s representing 1<sup>st</sup> order streams, those in the 200s representing 2<sup>nd</sup> order, etc. Designation ‘S’ indicates long-term monitoring sites which have historical data sets, and those with ‘D’ are newly established monitoring sites. Summer 2014 site names are associated with the stream where the site is found, with HELL representing Hellen Creek, GRAY representing Grays Creek, PARK representing Parkers Creek, and THOM representing Thomas Branch. Note that for site THOM01, June and July sampling locations are slightly different due to higher water levels in July at Thomas Branch. The characteristic site environment is given in the ‘Environment’ column.

**Table 2.2** Saturation state ( $\Omega$ ) of western MD samples found to be oversaturated in  $\text{BaSO}_4$ , with calculated free  $\text{Ba}^{2+}$  concentration (nM), free  $\text{SO}_4^{2-}$  concentration ( $\mu\text{M}$ ), and Ion Concentration Product (ICP) of each sample.

**Table A1** Stream concentrations of  $\text{Na}^+$ ,  $\text{K}^+$ ,  $\text{Mg}^{2+}$ , and  $\text{Ca}^{2+}$  ( $\mu\text{M}$ ),  $\text{Sr}^{2+}$  and  $\text{Ba}^{2+}$  (nM),  $\text{Cl}^-$ ,  $\text{SO}_4^{2-}$ ,  $\text{NO}_3^-$ ,  $\text{HCO}_3^-$ , and DOC ( $\mu\text{M}$ ), and pH. Values of  $\text{HCO}_3^-$  were approximated from charge balance, unless marked by \* which indicates  $\text{HCO}_3^-$  measured by Gran Titration.

**Table B1** Dissolved  $\text{CH}_4$  concentrations (nM) in western MD streams from the Sep 2012–Feb 2013 sample set and the Apr 2013–Apr 2014 sample set. The meaning of site names is described in Chapter 2. Concentration values are taken as the mean of sample duplicates, and relative errors, determined as half the difference between duplicate samples, is <8% for most values. The designated site environment is given in the column labeled ‘Env.’ with ‘A’ indicating anthropogenically influenced sites, ‘F’ indicating forested sites, and ‘W’ indicating wetland sites.

**Table B2** Values of  $\delta^{13}\text{C-CH}_4$  (‰) measured in western MD streams from the Sep 2012–Feb 2013 sample set as well as the Apr 2013–Apr 2014 sample set. Values were determined from the mean  $\delta^{13}\text{C-CH}_4$  measurement of sample duplicates, and the relative error, determined as half the difference between duplicate samples, was <2% for most samples.

**Table B3** Dissolved  $\text{CH}_4$  concentrations (nM) and  $\delta^{13}\text{C-CH}_4$  values (‰) in Calvert County streams in June and July of 2014. Site names were designated based on the stream in which sites were located, as defined in Chapter 2. Concentration values were determined from the mean of sample duplicates and showed relative error <8% for most measurements.  $\delta^{13}\text{C-CH}_4$  values were taken from the mean of sample duplicates and relative errors were <2% for most samples.

**Table B4** Longitudinal gradient of dissolved  $\text{CH}_4$  concentrations (nM) measured in Sep 2013. Duplicate samples were measured at the CASS101D site (0 m), as well as from locations downstream (–30 m and –20 m) and upstream (+10 m and +20 m). Errors were determined as half the difference between duplicate samples.

## List of Figures

**Figure 1.1** Map of shale formations with natural gas access in the lower 48 states. [http://www.eia.gov/oil\\_gas/rpd/shale\\_gas.pdf](http://www.eia.gov/oil_gas/rpd/shale_gas.pdf)

**Figure 1.2** Diagram showing conventional and unconventional drilling techniques for oil and natural gas. Conventional drilling accesses reservoirs of oil and gas trapped in reservoirs below a seal. Unconventional drilling utilizes a lateral wellbore and hydraulic fractures to extract oil and gas from shale formations. <http://www.eia.gov/todayinenergy/detail.cfm?id=110>

**Figure 1.3** Map of western Maryland showing areas underlain by the Marcellus Shale in blue. <http://www.wmrcd.org/>

**Figure 1.4** Map of the western Maryland study region with the study sites represented as purple points. Catchment areas studied are labeled, with the Youghiogheny River catchment shown in green, Casselman River catchment in yellow, Savage River catchment in blue, Georges Creek catchment in pink, and Potomac River Upper North Branch ('Potomac River U N Branch') catchment in orange. The wider Youghiogheny River basin is indicated in green, and the wider Potomac River North Branch basin in orange.

**Figure 2.1** Map of western MD stream sites for the Feb 2012–Feb 2013 and Apr 2013–Apr 2014 sampling sets. Background and symbol colors indicate catchment, with yellow indicating the Casselman River catchment, blue indicating the Savage River catchment, pink the Georges Creek catchment, orange the Potomac River Upper North Branch catchment, and green the Youghiogheny River catchment. Black symbol indicates the Frostburg WTP. The greater Youghiogheny River basin is indicated in green and the greater Potomac River North Branch in orange.

**Figure 2.2** Map of stream sites sampled in Calvert County, MD, in June and July 2014. Background and symbol colors correspond to stream catchment, with blue indicating the Patuxent River Lower catchment and purple indicating the West Chesapeake Bay catchment.

**Figure 2.3** Temporal variability in dissolved  $\text{Sr}^{2+}$  and  $\text{Ba}^{2+}$  concentrations (nM) across 1 year. Panels A, B, D, and F are sites in the Casselman River catchment, and panels C and E are sites in the Savage River catchment. SRPS indicates Savage River Pumping Station. Sites in Panels B, D, and E are from the 2012–2013 sample set, and those in Panels A, C, and F are from the 2013–2014 sample set.

**Figure 2.4** Values of  $\log([\text{Ba}]/[\text{Sr}])$  at each sampling site, with Feb 2012–Feb 2013 sites shown in the left panel, Apr 2013–Apr 2014 sites shown in the center panel, and June–July 2014 Calvert County sites shown in the right panel. Bars plotting above 0 indicate  $\text{Ba}^{2+}$  is elevated in concentration relative to  $\text{Sr}^{2+}$  and those plotting below 0 indicate  $\text{Sr}^{2+}$  is elevated.

**Figure 2.5** Concentrations of  $\text{Sr}^{2+}$  vs.  $\text{Ca}^{2+}$  in all stream waters.

**Figure 2.6** Concentrations of  $\text{Ca}^{2+}$  vs.  $\text{HCO}_3^-$  in western MD stream samples collected Oct' 2013.

**Figure 2.7.** Trilinear diagram showing relative contributions (%) of  $\text{Mg}^{2+}$ ,  $\text{Ca}^{2+}$ , and  $\text{Na}^+ + \text{K}^+$  cations in western MD and Calvert County streams. Marker color represents catchment as in Fig. 2.1. Average cation composition of shallow groundwater in a region overlying the Marcellus Shale (New York state) is represented by the red star (Lautz et al., 2014).

**Figure 2.8.** Geologic map of western MD by Brezinksi et al. (2013). Map background shades represent the underlying bedrock type. Green shades represent Mississippian and younger formations, and purple shades represent Devonian and older formations. All western MD stream sites are marked, with marker color indicating catchment as in Fig. 2.1

**Figure 2.9.** Bilinear plot of  $\text{K}^+$  vs.  $\text{Mg}^{2+}$  in western MD stream samples, with samples categorized by the underlying bedrock era, either Devonian or Pennsylvanian.

**Figure 2.10** Plot of  $\text{Na}^+$  vs  $\text{Cl}^-$  concentrations in deep Appalachian brines which occur in fracking fluids (Warner et al., 2012), in road salt effluent (Lautz et al., 2014), and in western MD streams.

**Figure 2.11** Plot of  $\text{Mg}^{2+}$  vs.  $\text{Cl}^-$  concentrations in deep Appalachian brines which occur in fracking fluids, in shallow groundwater overlying the Marcellus Shale (Warner et al., 2012), and in western MD streams.

**Figure 2.12** Values of  $\log([\text{Ba}]/[\text{Sr}])$  found in western MD streams (light gray) and in fracking fluids (dark gray). Western MD values were determined from average molar  $\text{Sr}^{2+}$  and  $\text{Ba}^{2+}$  concentrations from each time of sampling. Fracking fluid values were determined from molar concentrations from fracking fluid analyses as reported by Barbot et al. (2013) (A), Hayes et al. (2009) (B), He et al., (2014) (C, D, and E), Warner et al. (2012) (F), and Warner et al. (2013b) (G).

**Figure 3.1** Diagram showing a fracking well drilled into the Marcellus Shale, with red arrows indicating mechanisms for CH<sub>4</sub> contamination of water. Arrow A represents leakage of Marcellus Shale CH<sub>4</sub> through failed wellbore casing and B represents transport of intermediate formation CH<sub>4</sub> through annuli. Arrow C represents transport of CH<sub>4</sub> from shallow groundwater to streams. Arrow D represents a potential pathway of Marcellus Shale CH<sub>4</sub> from depth and E represents CH<sub>4</sub> migration from depth facilitated by pre-existing faults

**Figure 3.2** Temporal variability in western MD stream CH<sub>4</sub> concentrations (nM) across 1 year. Top panels (A and B) show sites from the 2012–2013 set, with high CH<sub>4</sub> concentration sites shown in A and low concentration sites in B. Bottom panels (C and D) show sites from the 2013–2014 set, with high concentration sites shown in C and intermediate concentration sites in D. SRPS indicates the Savage River Pumping Station. Note that the scale in panels B and D is an order of magnitude lower than in A and C. Bar color indicates site catchment, with yellow indicating Casselman River, blue Savage River, and green Youghiogheny River. Error bars indicate half of the difference between the sample duplicates, <8% of the concentration value in most cases.

**Figure 3.3.** Methane concentrations (nM) in Calvert County from June and July 2014 measurements, grouped by stream setting (forested, wetland, or anthropogenically influenced).

**Figure 3.4** Spatial distribution of CH<sub>4</sub> concentrations (nM) according to site setting, with sites characterized as forested, wetland, or anthropogenically influenced. Concentrations measured in Aug/Sep sampling in western MD (of both the 2012–2013 and 2013–2014 sets) are shown in (A) and those measured in July in Calvert County shown in (B). Concentrations shown in B are the same as those shown in Fig. 3.3 for July 2014. Note the order of magnitude higher concentrations in (B) which shows Calvert County measurements relative to (A) which shows those of western MD. Error bars indicate half of the difference between duplicate samples, <8% of the concentration values for most measurements.

**Figure 3.5** Longitudinal variability in dissolved CH<sub>4</sub> (nM) along the CASS101D stream reach in Sep 2013. Sampling occurred at CASS101D (0 m), 2 upstream locations (+10 m, +20 m), and 2 downstream locations (–20 m, –30 m). Error bars indicate half of the difference between duplicate samples.

**Figure 3.6** Measurements of  $\delta^{13}\text{C-CH}_4$  values (‰) for sites YOUG105D and YOUG106D across time (Apr 2013–Apr 2014).

**Figure 3.7**  $\delta^{13}\text{C}\text{-CH}_4$  values (‰) in Oct samples in western MD streams (A) and July samples in Calvert County streams (B), separated by stream setting (forested, wetland, or anthropogenically influenced). The range of  $\delta^{13}\text{C}\text{-CH}_4$  values characteristic of biogenic  $\text{CH}_4$ ,  $-110\text{‰}$  to  $-50\text{‰}$  (Whiticar, 1996), is indicated by the green bar. The range characteristic of Marcellus Shale  $\text{CH}_4$ , from  $-43\text{‰}$  to  $-27\text{‰}$  (Hakala, 2014), is indicated by the gray bar.

**Figure 3.8** Plot of  $\text{CH}_4$  concentration (nM) vs. water temperature ( $^{\circ}\text{C}$ ) for the 2012–2013 and 2013–2014 western MD sampling sets.

**Figure 3.9** Diagram of Principle Component Analysis (PCA) based on variables  $\text{CH}_4$  concentration, temperature, and streamflow for western MD samples. Color separates samples by environmental setting.

**Figure 3.10** Plot of  $\text{CH}_4$  concentration (nM) vs. streamflow for the 2013–2014 western MD sampling set. Streamflow values ( $\text{ft}^3/\text{s}$ ) obtained from each sampling trip were taken from the USGS gauge nearest to each site.

**Figure 3.11** Plot of  $\text{CH}_4$  concentration vs. Upstream Agricultural Land Use (%) for each site. April, August, and October samples are plotted, with each month including samples of the Sep 2012–Feb 2013 and the Apr 2013–Apr 2014 sample sets.

**Figure 3.12** Plot of  $\delta^{13}\text{C}\text{-CH}_4$  (‰) vs.  $\text{CH}_4$  concentration (nM) for each site's highest measured  $\text{CH}_4$  concentration, apart from site THOM02, for which  $\delta^{13}\text{C}\text{-CH}_4$  was measured in a sample with slightly lower  $\text{CH}_4$  concentration (July '14).

# Chapter 1: Hydraulic fracturing in the U.S. and its impact on the environment

## 1.1 Introduction

Rates of energy use by humans have steadily increased since the Industrial Revolution and continue to do so today (Carpenter, 2014). With high energy demands in the 21<sup>st</sup> century, novel resources and technologies are being developed and utilized with the intent of sustaining energy demands of the growing human population on a long-term scale.

Renewable resources have generated substantial interest and include hydropower, biofuels, geothermal energy, wind, and solar power. These energy sources are ultimately the most sustainable for human energy demands due to their very low greenhouse gas outputs to the atmosphere as well as their long-term energy potential. Solar power offers the largest reserve of energy, although it may be decades before developments occur to place solar energy in a competitive price range with hydrocarbon energy sources (Armor, 2014). It is estimated that currently approximately 11% of total world energy consumption comes from renewable resources, with the projection that the proportion of renewables will reach approximately 15% in 2040 (Letcher, 2014). For a significant emergence of renewable resource use, a combination of technological advances, cost breakthroughs, and legislation will be needed (Armor, 2014). Continued worldwide exploration of hydrocarbon repositories, including oil and natural gas, along with recent advancements in extraction techniques have allowed fossil fuels to remain the mainstay of world energy production and human consumption.

Oil, a prominent fossil fuel which is the largest contributor to world energy supplies, constitutes 31.4% of world energy sources (Key World Energy Statistics, 2014). Rates of discovery of oil have been declining since the 1960s (Hoffmann, 2014), however, and production of oil from conventional extraction methods is expected to drop by more than 50% over the next 20 years (Rhodes, 2014). Natural gas contributes 21.3% of world energy supplies and is growing in importance (Key World Energy Statistics, 2014). Between 1990 and 2009, global production of natural gas rose by almost 42%, nearly twice the 22% increase in global oil production over this period. Much of this growth is related to continuing discovery and expansion of gas reserves worldwide, and high natural gas production rates will likely be sustained. It is estimated that, outside of the U.S., less than 11% of natural gas reserves have been recovered (Moniz, 2011).

Of particular interest are novel techniques for stimulation of natural gas wells from impermeable deep shale formations, or shale gas drilling, which has vastly increased the availability of natural gas. Recent projections estimate that worldwide accessibility of shale-contained gas increases global recoverable gas resources by more than 40% (Rahm et al., 2013), with indications that more than 169 trillion m<sup>3</sup> of shale gas resources are potentially available (Soeder, 2012). Plans for drilling of newly available shale resources are underway in many countries that have access to the deep gas reservoirs, including Poland, Ukraine, Russia, China, and Australia (Malakoff, 2014; Vidic et al., 2013); however, some countries, such as England and France, are presently suspending or banning these drilling methods due to their potential environmental repercussions (Lewis, 2012).

The U.S. has been the first location of widespread natural gas extraction from deep shale formations, and is now the world's leading natural gas producer (Malakoff, 2014). With 29 known shale basins in the U.S. (Fig. 1.1), including the Marcellus Shale spanning 246,000 km<sup>2</sup> in the eastern U.S., shale gas is the fastest growing energy sector (Entrekin et al., 2011). Shale gas accounts for approximately 40% of total U.S. natural gas production and is expected to grow to 53% of the country's gas production by 2040 (Malakoff, 2014).

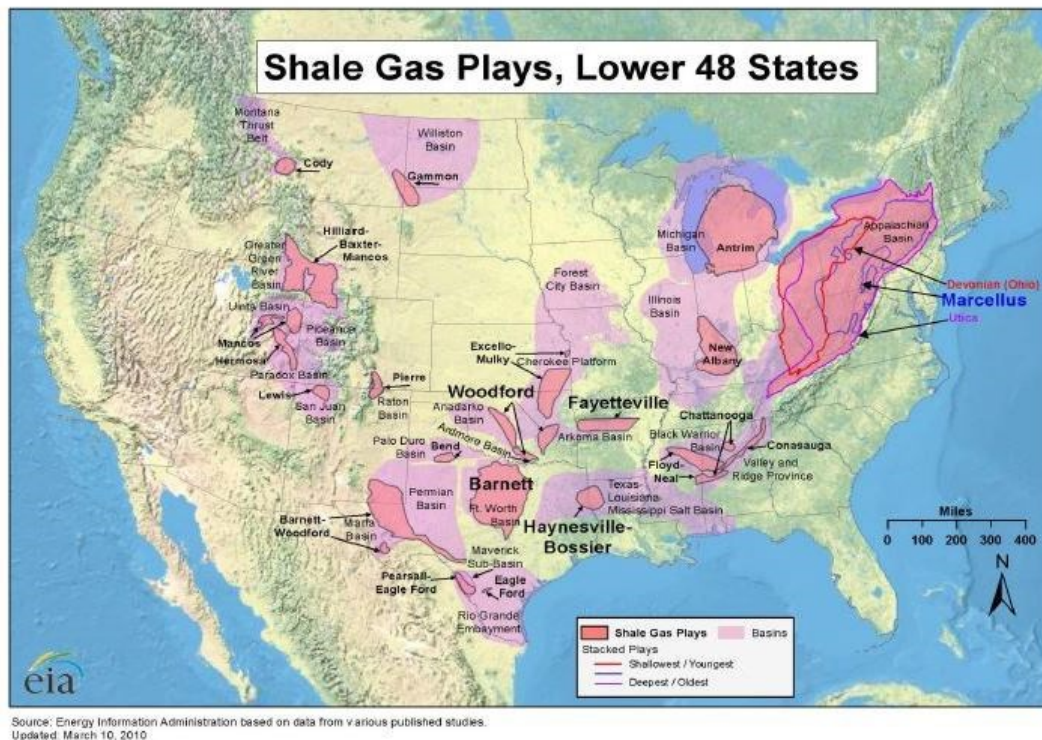


**Figure 1.1** Map of shale formations with natural gas access in the lower 48 states. [http://www.eia.gov/oil\\_gas/rpd/shale\\_gas.pdf](http://www.eia.gov/oil_gas/rpd/shale_gas.pdf)

In addition to the widespread availability of natural gas, there is also worldwide interest in this energy resource because it is relatively efficient and clean-burning. When considering greenhouse gases like carbon dioxide (CO<sub>2</sub>), methane (CH<sub>4</sub>), and nitrous oxide (N<sub>2</sub>O), released during fuel combustion, natural gas emits smaller

quantities per megajoule (MJ) of fuel combusted relative to both oil and coal (Burnham et al., 2012). One study has predicted that accelerated shale drilling of natural gas will reduce U.S. electricity sector emissions by 17% (Sovacool, 2014). Also, compared with oil and coal, natural gas combustion emits lower amounts of sulfur oxides, nitrogen oxides, and mercury (Sovacool, 2014). This has been an impetus for increasing utilization of natural gas worldwide. In China, for example, natural gas supplies 4% of total energy demands, and the country plans to increase its proportion of natural gas use to 8% by 2020 (Gregory et al., 2011).

## 1.2 Oil and natural gas production

### 1.2.1 Origins of oil and natural gas

Oil and natural gas are hydrocarbon fuels, often referred to as fossil fuels, which are formed from organic matter that deposits with lake or marine sediments and becomes buried and compacted over geologic time scales. This process occurs in aquatic areas of high productivity and low circulation, such as lagoons, deltas, or marshes, where high amounts of organic matter accumulate and stagnant conditions allow bottom waters to become anoxic. Settled organic matter may avoid decomposition and become buried as younger sediment layers are subsequently deposited. Buried layers are then subjected to increasingly higher temperatures and pressures which convert organic matter within sediments to hydrocarbon compounds over time (Keller, 1982).

With high pressure from the overlying rock as well as high temperature from the earth below, organic matter is first converted to kerogen, the high-molecular-weight

organic precursor to oil and gas. The next phase of breakdown of organic matter, in which kerogen undergoes thermal alteration to smaller organic compounds, is referred to as catagenesis and proceeds over thousands to millions of years (Schobert, 2013). When kerogen reaches temperatures of 60–170 °C, typically occurring at depths of 4–6 km, it is thermally broken down into hydrocarbons of oil, which mainly consists of compounds in the C<sub>3</sub>–C<sub>34</sub> size range (Marshak, 2005). With further increases to temperatures of 170–225 °C and depths of approximately 6–9 km, the *gas window* is reached (Marshak, 2005). Hydrocarbons are broken down to form compounds of natural gas, which include low-molecular-weight compounds in the C<sub>1</sub>–C<sub>7</sub> size range, with methane (CH<sub>4</sub>) being the predominant product at the hottest end of the gas window (Schobert, 2013).

### 1.2.2 Drilling of conventional oil and gas reservoirs

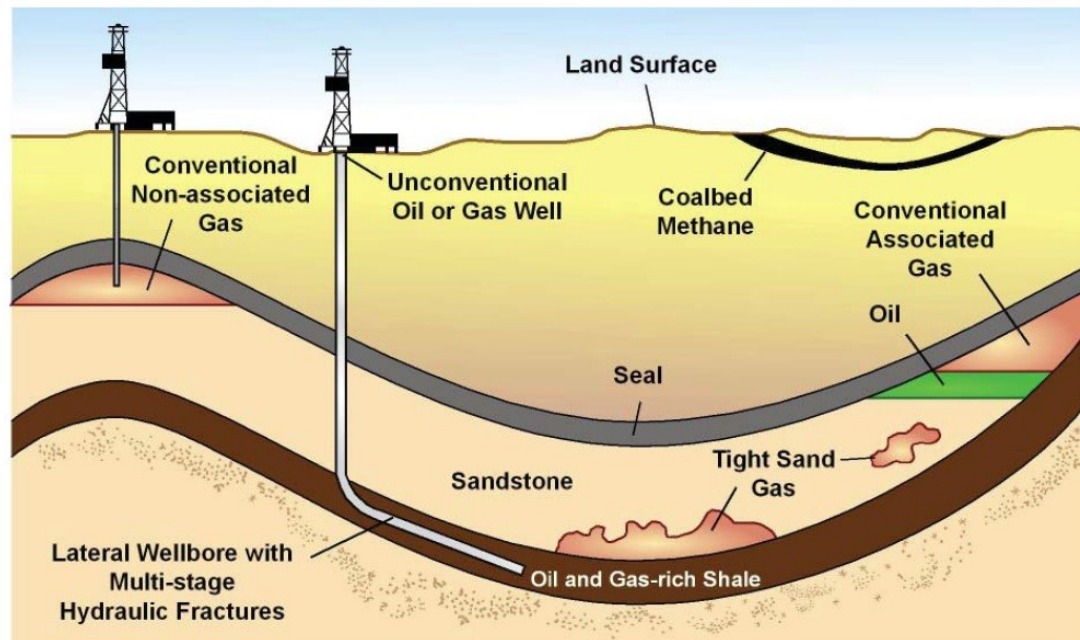
With exposure to high pressures and temperatures at depth, the organic material in the form of oil or natural gas is also prone to migrate to lower-pressure environments which have increased porosity. The oil and gas tend to migrate upward through the source rock, by way of faults, fractures, and more porous rock units, and upward migration continues until it is impeded by an impermeable overlying rock unit, or cap rock, under which oil and gas then accumulate (Letcher, 2014). These accumulations of “trapped” oil and natural gas create reservoirs which may be accessed by vertical drilling through the impervious cap rock into the reservoir, as illustrated by the image of a conventional gas well in Fig. 1.2. The compressed gas of the reservoir is then transported through the wellbore to the surface (Suarez, 2012).

These types of reservoirs have been accessed and drilled this way since the late nineteenth century, and the International Energy Agency (IEA) defines these resources as *conventional* because they are relatively easy and inexpensive to produce compared to oil and natural gas within deeper formations of low permeability (Letcher, 2014).

### 1.2.3 Drilling of unconventional oil and gas reservoirs

In some environments, sediments deposited with the organic matter are very fine-grained and the rock formed from the compaction of these sediments consequently has very low permeability. Oil and gas formed within this rock are unable to migrate and remain trapped within the formation (Kolb, 2014). If the impermeable rock formation is rich in organic matter and subjected to high temperature and pressure with very deep burial, the organic matter undergoes sufficient alteration over geologic time to form primarily natural gas within the rock (Judson, 1987). One type of low-permeability sedimentary rock is shale, which derives from fine sediments deposited under anaerobic conditions in biologically productive marine environments. Within shale formations there is an abundance of organic matter, and, with exposure to elevated temperatures and pressures, large amounts of natural gas are generated (Soeder, 2012).

## The Geology of Conventional and Unconventional Oil and Gas



Source: EIA

**Figure 1.2** Diagram showing conventional and unconventional drilling techniques for oil and natural gas. Conventional drilling accesses reservoirs of oil and gas trapped in reservoirs below a seal. Unconventional drilling utilizes a lateral wellbore and hydraulic fractures to extract oil and gas from shale formations.

<http://www.eia.gov/todayinenergy/detail.cfm?id=110>

These shale sources of natural gas were previously difficult and uneconomical to access due to shale's low permeability and also due to the relatively small vertical extent of shale formations, which are typically tens of meters thick, allowing only limited contact with a single conventional well that is drilled vertically (Soeder, 2012). In the 1990s, horizontal drilling techniques were developed, enabling extensive wellbore contact with shale throughout the formation. Around this time, methods were refined for extraction of hydrocarbons from rock by the high-pressure pumping of fluids into a formation, termed *hydraulic fracturing*. The development of hydraulic fracturing techniques facilitated stimulation of gas from low-permeability shale. These techniques were then combined with horizontal drilling, leading to

emergence of the first commercially viable shale gas production wells in North America's Barnett Shale in the early 21<sup>st</sup> century (Soeder, 2012). The term *hydraulic fracturing*, commonly referred to as *fracking*, is now used to refer to the combination of horizontal drilling and hydraulic fracturing for shale gas extraction. Shale gas accessed by fracking is considered an *unconventional* hydrocarbon resource because stimulation of gas trapped within shale is more difficult and requires advanced techniques, while conventional methods of gas production typically involve simpler withdrawal from a belowground gas reservoir within a more porous rock (Suarez, 2012).

In the typical fracking process for access to unconventional resources, a well is first drilled vertically. Upon reaching the shale, which may be between 600–4,000 m deep depending on the formation, drilling is redirected horizontally for well access within the formation, as is seen in the lateral wellbore diagram in Fig. 1.2 (Kell, 2009). The horizontal portion, called a *lateral*, may extend 300–3,000 m and multiple laterals may originate from one well, extending in different directions (Dale et al., 2013). Before drilling begins, the lateral is perforated using explosive charges on a wireline, generating holes which allow enhanced contact with the shale reservoir (Soeder, 2012).

For gas extraction, hydraulic fluids, containing water and numerous chemical additives, are pumped into the wellbore and then pressurized at 480–850 bar to generate new fractures in the shale and extend existing fractures (Soeder, 2012; Vidic et al., 2013). In the next phase, gas pressure in the rock is used to push the injected fluids back out of the well. Returning fluids are collected and referred to as *flowback*

*water* during this phase of drilling, which is termed *completion flowback* and may last up to several days (Allen et al., 2013). Any gas which returns to the surface during the completion flowback phase is sent to a flare, in which the majority of gas compounds are combusted (Soeder, 2012). After the initial period of completion flowback, gas production begins, although some fluid flow to the wellhead continues during the gas production phase, termed *produced water* (Soeder, 2012; Vidic et al., 2013). In total, 10–40% of injected fluids return and are collected at the surface wellhead during the life of the well (Gregory et al., 2011). The recovered fluids, including flowback water and produced water, are collectively referred to as *fracking fluids*.

Unconventional oil reserves, in addition to those of gas, are also found worldwide (Letcher, 2014). Accessibility of oil and gas reserves due to developments of unconventional drilling have significantly changed the global energy market and countries around the world planning for fracking development are looking to the U.S. and Canada, the first to extensively use fracking techniques, to take the lead in environmental research and Best Management Practices with regard to the drilling process (Soeder, 2012).

### 1.3 Environmental challenges related to fracking

#### 1.3.1 Range of environmental impacts

While fracking provides access to significant fuel resources, there are several potential environmental impacts related to fracking operations, some of which are not sufficiently understood. Infrastructure and well construction for this technology have

seen rapid growth in many areas of the U.S., and policies and enforcing personnel in many regions of fracking have not been able to expand regulatory activity at a pace to match that of drilling development (Soeder, 2012).

Aquatic, terrestrial, and atmospheric systems all may be affected by fracking development and its industrial nature. Compared with conventional drilling wells, well pads for fracking have a larger footprint, drilling time is typically longer, and transport of fluids leads to more extensive road traffic (Kolb, 2014). Environmental disturbances which may occur include light and noise pollution, atmospheric release of CH<sub>4</sub>, land fragmentation, non-native species introduction, habitat destruction, and degradation of water quality (Soeder, 2012). Although some of these impacts, such as light and noise pollution, may have short-term influence, others, such as land fragmentation and water quality degradation, may be more long-term and lead to a variety of effects on the surrounding ecosystem (Kolb, 2014).

Another aspect of fracking that may have long-term consequences is air pollution from various compounds emitted during operations. Heavy machinery is used considerably during construction and drilling, releasing a variety of compounds to the atmosphere including aromatic hydrocarbons benzene, toluene, ethylbenzene, and xylene (BTEX), carbon monoxide (CO), nitrous oxides (NO<sub>x</sub>), and fine particulate matter PM<sub>2.5</sub> (McKenzie et al., 2012). In addition, light alkanes, including propane and butane, and other volatile organic compounds (VOCs) are released from shale formations with gas extraction and may be emitted to the atmosphere during well operations (McKenzie et al., 2012; Petron et al., 2012).

Induction of earthquakes and seismic activity is also a potential risk of fracking processes. In 2012 the National Research Council (NRC) reviewed 154 worldwide reports of induced seismicity and found that there was no direct link between fracking and seismic events, but fracking fluid disposal by deep well injection was linked to induced seismicity in some areas (Hitzman, 2012). This finding has been supported by other studies in the U.S. which have linked seismic activity with deep well injection (Kim, 2013; van der Elst et al., 2013).

### 1.3.2 Impacts of fracking fluids on water resources

Surface and groundwater impacts constitute a major environmental concern surrounding fracking. Large quantities of water (between 1–100 million liters) are required for drilling of each well (Clark et al., 2013). Local water supplies, including surface water and groundwater sources, are employed in the process, leading to significant freshwater usage which may be deleterious in regions with stressed water supplies, particularly in periods of drought (Adair, 2012).

In addition to water quantity, water quality may also be jeopardized in areas of fracking activity. In recent years there has been increasing public consideration of water quality risks posed by fracking (Gregory et al., 2011). Aqueous fluids used for fracking contain numerous chemicals added prior to well injection; the major classes of additives include proppant material for keeping fractures open, acids which clean the wellbore, biocides for bacterial control, antiscalants for reducing precipitation of salts and metals, and surfactants which reduce surface tension to improve fluid recovery (Vidic et al., 2013). Although classes of chemical additives are known,

many specific compounds used in the fluids are considered proprietary and are not reported publicly. Some states, however, do require all fracking fluid compounds to be disclosed to regulatory authorities (Adair, 2012). A 2011 congressional investigation found that, over a 4-year period, a total of 750 chemicals were used in fracking fluids utilized by fourteen leading gas companies (Waxman et al., 2013), and many of these chemicals are not regulated by the U.S. Safe Drinking Water Act (Vidic et al., 2013).

Fracking fluids which are recovered at the wellhead after the fracking process typically contain compounds added before injection, degradation products of these compounds, and elements from brines and solutions within the shale and adjacent formations (Haluszczak et al., 2013). Due to interactions with formation solutions, high levels of total dissolved solids (TDS) are found in fracking fluids, with TDS commonly in the range 10,000–180,000 mg/L, while surface waters typically have TDS  $\ll$  1,000 mg/L (Vengosh et al., 2014). High levels of TDS may directly impair the normal metabolism of fish, amphibians, and aquatic plants (Canedo-Arguelles et al., 2013) and are also linked to the growth of harmful algae (Patino et al., 2014). In domestic and municipal water sources, elevated TDS may cause damage to water treatment equipment, increased water treatment costs, and undesirable drinking water taste (Anning, 2014).

Fracking fluids also contain radioactive material derived from the targeted formation in the form of radium (Ra) isotopes,  $^{226}\text{Ra}$  and  $^{228}\text{Ra}$ . These isotopes have been found in fracking fluids at levels 1,000–3,200 times higher than the EPA Maximum Contaminant Level (MCL) for radium in drinking water (Warner et al.,

2013a). Also present in fracking fluids are hydrocarbons including benzene, xylene, toluene, and naphthalene originating from the shale formation (Hayes, 2009); in surface and groundwater these have been linked to negative ecological and human health effects (Gross et al., 2013).

In addition to the variety of contained compounds, fracking fluids raise concern due to the large quantities which are collected at well sites and also due to the many possible pathways for their introduction to natural waters. During their flow to the surface from depth, fracking fluids may affect groundwater through potential belowground well casing failures or natural or induced fractures (Vidic et al., 2013). Upon their return to the surface, fracking fluids have potential for water contamination during on-site storage, transport, and disposal. Transport of large fluid quantities, required for many disposal methods, presents significant contamination risks (Skalak et al., 2014). Also particularly hazardous is disposal by fluid treatment and discharge, which releases many fracking fluid compounds to surface waters (Warner et al., 2013b). Deep underground injection of fracking fluids is another common disposal method which poses a contamination threat to groundwater in addition to the potential seismic effects (Vengosh et al., 2014).

Fracking fluids are not federally regulated, and states in which fracking occurs have addressed management of fluids in a variety of ways. In some states modifications of existing oil and gas regulations have been made for improved management of fracking fluids. In Colorado, requirements have been increased for pits storing hazardous substances, which are now more prevalent due to fracking. Ohio and Pennsylvania, two states with a high prevalence of fracking (Vidic et al.,

2013), have modified rules for treatment plants which receive fracking fluids (Adair, 2012). In Ohio, received fracking fluids must be below a threshold TDS level, and in Pennsylvania, treatment plant discharge is subject to average monthly TDS standards (Adair, 2012).

With a range of synthetic and naturally occurring constituents found in fracking fluids, as well as many opportunities for leakage and contamination, it is important to understand fates of these fluids and to be able to detect them in natural waters. A tool that has been used for this is the analysis of specific constituents which occur at very high levels in fracking fluids, on the order of thousands of mg/L, including chloride ( $\text{Cl}^-$ ), bromide ( $\text{Br}^-$ ), calcium ( $\text{Ca}^{2+}$ ), sodium ( $\text{Na}^+$ ), strontium ( $\text{Sr}^{2+}$ ), and barium ( $\text{Ba}^{2+}$ ) (Haluszczak et al., 2013; Warner et al., 2013a). Although some studies have reported high  $\text{Cl}^-$  and TDS levels in areas where treated fracking fluids are discharged (Olmstead et al., 2013; Wilson and VanBriesen, 2012),  $\text{Cl}^-$  and TDS also may become elevated in streams due to other human activities including suburban development and agriculture (Kaushal et al., 2005). Constituents such as  $\text{Ba}^{2+}$ ,  $\text{Sr}^{2+}$ , and  $\text{Br}^-$ , which occur at negligible or low levels in surface waters, are the most promising for detecting the presence of fracking fluids (Vidic et al., 2013).

### 1.3.3 Methane release associated with fracking

Due to the high-pressure stimulation of gas, there is potential for mobilizing methane ( $\text{CH}_4$ ) from the target shale formation or surrounding formations and this may lead to  $\text{CH}_4$  contamination of surface or groundwater as well as emission of  $\text{CH}_4$  to the atmosphere. In domestic water sources,  $\text{CH}_4$  contamination may be an

explosive hazard (Vidic et al., 2013). Methane in surface water environments and in the atmosphere is of concern since CH<sub>4</sub> is a powerful greenhouse gas (GHG) with global warming potential 28–32 times greater than that of CO<sub>2</sub> on the 100-year time scale (Caulton et al., 2014).

Although the predominant mechanisms for CH<sub>4</sub> contamination associated with fracking are not known, there are a number of suggested mechanisms through which CH<sub>4</sub> movement and contamination may occur with fracking activity (Osborn et al., 2011). One potential mechanism is the displacement of CH<sub>4</sub> present in the target shale formation leading to its upward migration into aquifers through faults or fracture networks. These networks are extensive in many shale basin regions, particularly that of the Marcellus Shale, and drilling may generate new or enlarged fractures which increase potential for CH<sub>4</sub> migration. In addition, numerous abandoned, uncased, and inadequately plugged wells exist in many areas of fracking development, further increasing systems of cross-formational connectivity (Osborn et al., 2011). Also possible with fracking is that the drilling stimulates upward migration of CH<sub>4</sub> from formations *above* the targeted shale formation (Osborn et al., 2011). Finally, fracking wells with faulty well casings or seals may allow CH<sub>4</sub> to leak from within the wellbore and to migrate laterally or vertically to water reservoirs, a phenomenon which has been documented in the conventional oil and gas industry (Vengosh et al., 2014).

While there are several pathways by which fracking may lead to CH<sub>4</sub> introduction to waters, dissolved CH<sub>4</sub> also occurs naturally in surface and groundwater. Methane forms at depth in sedimentary basins by high-temperature

maturation of organic matter, and this thermogenic CH<sub>4</sub> is able to migrate vertically to aquifers and also migrates laterally at faults and fractures (Etiope and Klusman, 2002). In addition, biogenic CH<sub>4</sub> is formed through microbial processes at shallow depths; this CH<sub>4</sub> may similarly reach groundwater or surface water through vertical or lateral migration (Vidic et al., 2013).

Because CH<sub>4</sub> may occur in surface and groundwater due to both natural processes and hydraulic fracturing activity, studies have been unable to clearly link fracking to elevated surface or groundwater CH<sub>4</sub> levels (Vidic et al., 2013). Long-term pre-drilling measurements of dissolved CH<sub>4</sub> in waters are needed to determine if dissolved CH<sub>4</sub> contamination correlates with fracking, and this type of long-term baseline data has not been available in the majority of active fracking areas (Adair, 2012).

Management actions have been taken in some states, however, to better understand drilling risks of CH<sub>4</sub> contamination and to better protect the water table. Michigan, Pennsylvania, and West Virginia have established Presumptive Liability, which assumes that the well operator is responsible for water contamination in the well vicinity unless there is evidence to the contrary. This incentivizes operators to monitor groundwater CH<sub>4</sub> prior to drilling. For reduction of groundwater contamination risks, several states have recently updated regulations to specify that surface casing must be in place to a depth of at least 50 ft below the deepest fresh groundwater sources (Trimble, 2012).

Although it is unknown whether there is a link between fracking and CH<sub>4</sub> contamination of waters, it is known that gas extraction by fracking releases gaseous

CH<sub>4</sub> to the atmosphere (Miller et al., 2013), which, as noted above, has climate implications because of the potency of CH<sub>4</sub> as a GHG in the atmosphere. Significant amounts of CH<sub>4</sub> are emitted at several points during the gas extraction process, including well completion, transport through seals and pipelines, and intentional venting practices (Allen et al., 2013; Eshleman, 2013). The EPA reports natural gas extraction systems to be the top source of anthropogenic CH<sub>4</sub> emissions (Hockstad, 2013). Estimates of CH<sub>4</sub> emission rates from a fracking well vary between 0.6–7.7% of the produced gas, with some estimates calculated from localized atmospheric sampling at well sites and others determined from aircraft or remote sensing measurements (Allen et al., 2013; Caulton et al., 2014; Miller et al., 2013). Recently it has been shown that if emission rates are greater than 3.2% of production gas, then, overall, natural gas combustion for fuel becomes worse than coal with respect to the global warming potential of released gases (Alvarez et al., 2012).

#### 1.4 Environmental management in the Marcellus Shale region of Maryland

Development of fracking wells has proceeded very rapidly in the U.S. over the last decade, particularly in eastern U.S. areas underlain by the Marcellus Shale, a gas-bearing formation of middle-Devonian age (Vengosh et al., 2014). Many states overlying the Marcellus Shale have moved forward quickly with fracking infrastructure and gas production, primarily West Virginia and Pennsylvania, in which a total of 8,000 gas wells have been drilled between 2008 and 2011 alone (Soeder, 2012). The Marcellus Shale also underlies Maryland in the western portion of the state, as is shown in Fig. 1.3, with areas underlain by the Marcellus Shale

shown in blue. Maryland is unique, however, in that it has not allowed fracking to date. A 2011 executive order was given for the state, The Marcellus Shale Safe Drilling Initiative, which suspended the licensing of fracking permits in Maryland for 3 years, allowing time for further study of potential environmental and public health effects of fracking (O'Malley and McDonough, 2011).

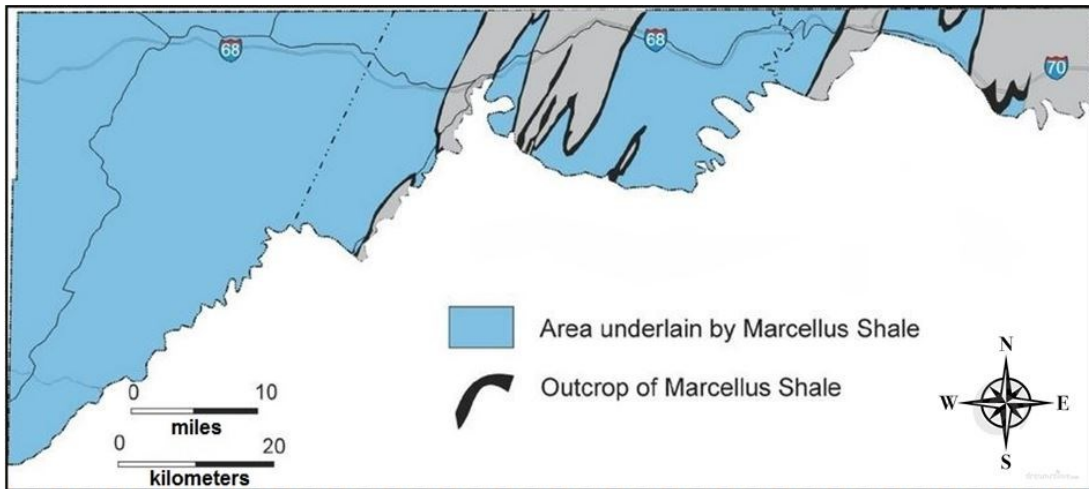


**Figure 1.3** Map of western Maryland showing areas underlain by the Marcellus Shale in blue. <http://www.wmrtd.org/>

The suspension of drilling under this policy initiated a 3-year pre-fracking period in Maryland and, in accordance with recommended management practices, monitoring of baseline conditions is being carried out during this period. Throughout the western Maryland region, the Maryland Department of Natural Resources (MD DNR) and researchers at the University of Maryland Center for Environmental Science (UMCES) have monitored streams at sites located downstream of areas leased for gas production. For the streams of interest, monitoring of stream water chemistry monitoring began in 2011, with continuous measurements of stream

temperature and specific conductance collected at all sites. Regular measurements of stream water pH, total suspended solids (TSS), and nutrients were taken at all sites starting in 2012. To assess stream biological conditions, regular monitoring of benthic macroinvertebrates, fish, mussel, and herpetofauna began in 2012. Monitoring of polycyclic aromatic hydrocarbons (PAHs) and surfactant compounds in streams was initiated in 2013 as these compounds are associated with fracking operations and may lead to water quality degradation. From 2012–2014, regular monitoring of dissolved CH<sub>4</sub>, Sr<sup>2+</sup>, Ba<sup>2+</sup>, and major ions occurred in view of their potential to be displaced and enter surface waters during fracking; the monitoring of the latter four constituents are the topic of this work.

The pre-drilling characterization of stream conditions and water chemistry in this region is unique and provides multi-faceted baseline data that were not collected in most U.S. states with fracking development. The pre-drilling stream water data for western Maryland inform resource managers in the state, and it will be most useful if collection of this data continues during drilling, production, and post-drilling periods, as was recommended in Maryland's Best Management Practices for Marcellus Shale Gas Development (Eshleman, 2013), so that potential changes in stream water quality may be observed over time. These datasets will aid in comprehension and potential mitigation of watershed impacts from fracking. They may also reveal the particular stages of the fracking process which are the most likely to have water quality impacts.

### 1.5 Study of dissolved methane and metals in Maryland surface waters

During the pre-fracking period in Maryland, I monitored surface water dissolved  $\text{CH}_4$ ,  $\text{Sr}^{2+}$ ,  $\text{Ba}^{2+}$ , and major ions for the current study, as these dissolved constituents may be indicators of watershed impacts from fracking. In particular, they may indicate two major types of water quality perturbations: contamination from fracking fluids and  $\text{CH}_4$  migration in proximity to fracking wells.

The western Maryland region examined in this study comprises the area underlain by the Marcellus Shale, shown in Fig. 1.3, and includes the state's westernmost county, Garrett, and the western portion of adjacent Allegany County. This region is primarily in the Allegheny Plateau physiographic province of the Appalachian mountains, with elevation ranging from 600–900 m (Roth, 1999). It remains largely undeveloped, with forest making up >75% of land cover and agriculture approximately 15% (Eshleman, 2013). There is a history of coal mining with many underground coal mines, both active and abandoned, as well as active and inactive gas wells and a gas storage field covering 138 km<sup>2</sup> (Eshleman, 2013). Existing mine and well infrastructure in areas of fracking development may compromise the integrity of drilled wells and may enable belowground migration of  $\text{CH}_4$  or fracking fluids to aquifers (Vidic et al., 2013). Also prevalent in the region are headwater streams, which warrant careful study before, during, and after drilling because of their strong aquatic–terrestrial linkages and the inherent vulnerability of their fauna (Pond, 2012). These streams contribute to the biological diversity and integrity of downstream systems (Meyer et al., 2007).

For monitoring streams in western Maryland in the current study, regular sampling was carried out in 25 stream reaches of varying topography and land use. These sites spanned five catchment areas across the region which are labeled on the map in Fig. 1.4: the Youghiogheny River catchment (green), Casselman River catchment (yellow), Savage River catchment (blue), Georges Creek catchment (pink), and Potomac River Upper North Branch catchment ('Potomac River U N Branch,' orange). Other areas of the greater Youghiogheny River basin are indicated in green on the map and areas of the greater Potomac River North Branch basin are shown in orange. Although fracking is not occurring in the western MD region, there is fracking activity just to the north in Pennsylvania as well as in West Virginia which borders the region on the south and west. Activity in West Virginia is notable since Maryland sites in the Youghiogheny River and Potomac River Upper North Branch catchments are located downstream of West Virginia land. The Casselman River, Savage River, and Georges Creek catchments drain Maryland land, with the Casselman and Savage Rivers flowing northward into Pennsylvania. Baseline measurements in the current study thus may not represent 'pristine' conditions but represent the current condition of western MD streams prior to MD fracking development.

Metals  $\text{Sr}^{2+}$  and  $\text{Ba}^{2+}$  occur at very high concentrations in fracking fluids as they are transported from *in situ* shale formations and are highly enriched in the fluids relative to surface waters (Barbot et al., 2013; Watmough, 2014). Strontium and  $\text{Ba}^{2+}$  may therefore act as tracers for the presence of fracking fluids and were monitored in

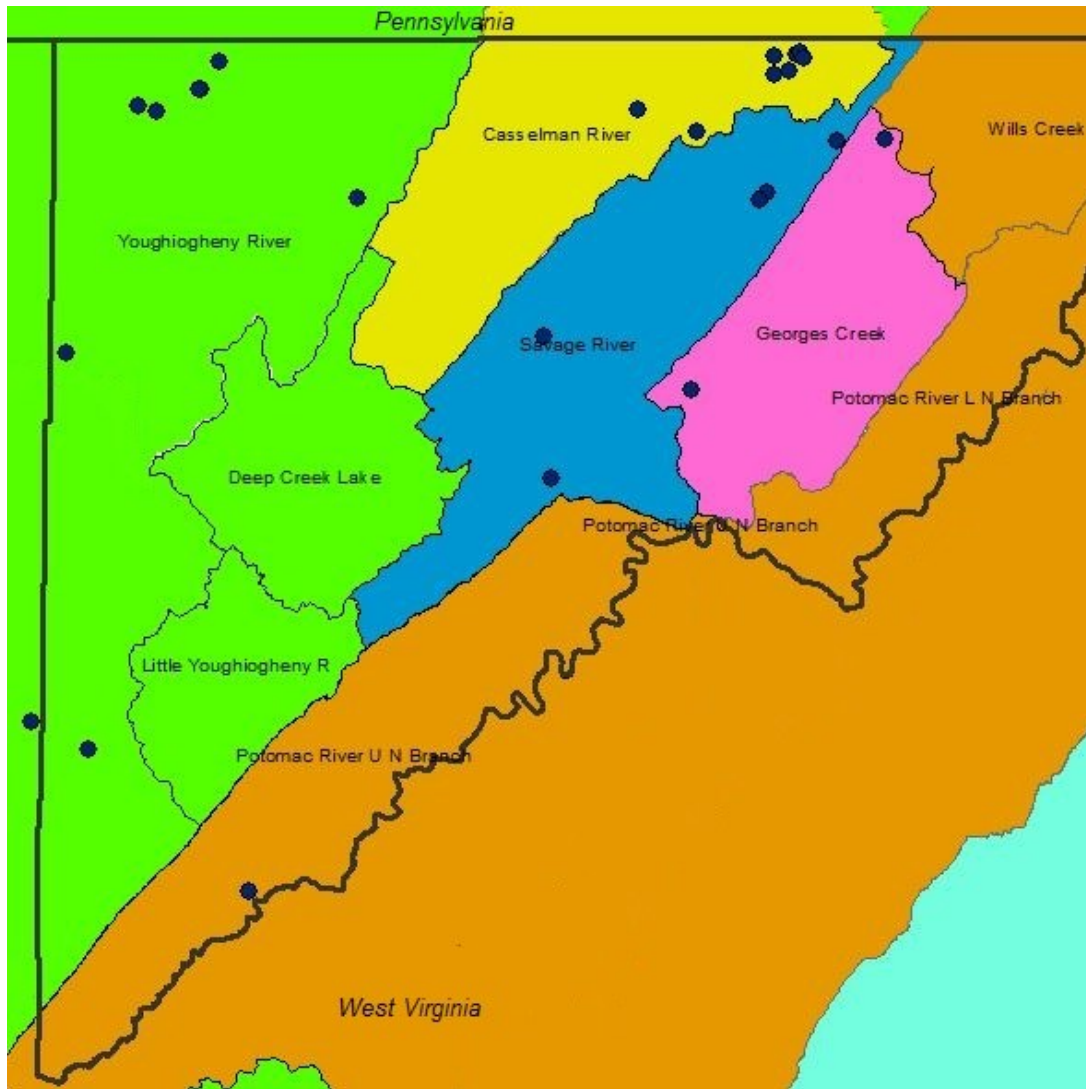


**Figure 1.4** Map of the western Maryland study region with the study sites represented as purple points. Catchment areas studied are labeled, with the Youghiogheny River catchment shown in green, Casselman River catchment in yellow, Savage River catchment in blue, Georges Creek catchment in pink, and Potomac River Upper North Branch ('Potomac River U N Branch') catchment in orange. The wider Youghiogheny River basin is indicated in green, and the wider Potomac River North Branch basin in orange.

western Maryland surface waters. Specifically, objectives with this monitoring were:

1. To determine temporal and spatial variability in stream concentrations of  $\text{Sr}^{2+}$  and  $\text{Ba}^{2+}$  throughout western Maryland across a 1-year period. This allowed determination of baseline concentrations in the region prior to fracking

development. With collection of baseline measurements, the applicability of  $\text{Sr}^{2+}$  and  $\text{Ba}^{2+}$  as fracking fluid tracers was also assessed. Monitoring of  $\text{Sr}^{2+}$  and  $\text{Ba}^{2+}$  stream concentrations is discussed in Chapter 2 of this work.

2. To determine relative concentrations in  $\text{Sr}^{2+}$  and  $\text{Ba}^{2+}$  using the Ba/Sr molar ratios in monitored stream waters. The Ba/Sr ratios were of interest as they may indicate different geologic  $\text{Sr}^{2+}$  and  $\text{Ba}^{2+}$  sources or may indicate relative patterns of  $\text{Ba}^{2+}$  and  $\text{Sr}^{2+}$  saturation in streams. In addition, stream ratios of Ba/Sr were assessed for their applicability as fracking fluid tracers.

Evaluation of Ba/Sr ratios is similarly discussed in Chapter 2.

Major ions  $\text{Na}^+$ ,  $\text{K}^+$ ,  $\text{Mg}^{2+}$ ,  $\text{Ca}^{2+}$ ,  $\text{Cl}^-$ , and  $\text{SO}_4^{2-}$  were measured in all streams for further characterization of stream waters. Nitrate ( $\text{NO}_3^-$ ), bicarbonate ( $\text{HCO}_3^-$ ), and dissolved organic carbon (DOC) were also measured in select sampling months.

Goals of the monitoring of major ions were:

1. To determine temporal and spatial variability of major ion concentrations in western Maryland streams monitored across 1 year. Monitoring of major ion levels allowed their assessment as potential fracking fluid tracers. Major ion measurements also enabled calculations of the ionic strength and charge balance of stream waters. Additionally, this monitoring allowed further interpretation of  $\text{Sr}^{2+}$  and  $\text{Ba}^{2+}$  concentration patterns, and, in particular, facilitated investigation of the potential for oversaturation with respect to  $\text{BaSO}_4$  or  $\text{SrSO}_4$ .

2. To determine major ion ratios in stream waters across both space and time. Major ion ratios in streams were used to determine probable geologic and anthropogenic sources to streamflow. The monitoring of major ion ratios also allowed determination of their viability as fracking fluid tracers. The assessment of major ion ratios is discussed in Chapter 2 of this work.

With the potential for upward CH<sub>4</sub> migration associated with fracking activity, dissolved CH<sub>4</sub> may shift from baseline surface water concentrations following fracking development, thus, in the current study, naturally occurring dissolved CH<sub>4</sub> was monitored in western Maryland headwater streams. The objectives of this part of the study were:

1. To determine temporal and spatial variability in stream concentrations of dissolved CH<sub>4</sub> over a year-long time span. Assessment of variability across time and space allowed determination of pre-fracking baseline concentrations which have not been previously measured in streams of western MD. With determining spatial and temporal concentration variability, I intended to verify whether CH<sub>4</sub> concentrations will be useful indicators of fracking-related stream contamination. Monitoring of dissolved CH<sub>4</sub> concentrations is discussed in Chapter 3 of this work.
2. To determine whether stream CH<sub>4</sub> is primarily supplied by microbial production or by migration from deep reservoirs of thermogenic CH<sub>4</sub>. The presence of thermogenic CH<sub>4</sub> was of particular interest since thermogenic inputs to streams may be affected by future fracking activity. The major CH<sub>4</sub>

stream sources were evaluated using analyses of the carbon isotopic composition of CH<sub>4</sub>, since microbially produced CH<sub>4</sub> has lower <sup>13</sup>C/<sup>12</sup>C ratios than thermogenic CH<sub>4</sub>. Carbon isotopic compositions of stream CH<sub>4</sub> and their use in determining CH<sub>4</sub> sources is presented in Chapter 3.

The characteristic stream baseline with respect to CH<sub>4</sub>, Sr<sup>2+</sup>, Ba<sup>2+</sup>, and major ions indicates expected ranges and variability of these constituents in streams unaffected by MD fracking. It allows for examining shifts in surface water chemistry over time related to fracking fluid contamination or to CH<sub>4</sub> migration to surface waters. Monitoring will be valuable for Maryland in the event that fracking is allowed, as potential short- and long-term impacts to surface waters may be observed. The identification of water quality impacts of fracking will also be useful outside of Maryland and will inform drilling practices so that they may be carried out with minimal impacts to the environment.

## Chapter 2: Baseline monitoring of dissolved metals in western Maryland streams

### 2.1 Introduction

#### 2.1.1 Hydraulic fracturing fluids as sources of water contamination

The use of hydraulic fracturing (*fracking*) fluids constitutes a major component of the fracking process, with 1–100 million L injected for the fracking process of each well (Clark et al., 2013). Fracking fluids may compromise surface and groundwater quality through a variety of contamination pathways. It is therefore necessary to detect and track the occurrence of fracking fluids in natural waters, for which tracer compounds may be useful. Tracking the fate of fracking fluids and its constituents requires that baseline conditions in natural waters are known. Baseline levels of dissolved strontium ( $\text{Sr}^{2+}$ ) and barium ( $\text{Ba}^{2+}$ ) in western Maryland (MD) streams are determined in this study as these metals may be used as tracers of fracking fluids in the future. In addition, stream water chemistry is assessed with respect to cations sodium ( $\text{Na}^+$ ), potassium ( $\text{K}^+$ ), magnesium ( $\text{Mg}^{2+}$ ), and calcium ( $\text{Ca}^{2+}$ ); anions chloride ( $\text{Cl}^-$ ), sulfate ( $\text{SO}_4^{2-}$ ), bicarbonate ( $\text{HCO}_3^-$ ), and nitrate ( $\text{NO}_3^-$ ); and dissolved organic carbon (DOC). Some of these ions were assessed for their applicability as fracking fluid tracers. They were also used to characterize stream waters and to determine ionic strength, charge balance, and the tendency for oversaturation with respect to  $\text{BaSO}_4$  and  $\text{SrSO}_4$  in streams of this region.

### 2.1.2 Characteristics of fracking fluids and wastes

Fracking fluids contain a variety of synthetic compounds added to enhance the drilling process. Although it is not required to disclose fracking fluid compounds in all U.S. states, the range of added compounds may include hydrochloric acid, ammonium persulfate, guar gum, isopropanol, citric acid, glutaraldehyde, ethylene glycol, acrylic polymers, and sand (Vengosh et al., 2014). During the fracking process fluids acquire natural compounds including dissolved solids, radioactive material, and hydrocarbon compounds from brines within the deep shale and adjacent formations (Vengosh et al., 2014). The natural compounds, synthetic compounds, and various degradation products all remain within the fracking fluid stream that is collected as waste at the end of the drilling process (Lester et al., 2015). The level of total dissolved solids (TDS) in recovered fracking fluids, which includes dissolved inorganic and organic constituents, varies widely among shale formations throughout the U.S., with Marcellus Shale drilling fluids typically having TDS of 180,000 mg/L or greater (Vengosh et al., 2014), well above TDS of seawater (35,000 mg/L) (Perlman, 2014). Some drilled shale formations, including the Marcellus Shale, produce fluids that have high levels of toxic metals such as arsenic (As) and selenium (Se) due to the high metal content of the shale (Vengosh et al., 2014). In addition to recovered fluids, the fracking process produces drill cuttings, which consist of drilled rock and clay remnants generated during wellbore drilling. Drill cuttings contain entrained salts, hydrocarbon compounds, and radionuclides. Like fracking fluids, the drill cuttings pose a contamination threat to surface and groundwater and are treated and disposed of off-site (Brantley et al., 2014; Kargbo et al., 2010).

Recovered fracking fluids and drill cuttings, as oil and gas industrial waste products, are exempt from U.S. Resource Conservation and Recovery Act (RCRA) hazardous waste provisions including “cradle to grave” surveillance of waste products (Hammer et al., 2012). Additionally, the 2005 Energy Policy Act exempted fracking operations from the Safe Drinking Water Act in the U.S. (Vengosh et al., 2014). State governments are the primary vehicles for regulating and documenting water contamination from fracking fluids and other waste materials (Vengosh et al., 2014). Maryland currently has in place regulations applicable to conventional oil and gas industries but does not have existing regulations and protocols addressing fracking activities and wastes (Eshleman, 2013).

### 2.1.3 Fates of fracking fluids in surface and groundwater

Throughout the life cycle of fracking fluids, many opportunities exist for fluid introduction to surface and groundwater. Groundwater may be affected upon fluid injection into wells. Fracking fluids may leak across failed well casings and migrate through underground systems of faults and fractures (Vidic et al., 2013). Such systems, which occur in the Marcellus Shale region, connect deep formation fluids with shallow aquifers (Llewellyn, 2014; Warner et al., 2012). Even without fracking fluid leakage, high-pressure fluid injections during drilling may stimulate upward migration of deep brines through the pre-existing fault systems (Vengosh et al., 2014). Abandoned oil and gas wells, which are prevalent in many areas of the Marcellus Shale, may also facilitate flow of brines or fracking fluids to shallow aquifers (Jackson et al., 2013b).

After fracking fluids are recovered at the wellhead, groundwater contamination may occur in association with spills or leaks of fluids during their storage or transport. Fracking fluids are often disposed of by deep well injection, which may be particularly hazardous to groundwater because of the potential for cement failure or compromised well integrity (Vengosh et al., 2014).

Fracking fluid contamination of groundwater has been suggested in some studies. A groundwater study in Colorado showed a link between fluid spill events and elevated levels of benzene, toluene, ethylbenzene, and xylene (BTEX) compounds in groundwater near fracking sites (Gross et al., 2013). Studies in an active fracking area in Wyoming showed elevated levels of specific conductance in groundwater, indicating increased concentrations of dissolved ionic constituents. High levels of ionic constituents as well as elevated groundwater dissolved methane, ethane, and propane found in this area indicated subsurface leakage of fracking fluids, although mechanisms of contamination were not determined (Wright, 2012). In the Barnett Shale region of Texas, a study reported elevated levels of As, Se, Sr, and Ba in groundwater located near fracking wells, with significantly lower concentrations of these constituents found at reference sites outside the fracking area (Fontenot et al., 2013).

Contamination of surface water may occur by inflow of contaminated groundwater (Heilweil et al., 2013), or it may occur via surface spills during fracking fluid recovery, storage, transport, or disposal. Recovered fluids are initially stored at the drilling site, which may allow surface water contamination in cases of storage pit breaching, insufficient pit linings, or other leakage incidents (Harkness et al., 2015;

Vengosh et al., 2014). After on-site storage, fracking fluids may be treated and reused at the well site or may be transported for off-site treatment and disposal (Shaffer et al., 2013). Long transport distances are often required, particularly for fluids disposed of in specified deep injection wells (Skalak et al., 2014). Long transport distances for large fluid volumes increase the risk of spills and impacts to surface waters.

Disposal of fracking fluids at municipal or industrial wastewater treatment plants influences surface waters because treatment plant outflow is discharged to streams and rivers, and wastewater treatment plants do not effectively remove all dissolved solids during treatment (Wilson and VanBriesen, 2012). Signals of fracking fluids have been found downstream of treatment plant discharge, with multiple studies showing elevated concentrations of dissolved constituents including  $\text{NH}_4^+$ ,  $\text{Na}^+$ ,  $\text{Mg}^{2+}$ ,  $\text{Ca}^{2+}$ ,  $\text{Sr}^{2+}$ ,  $\text{Ba}^{2+}$ ,  $\text{Cl}^-$ ,  $\text{Br}^-$ , and  $\text{I}^-$  in downstream waters (Ferrar et al., 2013; Harkness et al., 2015). In some regions, fluids are disposed of by land application or road spreading as deicer, and these practices affect surface waters through runoff (Vengosh et al., 2014). Road spreading of conventional drilling waste fluids has been linked to high levels of extractable  $^{226}\text{Ra}$ , Sr, Ca, and Na in soils and sediments (Skalak et al., 2014). Illegal disposal of untreated fracking fluids is an additional threat to surface waters and has been documented in some U.S. regions (Vengosh et al., 2014).

Surface water intrusion of inorganic ions such as those found in fracking fluids causes significant ecological problems. Increased ion levels interfere with normal osmoregulation and metabolism of aquatic organisms and may compromise functioning of aquatic plant species (Canedo-Arguelles et al., 2013). In addition, high

levels of dissolved ions may stimulate blooms of golden algae (*Prymnesium parvum*) which thrive in brackish environments and produce toxins lethal to fish (Patino et al., 2014).

Presence of the ions  $\text{Br}^-$  and  $\text{I}^-$  in surface waters are of particular concern for public health. Even slightly elevated concentrations of  $\text{Br}^-$  and  $\text{I}^-$  may lead to the formation of carcinogenic brominated and iodinated disinfection byproducts (DBPs) during drinking water chlorination or ozonation processes (Harkness et al., 2015; Warner et al., 2013a). Simulations show that surface waters receiving 0.01% fracking fluids by volume generate increased amounts of brominated and iodinated DBPs in drinking water (Parker et al., 2014).

The contaminant burden of fracking fluids is amplified in many regions because surface waters may already receive significant contaminant loads from sources including acid mine drainage, road salts, coal ash impoundment fluids, brines from abandoned oil wells, septic system effluent, and agricultural runoff. In such regions, surface water inputs of dissolved ions from fracking fluids may not be as readily diluted to safe levels (Ferrar et al., 2013). A recent study examining synergistic water quality impacts from mixtures of acid mine drainage and fracking fluids showed that the blended fluids were lower in metals and radionuclides; however, the mixtures formed precipitates that were high in radioactivity (Kondash et al., 2014).

Fracking fluid presence is also a major concern in surface waters because of exposure to naturally occurring radioactive material (NORM) derived from drilled shale formations (Vengosh et al., 2014). Discharge of treated fracking fluids to Pennsylvania streams has been linked to accumulation of radium isotopes  $^{226}\text{Ra}$  and

<sup>228</sup>Ra in sediments, with radioactivity levels approximately 200 times greater than those of background sediment samples (Warner et al., 2013a). The presence of Ra in freshwater sediments may allow significant Ra bioaccumulation in benthic organisms (Warner et al., 2013a).

Impacts of fracking fluids may be especially pronounced in headwater stream systems. Well pads for fracking sites are commonly in close proximity to headwater stream systems, allowing direct impacts from spills and other incidents (Brantley et al., 2014). Further, forest and vegetation are cleared for well construction and drilling, effectively removing buffers which normally protect high-quality headwater streams (Trexler et al., 2014). Small headwater streams, which are characterized by relatively low flow volumes, are innately sensitive to contaminants and thus highly vulnerable to water quality changes during fracking development.

#### 2.1.4 Use of metals as fracking fluid tracers

There are clearly numerous pathways for contamination of natural waters by fracking fluids as well as many serious ramifications of such contamination. It is therefore essential to understand the environmental fate of fracking fluids, particularly in headwater streams where their impacts may be greatest. Towards this objective, tracer compounds or elements are expected to be useful as indicators of fluid intrusion of surface waters (Mair et al., 2012). Tracers for identification of fracking fluids should be compounds that are known to occur in high concentrations in the fluids and found at very low concentrations in natural waters. A tracer compound should have relatively low variability in freshwater and should have no

major inputs from common contaminants or anthropogenic effluents, allowing the tracer to be definitively linked to fracking fluids. In addition, a tracer compound should be conducive to regular monitoring.

Several classes of synthetic organic compounds, such as surfactants, biocides, and scale-inhibiting species, are associated with fracking fluids and may signal fracking fluid presence since they otherwise do not occur in natural waters (Vengosh et al., 2014). Such organic compounds are difficult to use as tracers, though, since individual compounds in fluids are not disclosed and may vary widely among well operators (Arnaud, 2015). The degradation products of the compounds also vary depending on conditions and are not well known (Lester et al., 2015). Further, the organic compounds found in fluids are generally expensive to analyze and may require large sample volumes, making regular monitoring less practical.

Several major ions are elevated in fracking fluids and would be observed in surface waters in cases of fracking fluid contamination, including  $\text{Na}^+$ ,  $\text{Mg}^{2+}$ ,  $\text{Ca}^{2+}$ , and  $\text{Cl}^-$  (Barbot et al., 2013; Warner et al., 2013a). However, detection of these ions alone would not be distinctive of fracking fluids since such ions are supplied to surface waters from many different anthropogenic and geologic sources (Godwin et al., 2003; Likens et al., 1967). Still, a cumulative measure of total major ions, assessed as stream water specific conductance, can show spikes immediately following fracking fluid contamination (Brantley et al., 2014). Since specific conductance can be continuously recorded in streams by *in situ* data loggers (Stranko et al., 2013), such a tool would allow continuous observation and prompt detection of spikes signaling possible fracking fluid contamination. The specific conductance

measurements signaling potential contamination can be immediately followed by stream measurements of a tracer that is unique to fracking fluids.

The ions  $\text{Sr}^{2+}$ ,  $\text{Ba}^{2+}$ , and  $\text{Br}^-$  occur at very high levels in fracking fluids (Barbot et al., 2013) and are expected to be distinctive tracers of the fluids in streams. Concentrations of these elements are very low in natural waters relative to concentrations in fracking fluids. Based on reported  $\text{Sr}^{2+}$  and  $\text{Ba}^{2+}$  concentrations in fracking fluids and in streams (Brantley et al., 2014; Watmough, 2014), fracking fluids are expected to be enriched in  $\text{Sr}^{2+}$  and  $\text{Ba}^{2+}$  by a factor between 37,000 and 560,000 relative to streams. In low-order streams  $\text{Br}^-$  is not detected or detected at very low levels (Rai and Iqbal, 2015). The mere presence of  $\text{Br}^-$  therefore may be indicative of fracking fluid contamination. Regular monitoring on the order of weeks to months is feasible for these three constituents, with monitoring frequencies of once per 1–2 months assessed in the current study. In this study the 1–2 month sampling frequency was utilized for observation of natural concentration ranges in the stream constituents. With the potential for fracking fluid contamination events, however, a higher frequency monitoring tool, such as a field sensor of specific conductance, may be utilized for initial alert of stream contamination. Of the three elemental tracers  $\text{Sr}^{2+}$ ,  $\text{Ba}^{2+}$ , and  $\text{Br}^-$  which would distinguish fracking fluid presence,  $\text{Sr}^{2+}$  and  $\text{Ba}^{2+}$  were favored over  $\text{Br}^-$  in the current western MD study since they could be regularly analyzed at the Chesapeake Biological Laboratory.

### 2.1.5 Monitoring of Sr<sup>2+</sup> and Ba<sup>2+</sup> in western and southern MD streams

In order to use Sr<sup>2+</sup> and Ba<sup>2+</sup> as indicators of fracking fluid presence, it is important to understand their natural concentrations and ranges in aquatic environments. Dissolved Sr<sup>2+</sup> and Ba<sup>2+</sup> in freshwater are most commonly derived from weathering of compounds containing Sr and Ba in the mineral lattice, primarily carbonate rocks and weathered clay minerals, (Kravchenko et al., 2014; Negrel et al., 1993), both of which are abundant in western MD (Roth, 1999). Groundwater interacts considerably with these minerals and is enriched in Sr<sup>2+</sup> and Ba<sup>2+</sup>, acting as a source of Sr<sup>2+</sup> and Ba<sup>2+</sup> to overlying freshwater (Peek and Clementz, 2012). Surface runoff may acquire Sr<sup>2+</sup> and Ba<sup>2+</sup> through interactions with soil minerals, providing another freshwater source of these elements (Hogan and Blum, 2003). Strontium is more abundant than Ba in crustal minerals (Turekian and Wedepohl, 1961), and its salts are also more soluble than those of Ba (Peek and Clementz, 2012).

In some active fracking regions in Pennsylvania, surface water Sr<sup>2+</sup> and Ba<sup>2+</sup> concentrations have been measured and show high spatial and temporal variability (Brantley et al., 2014). This demonstrates the need for baseline measurements of Sr<sup>2+</sup> and Ba<sup>2+</sup> which can be compared with concentration measurements taken during and after fracking activity. Natural variability in surface water Sr<sup>2+</sup> and Ba<sup>2+</sup> in the region before the onset of fracking may be accounted for with baseline measurements at 1–2 month intervals in surface waters draining each potential well site, as was assessed in the current study.

With the suspension of permitting for fracking in MD under the Marcellus Shale Safe Drilling Initiative, an initial 3-year pre-drilling period occurred from 2011 to

2014, allowing for monitoring of dissolved  $\text{Sr}^{2+}$  and  $\text{Ba}^{2+}$  in the prospective drilling region of western MD, the topic of the current work. The first goal of this work was to determine both temporal and spatial variability of stream  $\text{Sr}^{2+}$  and  $\text{Ba}^{2+}$  concentrations. This allowed for characterization of baseline  $\text{Sr}^{2+}$  and  $\text{Ba}^{2+}$  concentrations prior to fracking activity. In addition, assessment of the spatial and temporal variability was used to determine the applicability of  $\text{Sr}^{2+}$  and  $\text{Ba}^{2+}$  as stream tracers for fracking fluids.

It was hypothesized that  $\text{Sr}^{2+}$  and  $\text{Ba}^{2+}$  temporal patterns are dependent upon relative inputs of surface and groundwater to a stream reach. Stream reaches which receive  $\text{Sr}^{2+}$  and  $\text{Ba}^{2+}$  from groundwater and which are strongly influenced by surface runoff were expected to show high concentrations of the metals in late summer and fall with lower concentrations in spring when runoff is greatest (Ahearn et al., 2004). Stream reaches which are predominantly groundwater fed with low influence from runoff were expected to show relatively low temporal variability. It was hypothesized that the spatial distribution of  $\text{Sr}^{2+}$  and  $\text{Ba}^{2+}$  concentrations follows patterns of bedrock geology which are highly variable in western MD (Brezinski, 2013). Despite the anticipated variability in concentrations, concentrations of these elements were expected to be very low relative to concentrations in fracking fluids based on previous  $\text{Sr}^{2+}$  and  $\text{Ba}^{2+}$  measurements in minimally disturbed streams of North America, as reported in the literature (Elias et al., 1982; Watmough, 2014);  $\text{Sr}^{2+}$  and  $\text{Ba}^{2+}$  were thus projected to be good fracking fluid tracers in streams. To evaluate naturally occurring temporal variability in stream  $\text{Sr}^{2+}$  and  $\text{Ba}^{2+}$ , regular concentration measurements were carried out at 4–8 week intervals over a 1-year

period. Baseline spatial variability in  $\text{Sr}^{2+}$  and  $\text{Ba}^{2+}$  was assessed through regular concentration measurements at 25 sites across western MD.

Another goal of this work was to assess naturally occurring stream ratios of Ba/Sr across time and space. These ratios, determined from  $\text{Sr}^{2+}$  and  $\text{Ba}^{2+}$  concentration measurements, allowed characterization of stream baselines with respect to the Ba/Sr ratio. Monitoring of Ba/Sr and its variability over time and space also allowed assessment of the Ba/Sr ratio as a potential tracer of fracking fluid. Finally, Ba/Sr ratios were used to interpret patterns observed in  $\text{Sr}^{2+}$  and  $\text{Ba}^{2+}$  concentrations across space and time. It was hypothesized that stream ratios of Ba/Sr vary based on underlying geology with which groundwater interacts, surface runoff interactions with soils, and extent of  $\text{BaSO}_4$  and  $\text{SrSO}_4$  precipitation. Ratios of Ba/Sr were assessed from  $\text{Sr}^{2+}$  and  $\text{Ba}^{2+}$  concentrations measured at 4–8 week sampling frequencies over 1 year, with measurements across the 25 western MD stream sites.

#### 2.1.6 Characterizing waters by major ion composition

In addition to baseline  $\text{Sr}^{2+}$  and  $\text{Ba}^{2+}$  concentrations, major ion concentrations were also of interest. A primary goal in this study then was to determine temporal and spatial variability in stream concentrations of major ions  $\text{Na}^+$ ,  $\text{K}^+$ ,  $\text{Mg}^{2+}$ ,  $\text{Ca}^{2+}$ ,  $\text{Cl}^-$ , and  $\text{SO}_4^{2-}$ . The monitoring of major ion concentrations enabled assessment of major ions as potential tracers of fracking fluids. The major ion measurements were also used to determine the ionic strength and relative charge contributions in stream waters. Additionally, major ion measurements allowed interpretation of  $\text{Sr}^{2+}$  and  $\text{Ba}^{2+}$  levels in streams since precipitation and dissolution of  $\text{Sr}^{2+}$  and  $\text{Ba}^{2+}$  salts are dictated

by the presence of certain ions; for example,  $\text{Ba}^{2+}$  concentrations in natural waters are affected by  $\text{SO}_4^{2-}$  levels because of the tendency for barite ( $\text{BaSO}_4$ ) formation (Kravchenko et al., 2014). Because of such effects of the major ions, observed temporal and spatial trends in  $\text{Sr}^{2+}$  and  $\text{Ba}^{2+}$  were compared with those of major cation and anion concentrations.

Acid neutralizing capacity (ANC), or the proton deficiency of a water sample which can be titrated to an equivalence point by a strong acid, was measured in some stream waters in this study. ANC is primarily controlled by  $\text{HCO}_3^-$  -content in river waters and was analyzed in stream waters for comparison with the unbalanced positive charge. Dissolved  $\text{NO}_3^-$  and DOC were measured in some stream samples for assessment of their anionic contributions.

With measuring of major ions, an additional goal of this study was to assess stream major ion ratios over time and space. Major ion ratios are useful for detecting various natural and anthropogenic impacts to streams; they have been used to indicate the presence in streams of migrated geologic brines, road salt effluent, abandoned mine drainage, conventional oil and gas production fluids, coal power plant wastewater, septic effluent, and agricultural wastewater (Dresel and Rose, 2010; Lautz et al., 2014; Wilson, 2014). Relative ion concentrations were compared across sites to determine similarities or differences among stream waters prior to fracking development. Also, major ion ratios were assessed for their viability as fracking fluid tracers.

As with stream  $\text{Sr}^{2+}$  and  $\text{Ba}^{2+}$  concentrations, it was hypothesized that absolute and relative major ion concentrations vary largely according to bedrock geology

underlying stream catchments. Seasonal influences were predicted to affect temporal variability of ion concentrations and ion ratios, with road salt effluent expected to be a major seasonal influence. Road salt effluent was expected to cause increases in stream levels of  $\text{Na}^+$  and  $\text{Cl}^-$  during winter, as well as slight increases in  $\text{Mg}^{2+}$  and  $\text{Ca}^{2+}$ . With major ions supplied to streams from several potentially variable sources, major ions as measured from grab sampling were not expected to be useful fracking fluid tracers. Spatial and temporal variability of major ions and major ion ratios were assessed through regular measurements of major cations and anions in streams throughout western MD, with sampling at 4–8 week time points over a 1-year period.

In addition to analysis of  $\text{Sr}^{2+}$  and  $\text{Ba}^{2+}$  in western MD streams, I compared stream concentrations in western MD with those of southern MD's coastal plain setting which is not underlain by the Marcellus Shale formation, with analysis of stream water  $\text{Sr}^{2+}$  and  $\text{Ba}^{2+}$  in Calvert County in June and July 2014. Along with  $\text{Sr}^{2+}$  and  $\text{Ba}^{2+}$ , major ion concentrations were assessed in Calvert County. Major ion measurements in Calvert County may further elucidate contrasts in major stream water influences between western and southern MD.

Monitoring of spatial and temporal ranges of  $\text{Sr}^{2+}$ ,  $\text{Ba}^{2+}$ , and major ions in streams allows for characterization of baseline water chemistry, which is particularly important for a region such as western MD that may be impacted by fracking in the future. These constituents and their relative concentrations are useful for categorizing stream water influences both currently and in the future following fracking development.

## 2.2 Materials and methods

### 2.2.1 Sampling sites

Samples for metals analysis were collected from first- to fourth-order stream reaches. As defined by Strahler (1952), first-order streams are perennial headwater streams with no tributaries, second-order streams are those formed from the joining of two first-order streams, third-order streams form from the joining of two second-order streams, and so on. Stream reaches sampled were downstream of potential fracking well pad locations in Garrett and Allegany Counties of western MD. In this region of MD, approximately 76% of land cover is forest. Agriculture and urban land use comprise approximately 16% and 3% of the region, respectively (Eshleman, 2013).

Sampling occurred in 5 catchment areas which are indicated by color in Fig 2.1: Casselman River, Georges Creek, Savage River, Potomac River Upper North Branch, and Youghiogheny River. Although the western MD study region does not presently have fracking activity, some sites within the Potomac River Upper North Branch and Youghiogheny River catchments may currently be influenced by fracking as they are downstream of West Virginia land where there is fracking activity. Fracking also occurs in Pennsylvania, although Pennsylvania land is downstream of all study sites.

Also monitored within the current study were the Savage River Pumping Station (SRPS), a groundwater reservoir within the Savage River catchment, and the Frostburg Water Treatment Plant (WTP), which provides drinking water for the city of Frostburg (Fig. 2.1). The WTP combines waters received from SRPS and from Frostburg's Piney Creek Reservoir. The treatment plant intake water monitored in this work is referred to as 'WTP Intake,' and the finished water from the plant which

was monitored is referred to as ‘WTP Finished’. The Piney Creek Reservoir, located in the Casselman River catchment, was regularly sampled in this study, along with several of its minor tributaries, and it is referred to as ‘Reservoir’.

In southern MD, stream samples for analysis of metals were collected from streams in the two major catchments of Calvert County: West Chesapeake Bay and Patuxent River Lower, both of which are delineated by background color on the map in Fig. 2.2. The Calvert County region is approximately 46% forest, 38% developed land, and 14% agricultural land (Maryland Dept of Planning, 2010).

Samples for analysis of dissolved metals were collected in three sets: two in western MD and one in southern MD’s Calvert County. The first set consists of six sites within Allegany and Garrett Counties which were sampled monthly during the period Feb 2012–Feb 2013. The second set includes fourteen sites in Garrett County which were sampled every 6–8 weeks in the period Apr 2013–Apr 2014. Samples within this set were collected with assistance from the Maryland Department of Natural Resources (MD DNR), who obtained landowner permission for site access, as necessary. Also within the second set are five sites which were sampled biannually (once each in winter and summer): PRUN301D, SAVA302D, YOUG201D, YOUG301D, and YOUG302D. All sites from the first and second sets are shown on the western MD map in Fig. 2.1. Apart from WTP Intake, WTP Finished, and SRPS, I designated all western MD sites as forested, wetland, or anthropogenically influenced, as indicated in Table 2.1, based on the observed surrounding environment of the site. Forested stream sites are characterized by significant tree and vegetation cover surrounding the stream. Wetland sites are characterized by inundated soils

surrounding the stream with vegetation and fewer tree stands than found at forested sites. Streamflow is relatively slow at wetland sites. Anthropogenically influenced sites are found in the immediate vicinity of anthropogenic developments including major roads, bridges, residential areas, and coal facilities.

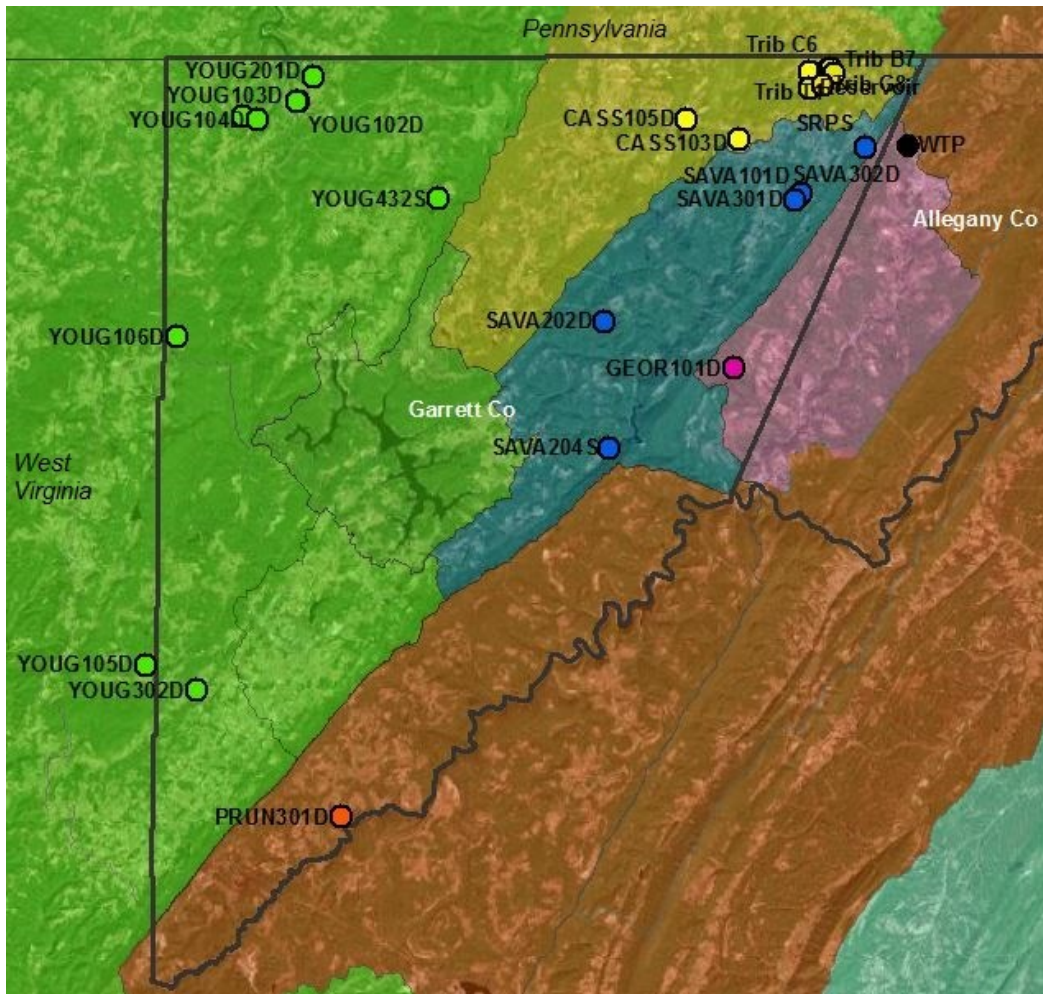


**Figure 2.1** Map of western MD stream sites for the Feb 2012–Feb 2013 and Apr 2013–Apr 2014 sampling sets. Background and symbol colors indicate catchment, with yellow indicating the Casselman River catchment, blue indicating the Savage River catchment, pink the Georges Creek catchment, orange the Potomac River Upper North Branch catchment, and green the Youghiogheny River catchment. Black symbol indicates the Frostburg WTP. The greater Youghiogheny River basin is indicated in green and the greater Potomac River North Branch in orange.

The third set of samples collected in this study includes seven sites in Calvert County which were sampled in June and July of 2014. These are shown on the map

in Fig. 2.2, with symbol color indicating the sampling stream and background color indicating catchment. Sites from all sampling sets are listed by site name in Table 2.1 with the corresponding stream name, catchment, geographic coordinates of the reference coordinate system WGS 84, and the site environment.

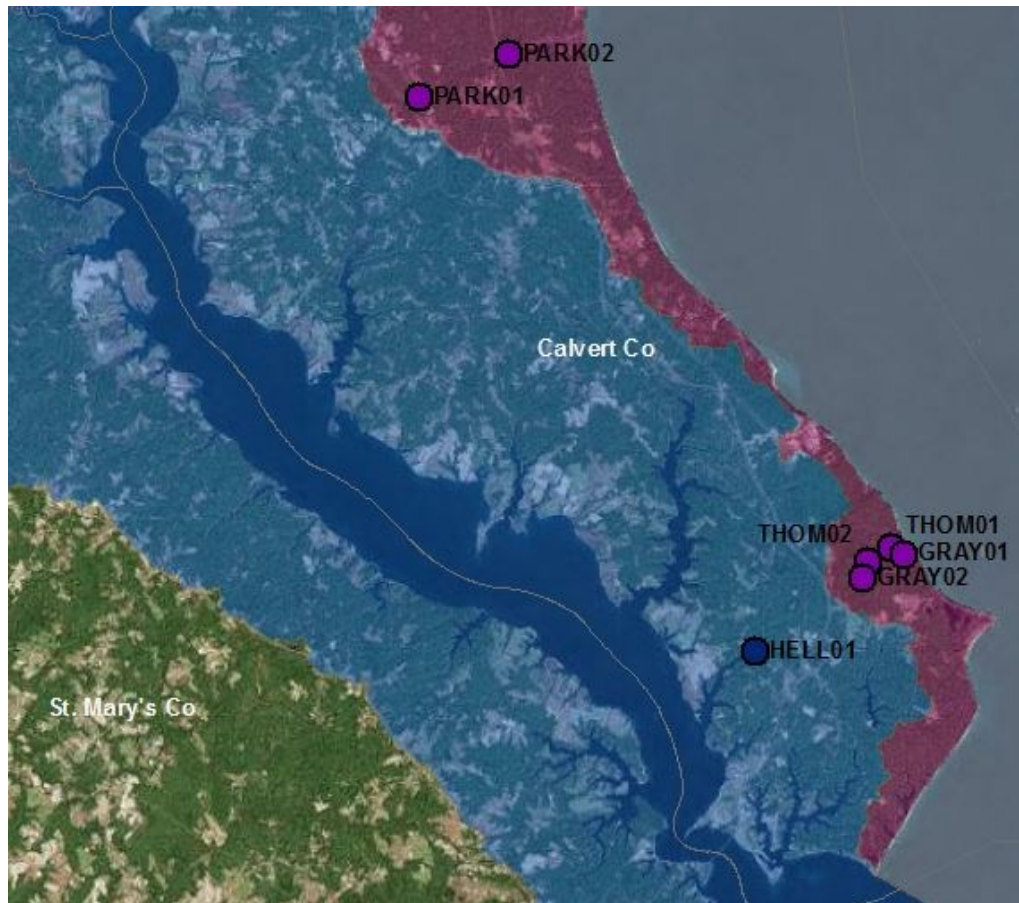


**Figure 2.2** Map of stream sites sampled in Calvert County, MD, in June and July 2014. Background and symbol colors correspond to stream catchment, with blue indicating the Patuxent River Lower catchment and purple indicating the West Chesapeake Bay catchment.

**Table 2.1** Names and locations of sampling sites in western MD for the Feb 2012–Feb 2013 and Apr 2013–Apr 2014 sets and sampling sites in Calvert County from the Summer 2014 set. Site name SRPS represents the Savage River Pumping Station and Reservoir represents the Piney Creek Reservoir. WTP Intake and WTP Finished represent the intake of the Frostburg City water treatment plant and the treated water from the plant, respectively. Sites in the Apr 2013–Apr 2014 set are named according to catchment, where CASS indicates the Casselman River catchment, GEOR the Georges Creek catchment, PRUN the Potomac River Upper North Branch catchment, SAVA the Savage River catchment, and YOUG the Youghiogheny River catchment. Sites in this set are numbered based on stream order, with numbers in the 100s representing 1<sup>st</sup> order streams, those in the 200s representing 2<sup>nd</sup> order, etc. Designation ‘S’ indicates long-term monitoring sites which have historical data sets, and those with ‘D’ are newly established monitoring sites. Summer 2014 site names are associated with the stream where the site is found, with HELL representing Hellen Creek, GRAY representing Grays Creek, PARK representing Parkers Creek, and THOM representing Thomas Branch. Note that for site THOM01, June and July sampling locations are slightly different due to higher water levels in July at Thomas Branch. The characteristic site environment is given in the ‘Environment’ column.

Site Name	Stream	Catchment Area	Latitude (N)	Longitude (W)	Environment
<b>Feb 2012–Feb 2013</b>					
SRPS	Savage River	Savage River	39° 40' 17.88"	78° 58' 14.94"	
Reservoir	Piney Creek	Casselman River	39° 42' 15.00"	79° 0' 40.80"	Anthropogenic
Tributary T1	Piney River Upper Tributary	Casselman River	39° 42' 52.62"	78° 59' 52.08"	Forested
Tributary C6	Piney Run Creek	Casselman River	39° 42' 55.38"	78° 59' 44.10"	Wetland
Tributary B7	Geatz Run	Casselman River	39° 42' 45.48"	78° 59' 35.22"	Wetland
Tributary G8	Blandy Run	Casselman River	39° 42' 21.6"	79° 0' 7.62"	Wetland
WTP Intake	Reservoir/SRPS	Casselman/Savage	39° 40' 19.55"	78° 56' 25.07"	
WTP Finished	Reservoir/SRPS	Casselman/Savage	39° 40' 19.55"	78° 56' 25.07"	
<b>Apr 2013–Apr 2014</b>					
CASS101D	Piney Creek Upper Tributary	Casselman River	39° 42' 47.10"	79° 0' 40.70"	Forested
CASS103D	Twomile Run	Casselman River	39° 40' 33.10"	79° 3' 43.20"	Anthropogenic
CASS105D	Meadow Run	Casselman River	39° 41' 13.40"	79° 6' 0.60"	Anthropogenic
GEOR101D	Mill Run	Georges Creek	39° 32' 53.10"	79° 3' 56.70"	Forested

**Table 2.1 (cont.)**

Site Name	Stream	Catchment Area	Latitude (N)	Longitude(W)	Environment
PRUN301D	Nydegger Run	Potomac River Upper North	39° 17' 51.10"	79° 21' 0.60"	Anthropogenic
SAVA101D	Savage River Upper Tributary	Savage River	39° 38' 45.6"	79° 1' 1.30"	Forested
SAVA202D	Big Run	Savage River	39° 34' 27.40"	79° 9' 35.40"	Forested
SAVA204S	Crabtree Creek	Savage River	39° 30' 13.10"	79° 9' 20.38"	Forested
SAVA301D	Savage River	Savage River	39° 38' 30.90"	79° 1' 18.40"	Forested
SAVA302D	Savage River	Savage River	39° 38' 35.50"	79° 1' 12.10"	Anthropogenic
YOUG102D	Youghiogheny River Upper Trib.	Youghiogheny River	39° 41' 48.50"	79° 22' 51.20"	Forested
YOUG103D	Youghiogheny River Upper Trib.	Youghiogheny River	39° 41' 48.40"	79° 22' 56.30"	Forested
YOUG104D	Buffalo Run Upper Tributary	Youghiogheny River	39° 41' 10.70"	79° 24' 36.50"	Wetland
YOUG105D	Laurel Run	Youghiogheny River	39° 22' 57.40"	79° 29' 28.60"	Anthropogenic
YOUG106D	Salt Block Run	Youghiogheny River	39° 33' 55.84"	79° 28' 6.38"	Wetland
YOUG201D	Mill Run	Youghiogheny River	39° 42' 37.8"	79° 22' 11.60"	Anthropogenic
YOUG301D	Buffalo Run	Youghiogheny River	39° 41' 20.10"	79° 25' 17.00"	Forested
YOUG302D	Cherry Creek	Youghiogheny River	39° 22' 6.90"	79° 27' 14.90"	Anthropogenic
YOUG432S	Bear Creek	Youghiogheny River	39° 38' 33.07"	79° 16' 47.28"	Forested
<b>Summer 2014</b>					
HELL01	Hellen Creek	Patuxent River Lower	38° 22' 37.20"	76° 27' 35.82"	Anthropogenic
GRAY01	Grays Creek	West Chesapeake Bay	38° 24' 6.96"	76° 24' 39.42"	Wetland
GRAY02	Grays Creek	West Chesapeake Bay	38° 23' 45.12"	76° 25' 27.54"	Forested
PARK01	Parkers Creek	West Chesapeake Bay	38° 31' 16.32"	76° 34' 18.48"	Anthropogenic
PARK02	Parkers Creek	West Chesapeake Bay	38° 31' 56.40"	76° 32' 30.84"	Forested
THOM01 June	Thomas Branch	West Chesapeake Bay	38° 24' 13.20"	76° 24' 55.02"	Wetland
THOM01 July	Thomas Branch	West Chesapeake Bay	38° 24' 13.74"	76° 24' 55.74"	Wetland
THOM02	Thomas Branch	West Chesapeake Bay	38° 24' 0.78"	76° 25' 21.66"	Forested

### 2.2.2 Field sampling

All field sampling was carried out when streams were at base flow stage, defined as normal flow conditions for the given season, with avoidance of sampling during high-flow conditions and following storm events. Prior to field sample collection, 60-mL Teflon sampling bottles were acid cleaned by immersion in sub-boiling 8 M HNO<sub>3</sub> for 24 hours and subsequently rinsed with Milli-Q water (18.2 MΩ cm). Bottles were transported to and from the field inside trace metal clean Ziploc<sup>®</sup> bags. Water samples were collected from the stream bank by hand at each site, except at site THOM01, where samples were collected from the wooden footbridge which crosses the stream. In June 2014, the sample was collected from the footbridge in the middle of the stream, and in July 2014, due to higher water levels, sample collection from the footbridge took place close to the north bank of the stream (Table 2.1). Because of the proximity of Calvert County surface waters to the Chesapeake Bay, salinity at each Calvert County site was tested with a refractometer and found to be <1 everywhere.

For sample collection, a plastic 60-mL Luer-lok syringe (Becton Dickinson) was used to collect stream water from mid-depth at each stream site. The syringe was first rinsed three times with 60 mL stream water. Following the rinses, 60 mL of water was taken into the syringe and a 0.2-μm filter (Corning) was attached to the syringe tip. The filter was rinsed by expelling 10 mL water through the syringe filter as waste. The Teflon sample bottle was rinsed three times with 10 mL of filtered stream water and was then filled to the bottle neck. After being transported to the laboratory, each sample was acidified with 50 μL concentrated HNO<sub>3</sub> (TraceMetal Grade, Fisher

Scientific) to keep metals in solution. Acidified samples were allowed to equilibrate for 24 hours before analysis.

Stream pH values in Apr 2013 were determined from measurements by MD DNR, where water samples were collected in polyethylene syringes without exposure to the atmosphere. Upon returning to the laboratory, samples were analyzed using a combination pH electrode and Orion 611 pH meter. Stream pH values of the Sep 2012–2013 period were measured with an *in situ* field meter (values provided by Tom Kozikowski, Mountain Ridge High School, Frostburg, MD).

### 2.2.3 Analysis of Sr<sup>2+</sup> and Ba<sup>2+</sup>

All preparation of samples and standards for elemental analyses was conducted in a class-100 laminar flow bench. Solutions were prepared with Milli-Q water (18.2 MΩ cm) from a Millipore Direct-Q 3UV purification system. For analysis by inductively coupled plasma mass spectrometry (ICP-MS), an aliquot of acidified field sample was diluted 1 in 10 in 1% HNO<sub>3</sub> and was spiked with an internal standard solution with 2 µg/L each of In and Cs. Diluted samples were then analyzed for Sr and Ba concentrations on an Agilent 7500cx ICP-MS, with concentrations measured against an external 5-point calibration line which was 0, 1, 2, 5, and 10 µg/L in both Sr and Ba. For Sr, masses 86 and 88 were measured, which were normalized to <sup>115</sup>In. For Ba, masses 135, 137, and 138 were measured, which were normalized to <sup>133</sup>Cs. For each element, measurements of separate isotopes were averaged to determine the element concentration. The set of diluted samples was analyzed by ICP-MS twice in random order. After each sample injection, the autosampler probe and sample

introduction system were rinsed by a 10 s aspiration of Milli-Q water followed by a 30 s aspiration of 1% HNO<sub>3</sub> rinse solution. After running the sample batch, stream samples were prepared in a second round of dilutions by diluting sample aliquots 1 in 20 in 1% HNO<sub>3</sub>. Three samples of high elemental concentrations from Aug 2013 were prepared with a 1 in 100 dilution in 1% HNO<sub>3</sub>. The second round of sample dilutions was analyzed by the same method on the ICP-MS. The average of concentration measurements of the two dilution rounds, each of which included two ICP-MS runs, was then used to determine sample Sr and Ba concentrations. Relative precision based on repeated measurements of samples was <1% for most samples.

#### 2.2.4 Analysis of major cations

Analysis of major cations Na<sup>+</sup>, K<sup>+</sup>, Mg<sup>2+</sup>, and Ca<sup>2+</sup> was carried out using a Perkin Elmer Optima 8300 Inductively Coupled Plasma Atomic Emission Spectrometer (ICP-AES) in Chesapeake Biological Laboratory's Nutrient Analytical Services Laboratory (NASL). Five-mL aliquots of each acidified sample were used for ICP-AES analysis. Cations Na<sup>+</sup>, Mg<sup>2+</sup>, and Ca<sup>2+</sup> were measured at two different emission wavelengths for each sample: Na<sup>+</sup> was measured in the visible spectrum at wavelengths 589.0 and 589.6 nm, Mg<sup>2+</sup> in the UV spectrum at wavelengths 279.1 and 285.2 nm, and Ca<sup>2+</sup> at wavelength 317.9 nm in the UV spectrum and at 422.7 nm in the visible spectrum. Potassium was measured at one visible wavelength, 766.5 nm, for each sample. For elements measured at two wavelengths, the measurements were averaged. Errors in each of the two wavelength measurements were propagated in the

average. All  $\text{Na}^+$  and  $\text{K}^+$  wavelengths were measured in the radial view and all  $\text{Ca}^{2+}$  and  $\text{Mg}^{2+}$  wavelengths measured in the axial view.

Cation concentrations were measured against a 5-point external calibration line, which was 0, 0.2, 0.4, 2, and 4 mg/L in  $\text{Mg}^{2+}$  and  $\text{K}^+$  and 0, 1, 2, 10, and 20 mg/L in  $\text{Ca}^{2+}$  and  $\text{Na}^+$ . Calibration standards were made from a multi-element stock solution containing  $\text{Na}^+$ ,  $\text{K}^+$ ,  $\text{Mg}^{2+}$ , and  $\text{Ca}^{2+}$  (SPEX CertiPrep). Samples whose concentrations exceeded the highest calibration standard were diluted in Milli-Q water for re-analysis, and cation concentrations of these samples were taken from the average of measurements of non-diluted and diluted runs. River water SLRS-5 SRM was analyzed for concentrations with each ICP-AES run. Concentration measurements agreed within 1.1%, 2.2%, 2.6%, and 0.9% of certified SRM concentrations of  $\text{Na}^+$ ,  $\text{K}^+$ ,  $\text{Mg}^{2+}$ , and  $\text{Ca}^{2+}$ , respectively. River water SRM was analyzed 27 times in total, and overall the concentration measurements gave relative precision of 1.3%, 2.7%, 1.2%, and 1.3% for  $\text{Na}^+$ ,  $\text{K}^+$ ,  $\text{Mg}^{2+}$ , and  $\text{Ca}^{2+}$ , respectively. Relative error of cation concentration measurements was <5% for most samples.

### 2.2.5 Analysis of major anions

For analysis of  $\text{Cl}^-$  and  $\text{SO}_4^{2-}$  concentrations, samples were run on a Dionex ICS-3000 Reagent-Free Ion Chromatography system with AS40 autosampler. An IonPac AG22 (4×50 mm) guard column and an ERS 500 suppressor with suppressor current of 50 mA were used in the system. As eluent, a carbonate/bicarbonate buffer was used, made fresh before each run from sodium carbonate and sodium bicarbonate (J.T. Baker). Buffer was made with deionized water and was allowed to degas by

sparging with He before IC runs. In the IC system the eluent flow rate was 1.2 mL/min. Six-mL aliquots of each acidified sample were used for analysis, and anion concentrations were measured against a 6-point calibration curve with concentrations 0, 0.8, 2, 4, 8, and 20 mg/L in  $\text{SO}_4^{2-}$  and concentrations 0, 2, 5, 10, 20, and 50 mg/L in  $\text{Cl}^-$ . The calibration standard solutions were made using a stock solution which was 1,000 mg/L in  $\text{Cl}^-$  and a stock solution which was 1,000 mg/L in  $\text{SO}_4^{2-}$  (VHG Labs). Calibration standards were acidified with  $\text{HNO}_3$  to match the sample matrix in order to account for effects of  $\text{HNO}_3$  on  $\text{SO}_4^{2-}$  sensitivity in the system. This precluded separate analysis of nitrate concentrations. The calibration curves for  $\text{Cl}^-$  and  $\text{SO}_4^{2-}$  were fitted with quadratic functions. Samples whose concentrations exceeded the highest calibration standard were diluted in deionized, acidified water for re-analysis by IC and final concentrations were determined from averages of diluted and non-diluted sample runs. Verification standards of 6.0 mg/L and 35.0 mg/L  $\text{Cl}^-$  were made from a separate lot of 1,000 mg/L stock  $\text{Cl}^-$  solution (VHG Labs) and, upon analysis, verification standards were found to be within 2.5% of the nominal concentrations. The two verification standards for  $\text{SO}_4^{2-}$ , similarly made from a separate lot of 1,000 mg/L stock  $\text{SO}_4^{2-}$  solution (VHG Labs), were 6.0 mg/L and 35.0 mg/L in  $\text{SO}_4^{2-}$ . Upon analysis, these were found to be within 0.9% of the nominal concentration. The SLRS-5 SRM was not used for verification of  $\text{Cl}^-$  and  $\text{SO}_4^{2-}$  concentrations since it is not certified for these ions. To determine reproducibility, SLRS-5 was analyzed for  $\text{Cl}^-$  and  $\text{SO}_4^{2-}$  with every IC run and gave

relative precisions of 1.6% and 0.8% for  $\text{Cl}^-$  and  $\text{SO}_4^{2-}$ , respectively, for a total of 33 measurements each.

#### 2.2.6 Analysis of Acid Neutralizing Capacity

During the Oct 2013 sampling in western MD, samples were collected for analysis of ANC to assess the levels of bicarbonate ( $\text{HCO}_3^-$ ) anions in stream samples. Samples were collected in 200-mL polyethylene bottles which had been previously washed in deionized water. At each site, bottles were rinsed three times with stream water. A sample of water from mid-depth of the stream was then collected in the bottle, filling it to the rim without headspace in order to avoid gas exchange. Sample bottles were stored in a cooler during transport to the laboratory and were refrigerated until ANC analysis.

Analysis of ANC was carried out by Gran Titration at University of Maryland Center for Environmental Science's Appalachian Laboratory in Frostburg, MD. For each sample, 50 mL was poured into a vial and 300  $\mu\text{L}$  of 2 M KCl was added to each to increase the ionic strength. While the sample was continuously stirred, a pH electrode was immersed in the sample and initial pH measured. The 0.01 M HCl titrant was then used to lower pH to approx. 4.7. Next, titrant was added in 8 increments to lower sample pH from 4.7 to 3.5. After each titrant addition, volume of cumulative acid added and pH were recorded as data pairs. After titration of the sample to pH 3.5 and recording of titration data, the pH electrode was rinsed thoroughly in deionized water before analysis of the next sample.

For each titrated sample, the Gran function  $F_{1a}$  was determined for each data pair of cumulative acid volume  $V_a$  (mL) and pH values.  $F_{1a}$  was determined by:

$$F_{1a} = (V_s + V_a)[H^+] \quad (2.1)$$

where  $V_s$  = total initial sample volume (mL). The  $F_{1a}$  value was then plotted against volume titrant added,  $V_a$ , to obtain a curve expressed by the linear equation

$$F_{1a} = b + aV_a \quad (2.2)$$

The equivalence volume  $V_1$  of the titration (mL) was determined as the point of interception with the  $V_a$  axis, calculated by

$$V_1 = \frac{-b}{a} \quad (2.3)$$

The ANC ( $\mu\text{eq/L}$ ) of the sample was then calculated from the equivalence volume by:

$$\text{ANC} = \frac{V_1 C_a}{V_s} \times 10^6 \quad (2.4)$$

where  $C_a$  = concentration of acid titrant (M).

### 2.2.7 Analysis of Dissolved Organic Carbon

During April 2014 sampling, western MD samples were collected for measurement of DOC in order to assess anionic contributions of DOC in stream waters. Prior to sampling, 30 mL polyethylene vials were immersed in 10% HCl for 12 hours and were rinsed with deionized water and dried. In the field, vials were

rinsed three times with stream water and then filled with water collected from mid-depth at each stream site.

For laboratory analysis, DOC was measured on a Shimadzu TOC-5000 in NASL at Chesapeake Biological Laboratory using a high-temperature combustion method (Sugimura and Suzuki, 1988). Samples were treated with HCl and then sparged with ultra-pure carrier grade air (a synthetic blend of oxygen and nitrogen) to remove inorganic carbon. In a high-temperature combustion (680°C), dissolved organic carbon was quantitatively oxidized on a catalyst bed of platinum-coated alumina to break down organic carbon to CO<sub>2</sub>. The CO<sub>2</sub> was carried by ultra-pure carrier grade air to the non-dispersive infrared detector (NDIR) for detection.

Concentrations of DOC were measured against a calibration line using the external standard potassium hydrogen phthalate (KHP). Standards in the calibration line were 0, 0.5, 1.0, 5.0, and 10.0 mg/L in KHP. The Continuing Calibration Verification (CCV) solution which contained 5.0 mg/L KHP was analyzed 5 times during sample analysis, with all measurements within 1.4% of the standard KHP concentration.

## 2.3 Results

### 2.3.1 Dissolved Sr<sup>2+</sup> and Ba<sup>2+</sup> concentrations

Dissolved Sr<sup>2+</sup> and Ba<sup>2+</sup> concentrations vary significantly in western MD streams throughout the Feb 2012–Feb 2013 and Apr 2013–Apr 2014 sample sets. Stream waters of the two western MD sample sets range between 100 nM and 700 nM in Ba<sup>2+</sup> across space and time. Strontium concentrations at sites in the region show a

greater range, with concentrations across both sample sets varying between 100 nM and 1,400 nM in space and time for most stream waters, although one site (PRUN301D) reached 3,200 nM in August 2013 (Table A1).

Spatially,  $\text{Sr}^{2+}$  and  $\text{Ba}^{2+}$  concentrations are significantly variable both within and among catchments. Strontium shows greater variability in space, with concentrations across the region varying by 1,000–3,000 nM in summer months when spatial variability is greatest (June and August). Variability in  $\text{Ba}^{2+}$  throughout the region is lower, with concentrations varying by 550 nM in August when spatial variability of  $\text{Ba}^{2+}$  is greatest. At the site PRUN301D, which was monitored biannually, exceptionally high  $\text{Sr}^{2+}$  concentrations were observed in Aug 2013 and Jan 2014, with concentrations of 3,151 nM and 1,453 nM, respectively (Table A1). The Ba/Sr ratio was accordingly very low relative to all other sites. Even when not including this site, the spatial variability of  $\text{Sr}^{2+}$  concentrations is greater than that of  $\text{Ba}^{2+}$  concentrations.

Significant temporal variability in dissolved  $\text{Sr}^{2+}$  and  $\text{Ba}^{2+}$  is also observed for western MD sites (Fig. 2.3). Concentrations range by 100 to 600 nM during one year in most streams. Certain sites, including Tributary T1 and Tributary C6, show strong seasonality for both metals, with concentrations highest between late summer and fall and lowest in early spring, while other sites show no distinct seasonal patterns. Figure 2.3 shows four sites in the Casselman River catchment (Panels A, B, D, and F) and two in the Savage River catchment (Panels C and E), illustrating the different temporal patterns both within and between catchments.

Most sites show consistent relative enrichment of either  $\text{Sr}^{2+}$  or  $\text{Ba}^{2+}$  throughout the year (Fig. 2.3). This is indicated by the logarithm of  $[\text{Ba}]/[\text{Sr}]$ , the ratio of molar Ba and Sr concentrations, where high  $\text{Ba}^{2+}$  concentration relative to  $\text{Sr}^{2+}$  gives a value  $>0$  and high  $\text{Sr}^{2+}$  concentration relative to  $\text{Ba}^{2+}$  give a value  $<0$ . Values of  $\log([\text{Ba}]/[\text{Sr}])$  determined for western MD stream sites ranged between  $-0.85$  and  $+0.37$ , as shown in Figure 2.4. Although most sites show consistent enrichment of one element, a number of sites in the Casselman River and Youghiogheny River catchments were found to alternate between enrichment of  $\text{Sr}^{2+}$  and  $\text{Ba}^{2+}$  throughout the year (Fig. 2.4). Among these sites, enrichment of  $\text{Sr}^{2+}$  was typically observed in fall and enrichment of  $\text{Ba}^{2+}$  observed in winter, spring, and summer. Among sites with continual enrichment of  $\text{Sr}^{2+}$  or  $\text{Ba}^{2+}$ , the dominance of a particular constituent—either  $\text{Sr}^{2+}$  or  $\text{Ba}^{2+}$ —was not found to be related to catchment but varied within catchments as much as throughout western MD.

In Calvert County streams,  $\text{Ba}^{2+}$  concentrations are between 100 nM and 300 nM, within the range of concentrations measured in western MD. Strontium concentrations in Calvert County have a slightly greater range than concentrations of most western MD streams, with concentrations between 100 nM and 1,800 nM (Table A1). The Parkers Creek sites in this region show  $\text{Sr}^{2+}$  concentrations at the high end of this range, varying between 1,400 nM and 1,800 nM, while all other Calvert County sites are between 100 nM and 500 nM. For both  $\text{Sr}^{2+}$  and  $\text{Ba}^{2+}$ , significant spatial variability is observed across Calvert County as well as for multiple sites within the same stream, although Grays Creek is an exception with similar  $\text{Sr}^{2+}$  concentrations at both stream sites (GRAY01 and GRAY02) in June and July 2014.

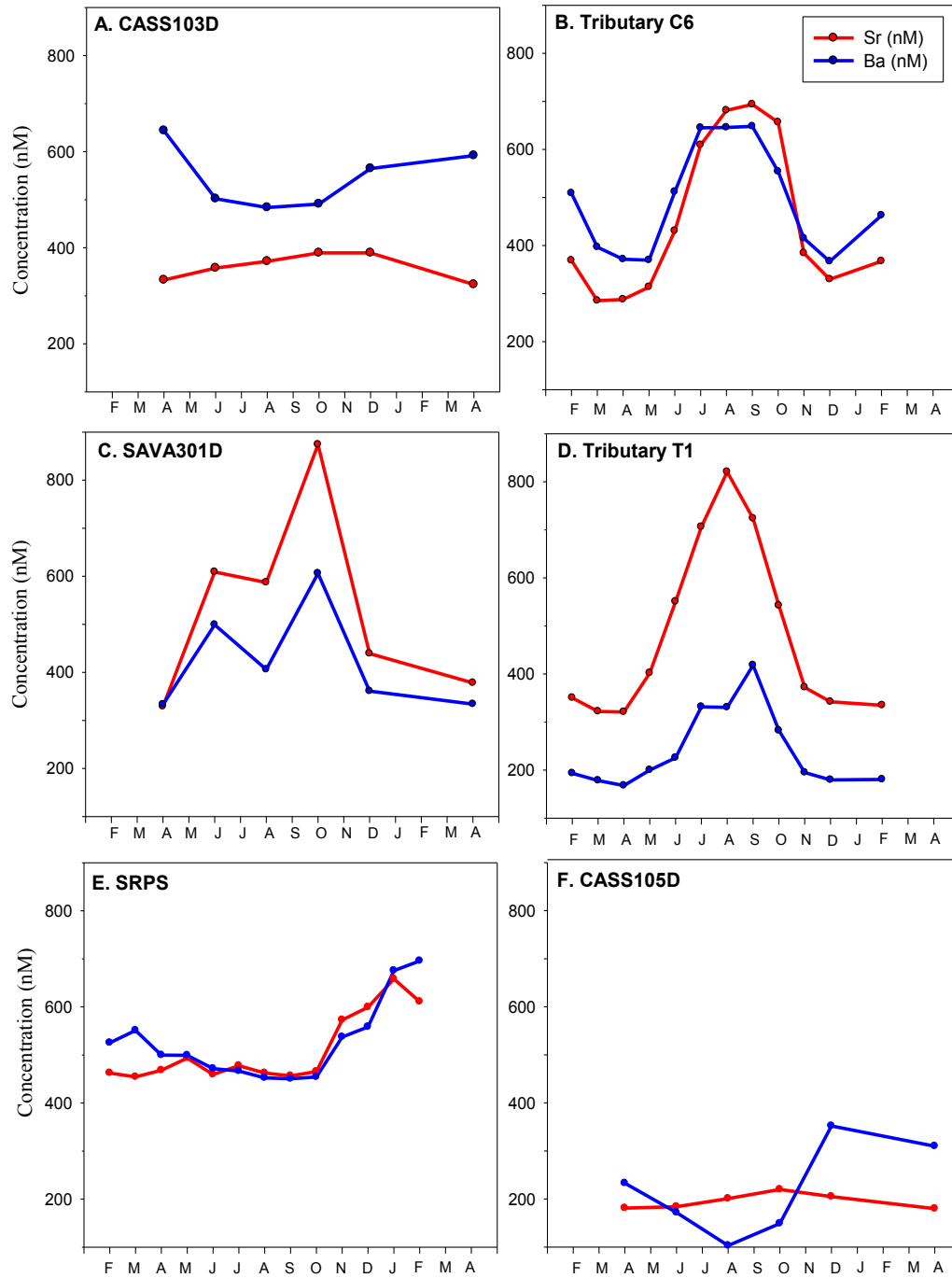


**Figure 2.3** Temporal variability in dissolved  $\text{Sr}^{2+}$  and  $\text{Ba}^{2+}$  concentrations (nM) across 1 year. Panels A, B, D, and F are sites in the Casselman River catchment, and panels C and E are sites in the Savage River catchment. SRPS indicates Savage River Pumping Station. Sites in Panels B, D, and E are from the 2012–2013 sample set, and those in Panels A, C, and F are from the 2013–2014 sample set.

Between June and July, most sites in Calvert County were stable in  $\text{Sr}^{2+}$  concentrations, although Parkers Creek sites increased. Barium concentrations increased between the two months for most sites, apart from sites in Grays Creek which were relatively constant. At Parkers Creek and Grays Creek sites,  $\text{Sr}^{2+}$  and  $\text{Ba}^{2+}$  showed the same concentration pattern between June and July, with both metals temporally constant at Grays Creek sites and both metals showing increases over time at Parkers Creek.

Relative concentrations of  $\text{Ba}^{2+}$  and  $\text{Sr}^{2+}$  in Calvert County show that sites have consistent enrichment of either  $\text{Sr}^{2+}$  or  $\text{Ba}^{2+}$  across June and July, indicated in the plot of  $\log([\text{Ba}]/[\text{Sr}])$  (Fig 2.4). As in western MD, the dominance of a particular element varies throughout Calvert County. The dominant element also varies within a single stream, as is observed in Grays Creek and Thomas Creek, although Parkers Creek shows dominance of  $\text{Sr}^{2+}$  at both sampled sites. As  $\text{Sr}^{2+}$  concentrations in Parkers Creek were relatively high and above the range measured for most western MD sites, the Ba/Sr ratios are very low and the  $\log([\text{Ba}]/[\text{Sr}])$  values, between  $-0.8$  and  $-1.0$ , are the most negative of both western MD and Calvert County samples. All other Calvert County sites show  $\log([\text{Ba}]/[\text{Sr}])$  values between  $-0.2$  and  $+0.13$  (Fig. 2.4), within the range of values observed for western MD sites.

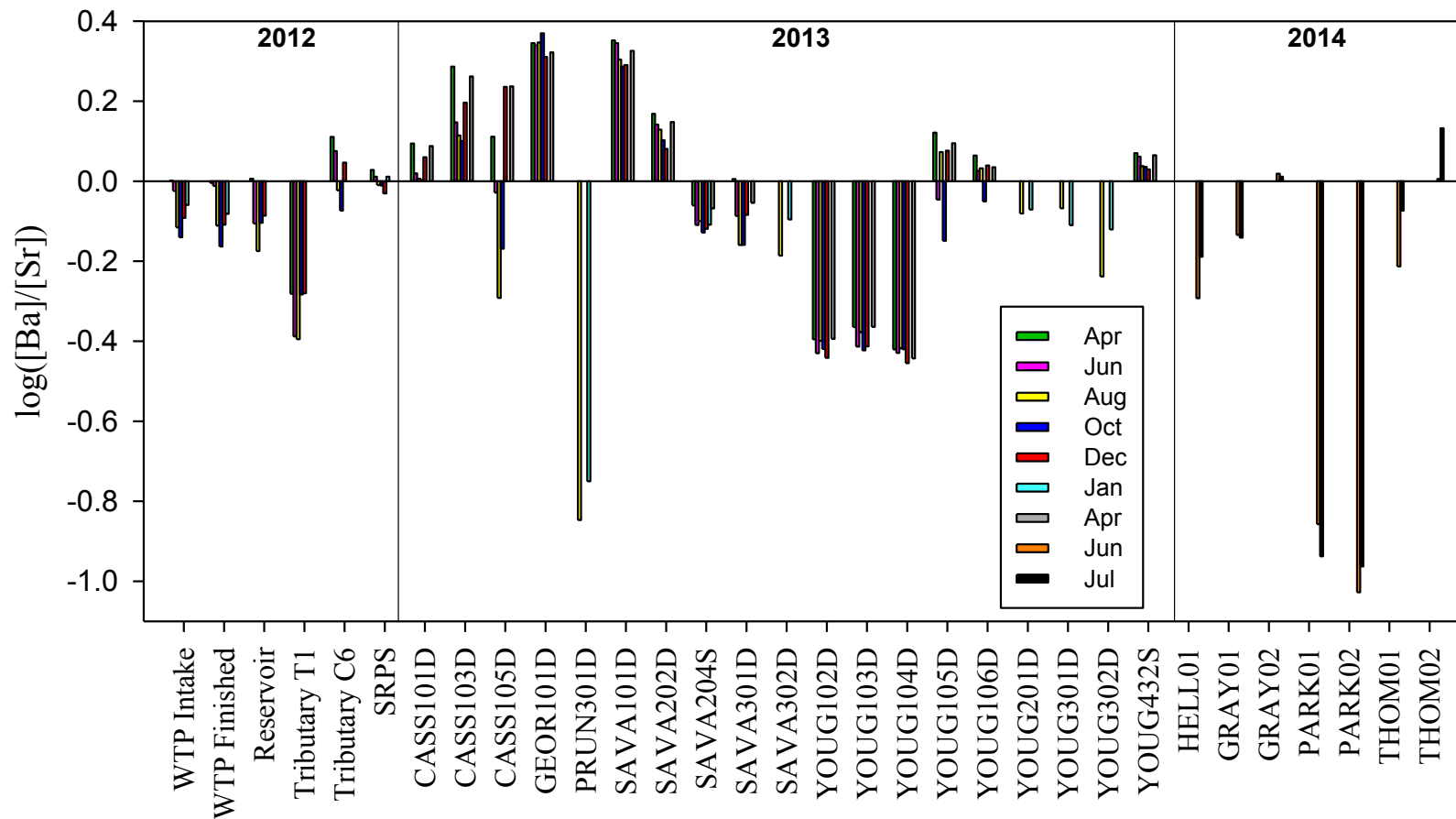


**Figure 2.4** Values of  $\log([Ba]/[Sr])$  at each sampling site, with Feb 2012–Feb 2013 sites shown in the left panel, Apr 2013–Apr 2014 sites shown in the center panel, and June–July 2014 Calvert County sites shown in the right panel. Bars plotting above 0 indicate  $Ba^{2+}$  is elevated in concentration relative to  $Sr^{2+}$  and those plotting below 0 indicate  $Sr^{2+}$  is elevated.

### 2.3.2 Major ion concentrations

Major ions are highly variable across western MD streams. Potassium concentrations show the lowest range among major cations, with concentrations found between 10–160  $\mu\text{M}$  (Table A1). Sodium ( $\text{Na}^+$ ) concentrations are highly variable and span a range of 10–2,600  $\mu\text{M}$  throughout space and time, with most values in the range of 10–1,100  $\mu\text{M}$ . Concentrations of  $\text{Ca}^{2+}$  and  $\text{Mg}^{2+}$  in western MD streams are primarily between 30  $\mu\text{M}$  and 800  $\mu\text{M}$ , although  $\text{Ca}^{2+}$  levels reach as high as 1,350  $\mu\text{M}$  in some sites and seasons. Sodium and  $\text{Ca}^{2+}$  are the dominant cations in all streams, with relative levels of each varying throughout western MD.

Anion concentrations are highly variable over space and time throughout western MD streams. Concentrations of  $\text{SO}_4^{2-}$  range between 10–1,600  $\mu\text{M}$ , although concentrations are most frequently between 10–400  $\mu\text{M}$  (Table A1). Levels of  $\text{Cl}^-$  show greater variability through space and time, with concentrations found between 10–3,200  $\mu\text{M}$ . Chloride concentrations are predominantly in the range of 10–1,300  $\mu\text{M}$  (Table A1).

Values of ANC measured for Oct 2013 samples ranged between 38.5  $\mu\text{eq/L}$  and 2,334  $\mu\text{eq/L}$  and are taken to be equivalent to concentrations of  $\text{HCO}_3^-$  ( $\mu\text{M}$ ) based on the pH values of stream waters, which range between 5.5 and 7.7 (Table A1). Also within this range are  $\text{HCO}_3^-$  concentrations estimated from the excess of cation charge in all samples not analyzed for  $\text{HCO}_3^-$  by ANC (Section 2.4.1). The positive charge excess was attributed to  $\text{HCO}_3^-$  anions, as samples which were analyzed for  $\text{HCO}_3^-$  show a balance of ionic charge within 10%, with the spread of 10% associated

with charge contributions of DOC and  $\text{NO}_3^-$  as well as variability within major cation and anion analyses (section 2.4.1).

Measurements of DOC taken in western MD streams in April 2014 ranged between 49.1–166  $\mu\text{M C}$ , an order of magnitude lower range than is found in  $\text{HCO}_3^-$  concentrations (Table A1). The range is lowest in the Youghiogheny River catchment, with concentrations spanning 49.1–76.6  $\mu\text{M C}$ , while within other catchments concentrations range between 50.0–166  $\mu\text{M C}$ .

Anionic charge contributed from DOC was determined for samples in which DOC was analyzed (Apr 2014) and used in calculations of ion balance. Anionic charge equivalents  $[A^-]$  (meq/L) of DOC were determined from the following equation:

$$[A^-] = \frac{\bar{K}[C_T]}{\bar{K} + [H^+]} \cdot 1000 \quad (2.5)$$

where  $\bar{K}$  is the pH-dependent mass action quotient determined from titration of humic and fulvic organic acids (Oliver et al., 1983), and  $C_T$  is the organic acid concentration (eq/L), which was determined by assigning a carboxyl concentration of 10  $\mu\text{eq/mg C}$  in DOC (Oliver et al., 1983). Measured values of pH from April 2013 were used in the calculation.

Concentrations of  $\text{NO}_3^-$  were measured in western MD samples from Feb 2012–May 2012. Ranging between 44–244  $\mu\text{M}$  (Table A1),  $\text{NO}_3^-$  concentrations are also an order of magnitude lower in range than those of  $\text{HCO}_3^-$ . Nitrate

concentrations were temporally variable at each site, with highest concentrations observed in February and March and lower concentrations in April and May.

Ancillary analysis of  $\text{Br}^-$  concentrations was carried out by ion chromatography at NASL. Six samples (WTP Intake, WTP Finished, Reservoir, SPRS, Trib. T1, and Trib. C6) were analyzed from collections in Feb 2012–June 2012. All samples showed  $\text{Br}^-$  concentrations below the detection limit of 1  $\mu\text{M}$ .

Major cation concentrations in Calvert County streams are similar to those in western MD. Levels of  $\text{K}^+$  are relatively low, as in western MD, and fall within the range of 10–100  $\mu\text{M}$  (Table A1). Sodium is the dominant cation at most sites, with concentrations ranging between 100  $\mu\text{M}$  and 2,000  $\mu\text{M}$  in concentration, although  $\text{Ca}^{2+}$  is the dominant cation at Parkers Creek sites. Concentrations of both  $\text{Mg}^{2+}$  and  $\text{Ca}^{2+}$  range from 20–800  $\mu\text{M}$  among sites in Calvert County.

Stream concentrations of  $\text{Cl}^-$  in Calvert County waters range from 100–2,600  $\mu\text{M}$ , within the range of western MD  $\text{Cl}^-$  concentrations (Table A1). Concentrations of  $\text{SO}_4^{2-}$  are between 30–140  $\mu\text{M}$ , falling at the lower end of the  $\text{SO}_4^{2-}$  concentration range found in western MD despite the proximity to Chesapeake Bay.

## 2.4 Discussion

### 2.4.1 Charge balance in western MD streams

Charge contributions of all measured cations and anions were determined in each stream sample. Sodium and  $\text{Ca}^{2+}$  are the greatest contributors to the cationic charge, with  $\text{Na}^+$  contributing up to 75% of positive charge and  $\text{Ca}^{2+}$  contributing up to 80%

among all samples. Magnesium contributes between 8–40% of positive charge, and  $K^+$  contributes less than 8% among all samples. Total equivalents of cationic charge, in meq/L, ranged between 0.2–4.4.

Relative to total equivalents of positive charge,  $Cl^-$  is the dominant anion in 43% of samples and contributes up to 85% of anionic charge. For low  $Cl^-$  samples in which it is not dominant,  $Cl^-$  may contribute as little as 2% of anionic charge. Sulfate is dominant in 18% of samples and contributes up to 95% of the balance of negative charge, although it also may contribute as little as 2% in samples for which it is not dominant. In all other waters where  $Cl^-$  and  $SO_4^{2-}$  are not dominant, it is expected that  $HCO_3^-$  is the dominant anion.

In samples not analyzed for  $HCO_3^-$ , an excess of cations is found for the charge balance. It is expected that the unaccounted for negative charge from this calculation is primarily attributable to  $HCO_3^-$ , as samples for which  $HCO_3^-$  was analyzed by ANC titration show relatively large contributions from this constituent. Samples analyzed for  $HCO_3^-$  show a balance of charge within 10% of 0 for most waters, which is likely attributable to charge contributions of DOC and  $NO_3^-$  and to variability from error in the major cation and anion analyses. Charge contributions of DOC are estimated to account for <5% of anionic charge in samples, and  $NO_3^-$  contributes <10% for most samples in which it was analyzed. Other analyses of headwater streams in several Appalachian highlands regions have similarly shown low contributions of  $NO_3^-$  and DOC relative to other ions (Mast, 1999).

The charge contributed from  $\text{HCO}_3^-$ , estimated from the excess of positive charge in samples, is found to be dominant in 38% of samples and contributes up to 90% of anionic charge, although, in samples for which it is not dominant it may contribute negligible charge (Table A1). Analyses of charge contributions in western MD stream waters indicate the dominant ions in this region, demonstrating the current pre-fracking conditions of western MD streams.

#### 2.4.2 Major ions as tracers of fracking fluids

All major ions were found to be 1–3 orders of magnitude greater in concentration than  $\text{Sr}^{2+}$  and  $\text{Ba}^{2+}$  in streams and were highly variable throughout space and time, with each measured ion ranging over 1–2 orders of magnitude in concentration, suggesting that individual major ion measurements may not be useful as tracers of fracking fluids.

To investigate possible patterns in variability, relative concentrations of major ions were evaluated. Sodium and  $\text{Ca}^{2+}$  were found to be the dominant cations in all western MD and Calvert County streams although the dominance of  $\text{Na}^+$  vs.  $\text{Ca}^{2+}$  varies spatially both within and among catchments. Other studies in Appalachian highland streams similarly show dominance of  $\text{Na}^+$  and  $\text{Ca}^{2+}$  with relative abundance of each varying within single catchments (Johnson et al., 2000; Timpano et al., 2015). The dominance of  $\text{Ca}^{2+}$  in certain streams is likely associated with areas of carbonate mineral bedrock (Roth, 1999). Stream water  $\text{Sr}^{2+}$  and  $\text{Ca}^{2+}$  showed correlation among all sampled streams (Fig. 2.5), a reasonable finding since  $\text{Sr}^{2+}$  substitutes for  $\text{Ca}^{2+}$  in

Ca-bearing minerals (Peek and Clementz, 2012). The strength of this correlation varied among western MD waters, though, likely related to varying mineral ratios of

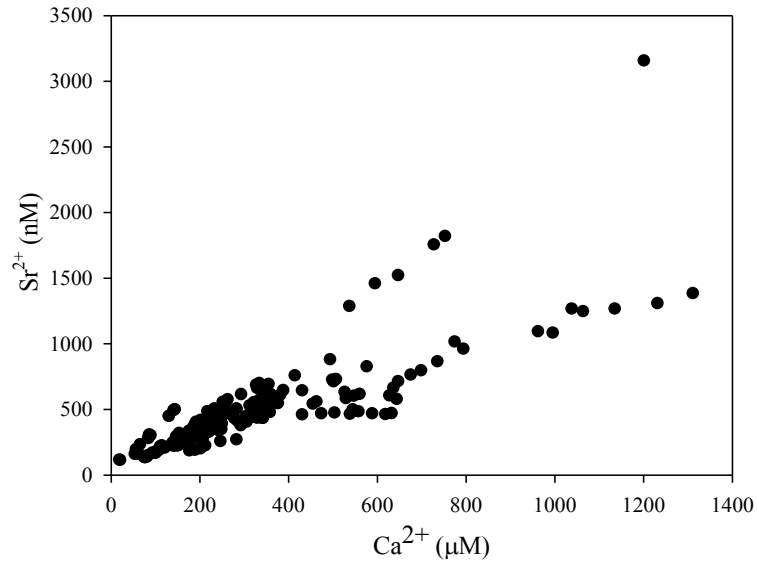


**Figure 2.5** Concentrations of Sr<sup>2+</sup> vs. Ca<sup>2+</sup> in all stream waters.

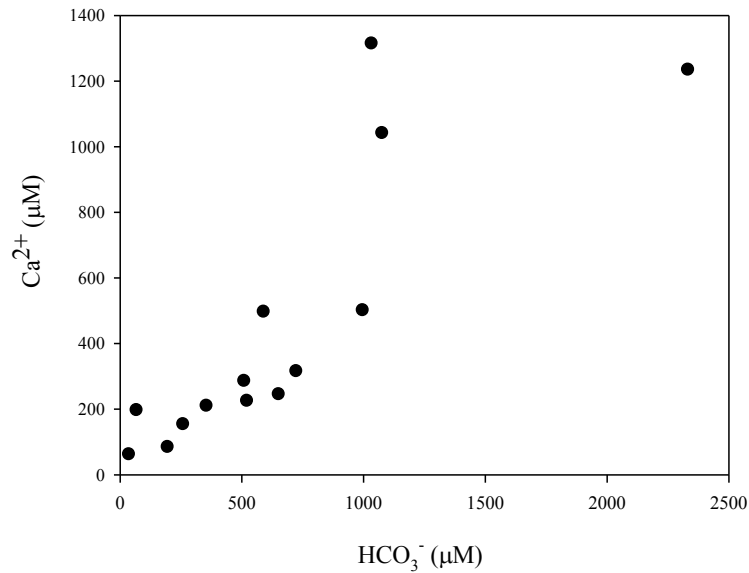


**Figure 2.6** Concentrations of Ca<sup>2+</sup> vs. HCO<sub>3</sub><sup>-</sup> in western MD stream samples collected Oct 2013.

Sr/Ca (Land et al., 2000) (Fig 2.5). Calcium concentrations were also correlated with  $\text{HCO}_3^-$  concentrations during Oct 2013 when  $\text{HCO}_3^-$  was measured (Fig. 2.6), supporting the theory that high- $\text{Ca}^{2+}$  sites are associated with locations of underlying carbonate rock. In Calvert County where carbonate bedrock is less prominent (Roth, 1999),  $\text{Ca}^{2+}$  is not found to be a dominant cation, although Parkers Creek sites, which show relatively high  $\text{Ca}^{2+}$  and  $\text{Sr}^{2+}$ , are an exception and may be influenced by localized carbonate minerals in proximity to Parkers Creek (Carnevale et al., 2011).

Variability in major cation composition was further evaluated by plotting stream waters on a trilinear diagram of relative cation concentrations which shows distinctions of stream waters in western MD and Calvert County (Fig. 2.7). Major cation composition may be dictated in part by catchment area in which the stream is found, as some stream samples in the diagram plot in groups according to catchment, which is indicated by color. Some stream waters within the same catchment, though, plot in separate areas of the diagram. For example, some waters in the Savage River catchment plot in an area indicating relatively high  $\text{Ca}^{2+}$  contribution (45%–60%) and fairly low  $\text{Na}^+ + \text{K}^+$  contribution (20%–25%), and other Savage River waters show a grouping of relatively high  $\text{Na}^+ + \text{K}^+$  (60%–70%) with fairly low contributions of  $\text{Ca}^{2+}$  (20%–30%). This suggests that another major factor affects stream water chemistry. It is suspected that variable bedrock geology of the region has a predominant influence on ion composition as groundwater is expected to be a major stream water source under base flow conditions (Ahearn et al., 2004). In the trilinear diagram, the point marked with a star represents average cation composition of shallow groundwater overlying the Marcellus Shale in southern New York (Fig. 2.7)

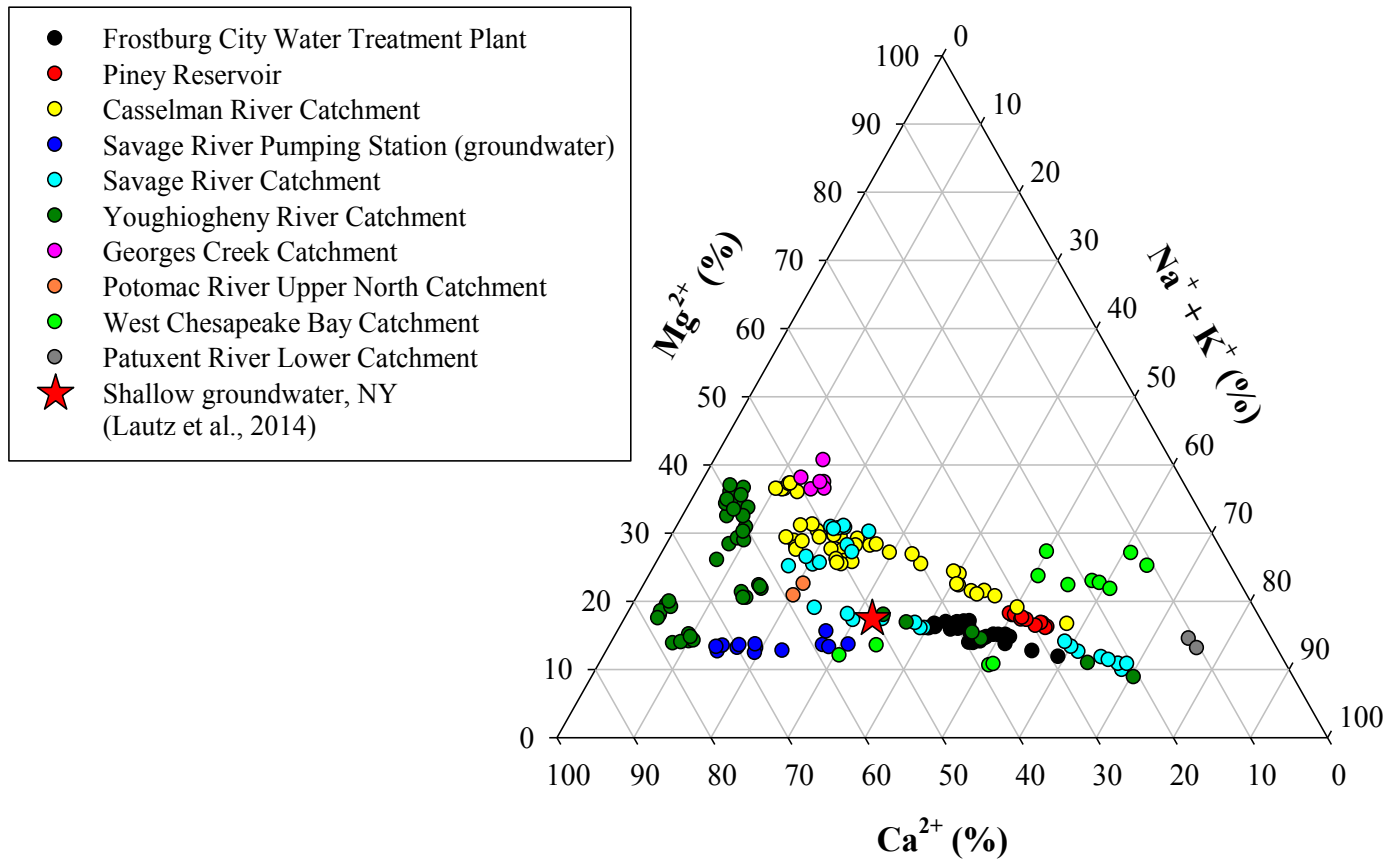


**Figure 2.7.** Trilinear diagram showing relative contributions (%) of  $Mg^{2+}$ ,  $Ca^{2+}$ , and  $Na^+ + K^+$  cations in western MD and Calvert County streams. Marker color represents catchment as in Fig. 2.1. Average cation composition of shallow groundwater in a region overlying the Marcellus Shale (New York state) is represented by the red star (Lautz et al., 2014).

(Lautz et al., 2014), with the shallow groundwater plotting among most stream water samples in the diagram. This demonstrates the similarity in composition of shallow groundwater and stream water, further suggesting that groundwater is an important contributor to western MD streams.

Bedrock geology is variable in western MD, as illustrated in the Geologic Map of Western Maryland (Brezinski, 2013) (Fig. 2.8), with the two map background colors representing different bedrock formations. In this region, bedrock geology was previously shown to be an important factor in stream chemistry responses to acidic deposition (Roth, 1999). In the current study, plotting of sites on the geologic map

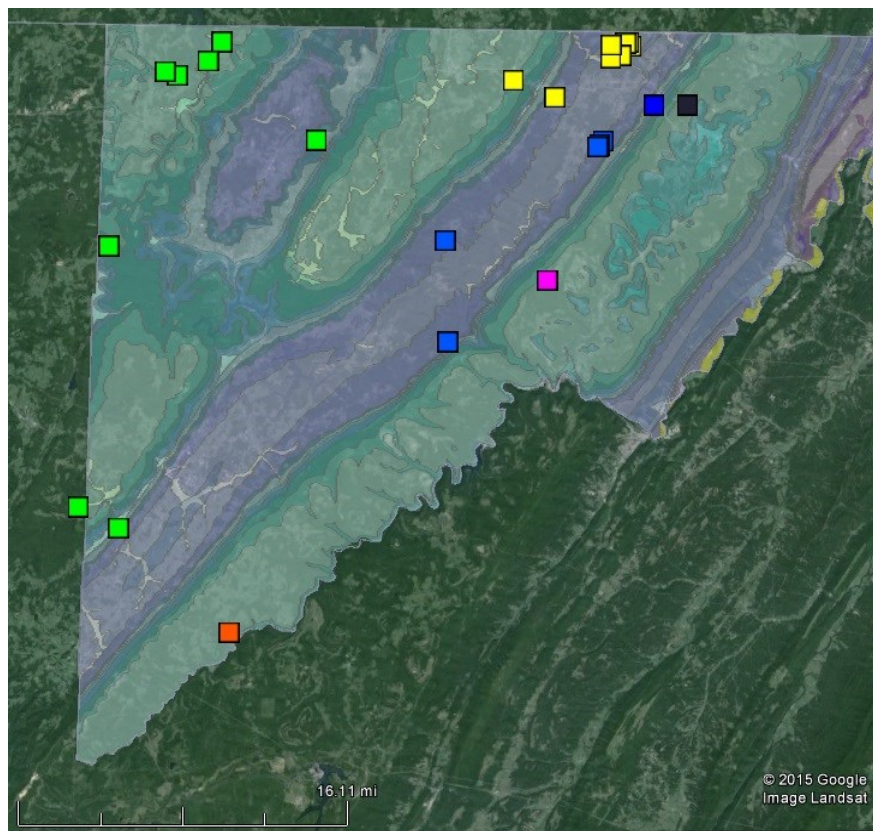


**Figure 2.8.** Geologic map of western MD by Brezinski et al. (2013). Map background shades represent the underlying bedrock type. Green shades represent Mississippian and younger formations, and purple shades represent Devonian and older formations. All western MD stream sites are marked, with marker color indicating catchment as in Fig. 2.1.

(Fig. 2.8) shows that underlying bedrock type varies within and among catchments, with marker color corresponding to catchment as in Fig. 2.1. To assess the influence of underlying bedrock on stream water chemistry, study sites were categorized according to underlying bedrock era and stream waters were plotted bilinearly with  $K^+$  vs.  $Mg^{2+}$  concentrations (Fig. 2.9). The bilinear plot of major cation composition shows separation of stream waters according to bedrock formation era, either Devonian, shown in purple points, or Pennsylvanian, shown in green points in Fig. 2.9. The differentiation of waters based on underlying bedrock demonstrates the influence of bedrock geology on overlying stream water composition.

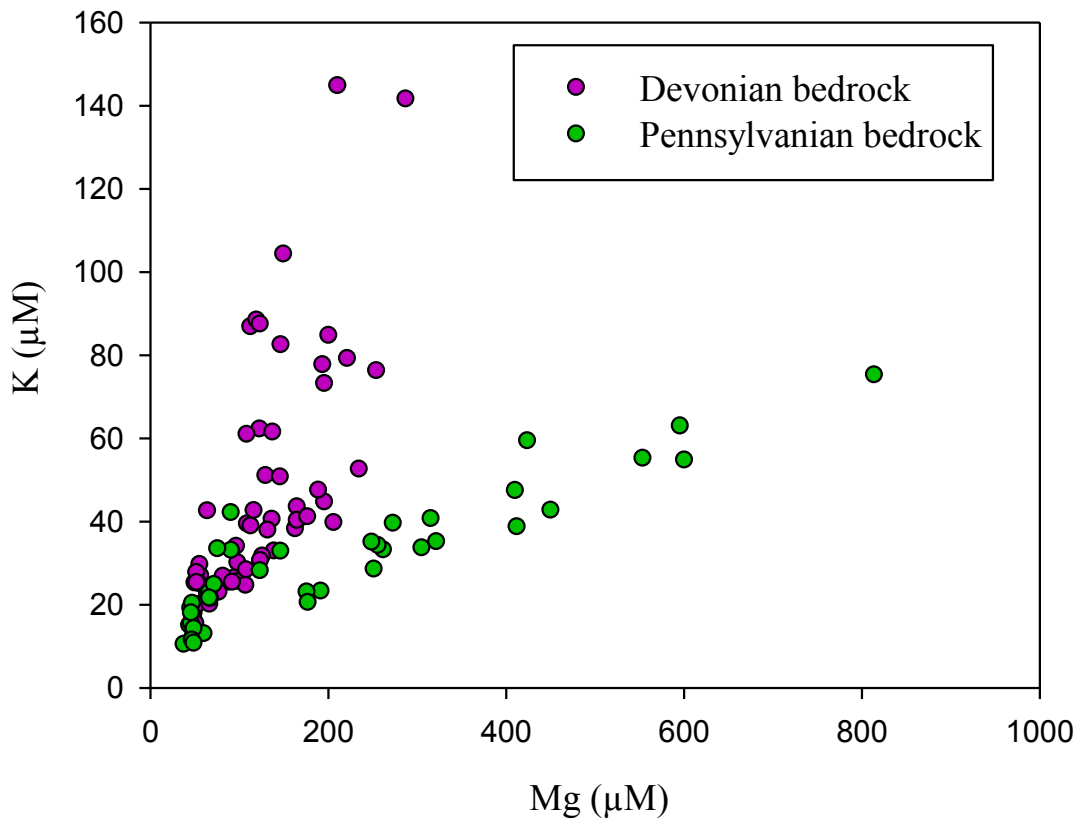


**Figure 2.9.** Bilinear plot of  $K^+$  vs.  $Mg^{2+}$  in western MD stream samples, with samples categorized by the underlying bedrock era, either Devonian or Pennsylvanian.

Although geology and its impact on groundwater affect stream water chemistry, runoff from road salt is a major factor as well. A plot of  $\text{Na}^+$  vs.  $\text{Cl}^-$ , the main constituents of road salt, shows that stream waters generally plot along a line of mixing with road salt effluent (Lautz et al., 2014) (Fig. 2.10). This is in agreement with speculation following other northern U.S. studies that consistent seasonal road salt application has increased groundwater stores of mobile  $\text{Na}^+$  and  $\text{Cl}^-$  which drive surface water levels of these ions (Thompson et al., 2011).

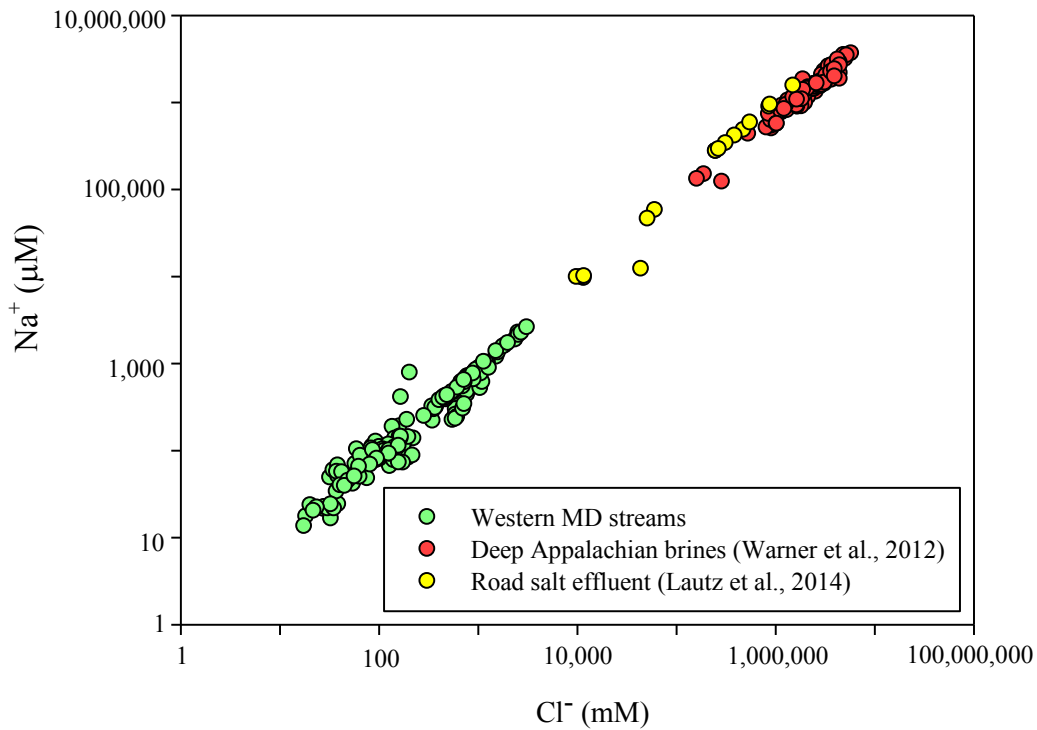


**Figure 2.10** Plot of  $\text{Na}^+$  vs.  $\text{Cl}^-$  concentrations in deep Appalachian brines which occur in fracking fluids (Warner et al., 2012), in road salt effluent (Lautz et al., 2014), and in western MD streams.

The plot in Fig. 2.10 also shows  $\text{Na}^+$  vs.  $\text{Cl}^-$  concentrations of deep Appalachian brines, a major influence in fracking fluids from the Marcellus Shale. As observed in the plot,  $\text{Na}^+/\text{Cl}^-$  ratios are similar for western MD streams, fracking fluids, and road

salt effluents. Ratios of  $\text{Na}^+/\text{Cl}^-$  will therefore not be useful as fracking fluid tracers. The plot also demonstrates that stream water variability of  $\text{Na}^+$  and  $\text{Cl}^-$  concentrations is about 3 orders of magnitude, indicating that the individual ions will not be suitable as fracking fluid tracers.

The bivariate plot of  $\text{Mg}^{2+}$  vs.  $\text{Cl}^-$  shows similarities in composition of western MD streams and fracking fluids containing Appalachian brines (Warner et al., 2012) (Fig. 2.11). The similarity means that  $\text{Mg}^{2+}/\text{Cl}^-$  ratios cannot be used to track fracking fluids in streams. Shallow groundwater overlying the Marcellus Shale in Pennsylvania is also plotted in Fig. 2.11 and shows close resemblance to headwater streams in MD, indicative of a groundwater origin of these streams (Lautz et al., 2014).

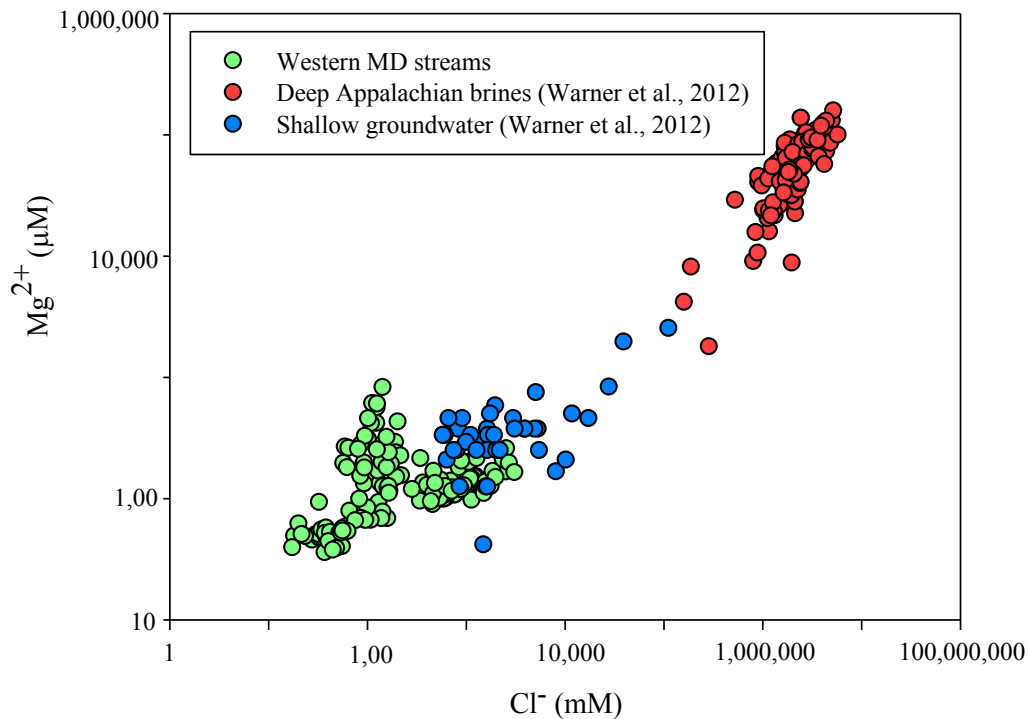


**Figure 2.11** Plot of  $\text{Mg}^{2+}$  vs.  $\text{Cl}^-$  concentrations in deep Appalachian brines which occur in fracking fluids, in shallow groundwater overlying the Marcellus Shale (Warner et al., 2012), and in western MD streams.

With the variability in major cation and anion concentrations across western MD streams, these constituents are not useful tracers of fracking fluids. Values of major ion ratios are also not desirable as tracers without other constraining constituents, although analysis of ion ratios indicates predominant stream water sources. In addition to the variability, the major ions are relatively abundant, particularly in comparison to trace metal tracers such as  $\text{Sr}^{2+}$  and  $\text{Ba}^{2+}$ . Relative to streams, fracking fluids are enriched in  $\text{Sr}^{2+}$  and  $\text{Ba}^{2+}$  by factors of 25,000–50,000, while fluids are enriched in the major ions by factors of 100–1,000 (Barbot et al., 2013; Warner et al., 2013a). Major ion levels in streams are likely to show lower shifts in cases of fracking fluid intrusion compared to other tracers.

Dissolved  $\text{Br}^-$ , which was measured irregularly for samples of the Feb 2012–Feb 2013 set, was found to be below detection limits in all analyzed stream samples. Although it could not be regularly measured in this study due to instrument limitations, the preliminary analyses show that  $\text{Br}^-$  may be the optimal fracking fluid tracer in western MD since it is enriched in fracking fluids and occurs at very low levels in streams of this region.

#### 2.4.3 $\text{Sr}^{2+}$ and $\text{Ba}^{2+}$ as tracers of fracking fluids

Strontium and  $\text{Ba}^{2+}$  concentrations in western MD streams, although variable over space and time, agree with concentrations measured for a range of other minimally disturbed catchments in North America. Stream waters were found to have ranges of 140–800 nM in  $\text{Sr}^{2+}$  and 10–250 nM in  $\text{Ba}^{2+}$  (Elias et al., 1982; Fitzpatrick et al., 2007; Watmough, 2014), with a greater range for  $\text{Sr}^{2+}$  as was found

in the current study. This observation is due to higher solubility of  $\text{Sr}^{2+}$  than  $\text{Ba}^{2+}$  in minerals as well as the greater abundance of  $\text{Sr}^{2+}$  in nature relative to  $\text{Ba}^{2+}$  (Nesbitt et al., 1980; Turekian and Wedepohl, 1961).

Stream concentrations of  $\text{Sr}^{2+}$  and  $\text{Ba}^{2+}$  in Calvert County are in the same ranges as concentrations found in western MD streams, although  $\text{Sr}^{2+}$  concentrations show a greater range in Calvert County with Parkers Creek sites showing high  $\text{Sr}^{2+}$  outside the concentration range of most western MD streams. This occurrence may be associated with marine carbonates which have outcrops along the mouth of Parkers Creek (Carnevale et al., 2011).

In western MD, a distinct temporal pattern in  $\text{Sr}^{2+}$  and  $\text{Ba}^{2+}$  levels is observed for sites Tributary T1, Tributary C6, and SAVA301D which have concentrations highest in late summer and fall and lowest concentrations in spring (Fig. 2.3). This indicates that these streams may be influenced by seasonal inputs of surface runoff. With groundwater supplying dissolved  $\text{Sr}^{2+}$  and  $\text{Ba}^{2+}$  year-round, metal concentrations are lowest in spring when surface runoff is high and highest in fall when runoff is minimal (Stranko et al., 2013). A number of other sites, including SAVA204S, YOUNG102D, and YOUNG104D, similarly show maximum concentrations in fall with large concentration decreases by spring, suggesting that  $\text{Sr}^{2+}$  and  $\text{Ba}^{2+}$  are primarily from groundwater and that streamflow is influenced by surface runoff in these streams. The temporal pattern may be less clear at these sites as there may be a portion of  $\text{Sr}^{2+}$  and  $\text{Ba}^{2+}$  supplied by surface runoff that has interacted with soil minerals (Hogan and Blum, 2003). Also, the sites with less distinct temporal patterns were sampled bimonthly (Apr 2013–Apr 2014), allowing lower resolution in

observed patterns, while the sites showing the most distinct temporal cycles are those sampled monthly (Feb 2012–Feb 2013). This suggests that monthly measurements of  $\text{Sr}^{2+}$  and  $\text{Ba}^{2+}$  may be optimal.

Many western MD streams show temporal variability in  $\text{Sr}^{2+}$  and  $\text{Ba}^{2+}$  but no distinct temporal pattern (Fig. 2.3, panels A and E). This may indicate that these streams receive relatively low amounts of flow from surface runoff and are predominantly fed by groundwater throughout the year. Other sites in the region show relatively low  $\text{Sr}^{2+}$  and  $\text{Ba}^{2+}$  concentrations as well as relatively low temporal variability in concentrations, such as CASS105D (Fig 2.4, panel F), SAVA101D, GEOR101D, YOUG105D, and YOUG106D. For these sites, streamflow may be substantially supplied by surface runoff which is less enriched in  $\text{Sr}^{2+}$  and  $\text{Ba}^{2+}$  relative to groundwater (Peek and Clementz, 2012). Alternatively, for sites of this type, low concentrations and low temporal variability may indicate a groundwater source which has short aquifer residence time and therefore lower  $\text{Sr}^{2+}$  and  $\text{Ba}^{2+}$  concentrations, yet still provides these species at constant levels to streams (Peek and Clementz, 2012).

Spatial variability of  $\text{Sr}^{2+}$  and  $\text{Ba}^{2+}$  concentrations is found both within and among catchments. Groundwater, the major contributor of  $\text{Sr}^{2+}$  and  $\text{Ba}^{2+}$  to surface waters (Peek and Clementz, 2012) is influenced by bedrock geology, a factor which is highly variable across space in western MD (Brezinski, 2013). Bedrock minerals found in western MD, including carbonates and weathered clay minerals, vary in abundance of  $\text{Sr}^{2+}$  and  $\text{Ba}^{2+}$  (Brezinski, 2013; Turekian and Wedepohl, 1961). In addition to variability in abundances of these trace metals, minerals vary in their

weathering rates, affecting the release of  $\text{Sr}^{2+}$  and  $\text{Ba}^{2+}$  to groundwater (Land et al., 2000).

Heterogeneity of mineral  $\text{Sr}^{2+}$  and  $\text{Ba}^{2+}$  sources to streams is reflected in the Ba/Sr ratios, assessed as  $\log([\text{Ba}]/[\text{Sr}])$  values here, which show greater variability over space than over time. Relatively stable Ba/Sr ratios across time are likely indicative of a temporally consistent geologic source of  $\text{Sr}^{2+}$  and  $\text{Ba}^{2+}$ . In sites where seasonal shifts in concentrations are observed despite a stable ratio, dilution from runoff is likely affecting these constituents.

The variability in  $\log([\text{Ba}]/[\text{Sr}])$  values across the region may demonstrate the spatial variability of mineral sources underlying stream beds (Fig. 2.4). The irregularity of weathering of Sr- and Ba-bearing minerals also affects  $\log([\text{Ba}]/[\text{Sr}])$  values across the region. Land et al (2000) found that, within a forested catchment, groundwater derived from deeper flowpaths showed lower Ba/Sr ratios compared to shallower groundwater and soil water. This was attributed to less intensive weathering environments at greater depths, where Sr is released at greater rates than is Ba, since Sr-containing minerals are overall more soluble.

In western MD streams, molar Ba/Sr ratios reported as  $\log([\text{Ba}]/[\text{Sr}])$  are in agreement with  $\log([\text{Ba}]/[\text{Sr}])$  ranges occurring in other first-order North American streams (Hogan and Blum, 2003; Land et al., 2000). Values obtained in these studies, though, show lower ranges of  $\log([\text{Ba}]/[\text{Sr}])$  than observed here, which may be indicative of the high spatial variability of bedrock underlying western MD streams.

Although stream dissolved  $\text{Sr}^{2+}$  and  $\text{Ba}^{2+}$  vary throughout western MD, stream concentrations, in the range of 100–1,400 nM for most sites, are very low in relation

to fracking fluids, which may allow observation of concentration spikes with spill events. Fracking fluid spill events are reported to be 2,900 L on average (Gross et al., 2013), as determined in a western U.S. shale region, although most documented spills in the Marcellus Shale region from 2009–2013 were larger (Brantley et al., 2014). Considering a 2,900 L spill from a well pad which drains to a nearby headwater stream over five hours, the discharge of fluids to the stream would comprise approximately 0.2% of streamflow, based on average discharge of 66 L/s, as determined on average from long term (2000–2014) monitoring stream sites in western MD (Saville et al., 2014). With this 0.2% contribution of fracking fluid at the site of discharge to the stream, the  $\text{Sr}^{2+}$  and  $\text{Ba}^{2+}$  levels in the stream may reach 38,690 nM and 32,400 nM, respectively, based on reported  $\text{Sr}^{2+}$  and  $\text{Ba}^{2+}$  levels in fluids (Barbot et al., 2013). As monitored stream sites are positioned just downstream of proposed well pad locations, these high concentrations which are 1–2 orders of magnitude greater than background concentrations would likely be observable above normal variability. Still, if stream sampling is not carried out within 1–2 days of a spill event, signals of  $\text{Sr}^{2+}$  and  $\text{Ba}^{2+}$  may be dampened and would be within normal concentration variability. It may therefore be best to use a continuous online monitoring tool for preliminary detection of potential fracking fluid contamination. Stream specific conductance, as noted, may be monitored this way using *in situ* sensors, where the specific conductance, a measure of stream water dissolved ions, would show significant spikes immediately following fracking fluid contamination (Brantley et al., 2014). Upon observance of spikes in conductivity, measurements of  $\text{Sr}^{2+}$  and  $\text{Ba}^{2+}$  concentrations could then be taken for verification that contamination is

from fracking fluids and not from other anthropogenic effluents which would be relatively low in  $\text{Sr}^{2+}$  and  $\text{Ba}^{2+}$  (Vidic et al., 2013). Measurements of  $\text{Sr}^{2+}$  and  $\text{Ba}^{2+}$  would show elevated concentrations following spill events and would confirm the presence of fracking fluids.

#### 2.4.4 Sr and Ba solubility and its effect on tracer use

The saturation states of  $\text{BaSO}_4$  and  $\text{SrSO}_4$  were calculated for western MD and Calvert stream waters in order to determine whether oversaturation affects  $\text{Ba}^{2+}$  and  $\text{Sr}^{2+}$  levels. The solubility product ( $K_{sp}$ ) values were determined from literature values for 25°C and 0 ionic strength conditions, where  $K_{sp} = 1.102 \times 10^{-10}$  for  $\text{BaSO}_4$  (Templeton, 1960) and  $K_{sp} = 2.344 \times 10^{-7}$  for  $\text{SrSO}_4$  (Prieto et al., 1997). Ionic strength was determined according to the equation

$$I = \frac{1}{2} \sum_i c_i z_i^2 \quad (2.6)$$

where  $c_i$  is the concentration of the  $i^{\text{th}}$  ionic species and  $z_i$  is the charge of the species. Ionic strength was found to be below 0.007 for stream waters and was approximated to be zero. The ion concentration product (ICP) was determined with respect to  $\text{BaSO}_4$  and  $\text{SrSO}_4$  in each stream sample and was compared to  $K_{sp}$  to determine saturation state  $\Omega$  according to the equation

$$\Omega = \frac{\text{ICP}}{K_{sp}} \quad (2.7)$$

The ICP values for  $\text{BaSO}_4$  and  $\text{SrSO}_4$  were calculated according to the equations

$$\text{ICP}_{\text{BaSO}_4} = [\text{Ba}^{2+}]_f [\text{SO}_4^{2-}]_f \quad (2.8)$$

$$ICP_{SrSO_4} = [Sr^{2+}]_f [SO_4^{2-}]_f \quad (2.9)$$

where total measured molar concentrations of  $Ba^{2+}$ ,  $Sr^{2+}$ , and  $SO_4^{2-}$  were taken to be equal to the free concentrations  $[Ba^{2+}]_f$ ,  $[Sr^{2+}]_f$ , and  $[SO_4^{2-}]_f$ , respectively, or  $[Ba^{2+}]_T \approx [Ba^{2+}]_f$ ,  $[Sr^{2+}]_T \approx [Sr^{2+}]_f$ , and  $[SO_4^{2-}]_T \approx [SO_4^{2-}]_f$ . This was a conservative approximation since free concentrations are slightly lower than total concentrations due to complexation of  $Ba^{2+}$  and  $Sr^{2+}$  with  $Cl^-$  and  $OH^-$ , and of  $Na^+$  with  $SO_4^{2-}$ .

Ratios of  $\frac{[Ba^{2+}]_f}{[Ba^{2+}]_T}$  and  $\frac{[Sr^{2+}]_f}{[Sr^{2+}]_T}$ , which account for this complexation, were

calculated from the following equations:

$$\frac{[Ba^{2+}]_f}{[Ba^{2+}]_T} = \frac{1}{\left(1 + [Cl^-] \beta_{BaCl} + \frac{\beta_{BaOH}^*}{[H^+]}\right)} \quad (2.10)$$

$$\frac{[Sr^{2+}]_f}{[Sr^{2+}]_T} = \frac{1}{\left(1 + [Cl^-] \beta_{SrCl} + \frac{\beta_{SrOH}^*}{[H^+]}\right)} \quad (2.11)$$

where  $\beta_{BaCl} = 0.363$ ,  $\beta_{BaOH}^* = 4.603 \times 10^{-14}$ ,  $\beta_{SrCl} = 0.603$ , and  $\beta_{SrOH}^* = 6.653 \times 10^{-14}$

(Martell, 2004). Values of stream pH collected for April 2013 were used for approximating pH values in each sample.

The ratios of  $\frac{[SO_4^{2-}]_f}{[SO_4^{2-}]_T}$  accounting for  $NaSO_4^-$  complexation were determined by:

$$\frac{[SO_4^{2-}]_f}{[SO_4^{2-}]_T} = \frac{1}{(1 + [Na^+] \beta_{NaSO_4})} \quad (2.12)$$

where  $\beta_{\text{NaSO}_4} = 5.495$  (Martell, 2004). Ratios of  $\frac{[\text{Sr}^{2+}]_f}{[\text{Sr}^{2+}]_T}$  were found to be between

0.998–1.000 for all samples. Ratios of  $\frac{[\text{Ba}^{2+}]_f}{[\text{Ba}^{2+}]_T}$  were between 0.999–1.000 for all

samples, and ratios of  $\frac{[\text{SO}_4^{2-}]_f}{[\text{SO}_4^{2-}]_T}$  were between 0.986–0.999 for all samples.

Using total concentrations  $[\text{Ba}^{2+}]_T$ ,  $[\text{Sr}^{2+}]_T$ , and  $[\text{SO}_4^{2-}]_T$ , to calculate ICP values, no samples were found to be oversaturated with respect to  $\text{SrSO}_4$ , whereas possible oversaturation with respect to  $\text{BaSO}_4$  ( $\Omega \geq 0.9$ ) was found to occur for 15 samples. For the 15 samples which showed oversaturation of  $\text{BaSO}_4$ , true  $[\text{Ba}^{2+}]_f$  and  $[\text{SO}_4^{2-}]_f$  concentrations were calculated from Equations (2.10) and (2.12) to verify the oversaturation state when accounting for  $\text{BaCl}^+$ ,  $\text{BaOH}^+$ , and  $\text{NaSO}_4^-$  ion pairs. Calculation of ICP using free concentrations confirmed that oversaturation occurred for each of the 15 stream samples, with saturation states of  $\sim 1.1$ – $7.5$  as shown in Table 2.2.

All occurrences of oversaturation were found at four sites located in the Youghiogheny River and Potomac River Upper North Branch catchments. In these stream reaches,  $\text{SO}_4^{2-}$  concentrations are high relative to all other sites (Table A1), which largely affects the degree of saturation. Each of these sites also shows relatively high  $\text{Sr}^{2+}$  and  $\text{Ca}^{2+}$  levels. Waters from three of the four sites (YOUG102D, YOUG103D, and PRUN301D) are elevated in  $\text{SO}_4^{2-}$  relative to  $\text{HCO}_3^-$ , indicating that underlying anhydrite minerals ( $\text{CaSO}_4$ ) may influence these areas. Relatively

high  $\text{HCO}_3^-$  as well as  $\text{Ca}^{2+}$  at site YOUG104D suggests that carbonate bedrock underlies this stream area. At all four sites,  $\text{Ba}^{2+}$  concentrations are relatively high, although oversaturation is not solely dependent upon  $\text{Ba}^{2+}$  concentration since other sites with similar  $\text{Ba}^{2+}$  levels, such as CASS101D and SAVA301D, are not oversaturated. All stream samples which show oversaturation were also found to be those with greatest enrichment of  $\text{Sr}^{2+}$  relative to  $\text{Ba}^{2+}$  with  $\log([\text{Ba}]/[\text{Sr}])$  values between  $-0.85$  and  $-0.36$  (Fig. 2.4). No sites in Calvert County were found to be oversaturated, likely related to the relatively low  $\text{SO}_4^{2-}$  concentrations in this region.

**Table 2.2** Saturation state ( $\Omega$ ) of western MD samples found to be oversaturated in  $\text{BaSO}_4$ , with calculated free  $\text{Ba}^{2+}$  concentration (nM), free  $\text{SO}_4^{2-}$  concentration ( $\mu\text{M}$ ), and Ion Concentration Product (ICP) of each sample.

Sample	$[\text{Ba}]_f$ (nM)	$[\text{SO}_4^{2-}]_f$ ( $\mu\text{M}$ )	ICP	$\Omega$
YOUG102D Apr 2013	285	757	$2.16 \times 10^{-10}$	1.96
YOUG102D Jun 2013	404	1011	$4.09 \times 10^{-10}$	3.71
YOUG102D Aug 2013	430	1174	$5.04 \times 10^{-10}$	4.58
YOUG102D Oct 2013	525	1575	$8.27 \times 10^{-10}$	7.50
YOUG102D Dec 2013	216	530	$1.15 \times 10^{-10}$	1.04
YOUG102D Apr 2014	234	549	$1.28 \times 10^{-10}$	1.17
YOUG103D Apr 2013	270	535	$1.45 \times 10^{-10}$	1.31
YOUG103D Jun 2013	390	667	$2.60 \times 10^{-10}$	2.36
YOUG103D Aug 2013	400	832	$3.33 \times 10^{-10}$	3.02
YOUG103D Oct 2013	476	1072	$5.11 \times 10^{-10}$	4.64
YOUG104D Jun 2013	469	311	$1.46 \times 10^{-10}$	1.33
YOUG104D Aug 2013	474	302	$1.43 \times 10^{-10}$	1.30
YOUG104D Oct 2013	495	336	$1.66 \times 10^{-10}$	1.51
PRUN301D Aug 2013	448	1541	$6.90 \times 10^{-10}$	6.27
PRUN301D Jan 2014	258	650	$1.68 \times 10^{-10}$	1.52

Although fracking fluids do not have a distinct  $\log([\text{Ba}]/[\text{Sr}])$  signature (Fig. 2.12), findings in this study suggest that  $\log([\text{Ba}]/[\text{Sr}])$  values may be suitable tracers

of fracking fluids in western MD due to the tendency for BaSO<sub>4</sub> oversaturation, which is expected to occur in streams with the intrusion of fracking fluids. The oversaturation with respect to BaSO<sub>4</sub>, which was found to occur in western MD streams, is expected to allow increased Sr<sup>2+</sup> concentrations with fracking fluid stream contamination. With BaSO<sub>4</sub> oversaturation, Ba<sup>2+</sup> concentrations would remain relatively constant in such contamination events. A significant decrease in log([Ba]/[Sr]) would then be observed in the affected stream, particularly as log([Ba]/[Sr]) values are relatively stable across time at most sites. The Sr<sup>2+</sup> and Ba<sup>2+</sup> stream concentrations described for a 0.2% fracking fluid introduction, 38,690 nM and 32,400 nM, respectively, will likely cause oversaturation of BaSO<sub>4</sub>, particularly

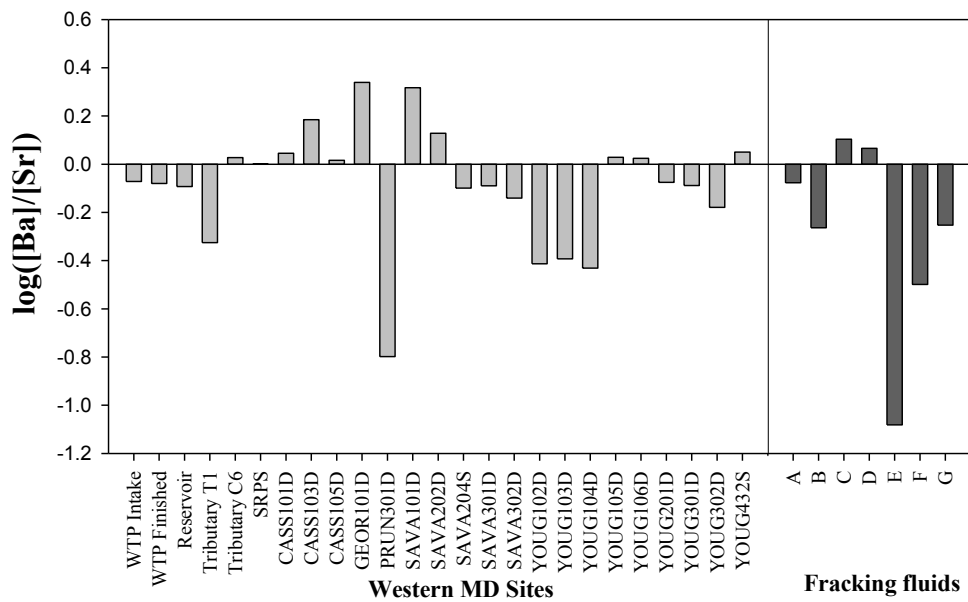


**Figure 2.12** Values of log([Ba]/[Sr]) found in western MD streams (light gray) and in fracking fluids (dark gray). Western MD values were determined from average molar Sr<sup>2+</sup> and Ba<sup>2+</sup> concentrations from each time of sampling. Fracking fluid values were determined from molar concentrations from fracking fluid analyses as reported by Barbot et al. (2013) (A), Hayes et al. (2009) (B), He et al., (2014) (C, D, and E), Warner et al. (2012) (F), and Warner et al. (2013b) (G).

with increased  $\text{SO}_4^{2-}$  supplied by fluids, with He et al (2014) having shown that  $\text{SO}_4^{2-}$  addition to fracking fluid samples results in rapid oversaturation with respect to  $\text{BaSO}_4$ . Fracking fluid contamination following a spill event could thus be further verified with evaluation of the stream water  $\log([\text{Ba}]/[\text{Sr}])$  value.

#### 2.4.5 Implications and Conclusions

Headwater streams in western MD show significant variability in  $\text{Sr}^{2+}$  and  $\text{Ba}^{2+}$  over space and time. Variability is expected to be primarily related to variability of underlying geology in the region since groundwater is a predominant source of  $\text{Sr}^{2+}$  and  $\text{Ba}^{2+}$  in streams. In headwater streams near well pads, dissolved  $\text{Sr}^{2+}$  and  $\text{Ba}^{2+}$  concentrations may be useful as tracers which verify stream intrusion of fracking fluids, with initial detection of contamination indicated by a continuous stream monitoring tool. Measured  $\log([\text{Ba}]/[\text{Sr}])$  values vary across space but show lower variability across time for each site. These values may be useful as fracking fluid tracers. Due to  $\text{BaSO}_4$  oversaturation which is expected to occur with introduction of fracking fluids to streams,  $\text{Sr}^{2+}$  is expected to increase to much greater levels than  $\text{Ba}^{2+}$ . The  $\log([\text{Ba}]/[\text{Sr}])$  in stream waters would then decrease from the baseline value with fracking fluid contamination.

Use of  $\text{Sr}^{2+}$ ,  $\text{Ba}^{2+}$ , and  $\log([\text{Ba}]/[\text{Sr}])$  values as tracers requires monitoring of concentrations of these metals before, during, and after fracking activity in order to observe departures from natural levels. In order to capture the naturally occurring temporal variability of  $\text{Sr}^{2+}$ ,  $\text{Ba}^{2+}$ , and  $\log([\text{Ba}]/[\text{Sr}])$ , it was determined that monthly baseline monitoring is suitable. Monthly concentration measurements are a sufficient

frequency for observation of patterns and variation in  $\text{Sr}^{2+}$  and  $\text{Ba}^{2+}$ , as observed in Fig. 2.4, Panels B, D, and E, while sampling bimonthly, as in Panels A, C, and F, shows lower resolution in concentration patterns. Monthly monitoring should then continue during and after fracking development, allowing for continued observation of trends and patterns in  $\text{Sr}^{2+}$ ,  $\text{Ba}^{2+}$ , and  $\log([\text{Ba}]/[\text{Sr}])$ . In addition, during fracking development, these tracers should be used for verification of the presence of fracking fluids in stream contamination events, with measurements immediately following such events, as elevated  $\text{Sr}^{2+}$  and  $\text{Ba}^{2+}$  and decreased  $\log([\text{Ba}]/[\text{Sr}])$  will be observed with fracking fluid intrusion. Contamination events can be initially detected using continuous monitoring tools such as the *in situ* specific conductivity sensor.

Similarly, with the indication that dissolved  $\text{Br}^-$  will be valuable as a fracking fluid tracer, regular monitoring of  $\text{Br}^-$  should be carried out on a monthly basis prior to fracking in order to capture temporal variability of this constituent. With the start of fracking activity in the region, monthly  $\text{Br}^-$  measurements should continue for observation of trends, and, in addition, this constituent may be used to verify presence of fracking fluids in cases where contamination is suspected based on continuous monitoring data.

For spatial considerations of  $\text{Sr}^{2+}$  and  $\text{Ba}^{2+}$ , these constituents should be monitored in streams immediately downstream of well pads. This was the basis for site choice in the current study, and, as new well pad locations are leased in MD or in other areas of fracking development, new stream monitoring sites should be established. Entekin et al (2011) found that Marcellus Shale gas wells are typically quite close to streams, with an average distance of 153 m to stream channels. It is

important to assess streams at these vulnerable locations which would likely be the first points to show water quality changes. For monitoring of  $\text{Sr}^{2+}$  and  $\text{Ba}^{2+}$ , in particular, stream sites should be immediately downstream of well pads since spill signals could be diluted further downstream and may appear to be within baseline variability. With the use of  $\text{Br}^-$  as a tracer, spatial distribution of monitoring would similarly include sites immediately downstream of well pads which may be most directly impacted by fracking activity.

Ions  $\text{Na}^+$ ,  $\text{K}^+$ ,  $\text{Mg}^{2+}$ ,  $\text{Ca}^{2+}$ ,  $\text{Cl}^-$ , and  $\text{SO}_4^{2-}$  all vary significantly across western MD streams, with bedrock geology and groundwater having considerable influence on variability. The high variability and relative abundance of major cations and anions demonstrate that periodic ion measurements are not applicable for detection of fracking fluids. Ion ratios allow assessment and comparison of stream waters, although major ion ratios also are not likely to be useful tracers due to their resemblance to fracking fluids. Monitoring of  $\text{Sr}^{2+}$ ,  $\text{Ba}^{2+}$ , and  $\log([\text{Ba}]/[\text{Sr}])$  values suggest that these constituents will be most beneficial for recognizing fracking fluid presence in western MD streams, and localized  $\text{Br}^-$  measurements in 2012 demonstrated this constituent should also be monitored as it will be an advantageous tracer of fracking fluids.

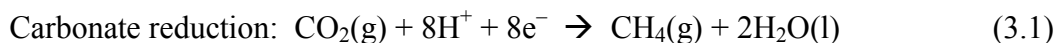
## Chapter 3: Monitoring of dissolved methane in western Maryland streams

### 3.1 Introduction

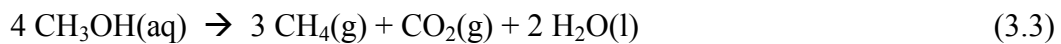
Methane (CH<sub>4</sub>) is found naturally in freshwater due to both groundwater inputs and *in situ* biological productivity, yet it may also be transferred to freshwater as a result of CH<sub>4</sub> migration linked to hydraulic fracturing (*fracking*) operations. Little is known of the natural spatial and temporal variability of CH<sub>4</sub> in streams which may be impacted by fracking (Brantley et al., 2014). To address this knowledge gap, naturally occurring dissolved CH<sub>4</sub> was monitored across spatial and temporal ranges in western Maryland (MD) streams. This may enable future identification of CH<sub>4</sub> contamination associated with fracking.

#### 3.1.1 Sources of methane in natural waters

Dissolved CH<sub>4</sub> is found naturally in most aquatic systems, including ocean waters, estuaries, groundwater, streams, lakes, and swamps (Whiticar and Faber, 1986). In many of these systems, CH<sub>4</sub> derives from biogenic production, referred to as *methanogenesis* (Schoell, 1988). In methanogenesis, microbes primarily produce CH<sub>4</sub> under anoxic conditions through one of the following reactions:



where CO<sub>2</sub> is carbon dioxide, H<sup>+</sup> represents protons, e<sup>-</sup> represents electrons, H<sub>2</sub>O is water, and CH<sub>3</sub>COOH is acetate, with CO<sub>2</sub> and CH<sub>3</sub>COOH representing competitive substrates as they are more effectively used by other microbial assemblages (Whiticar, 1999). In some cases CH<sub>4</sub> is also produced from non-competitive substrates such as methanol (CH<sub>3</sub>OH) and methylated amines (Whiticar, 1999). A methanogenic reaction utilizing CH<sub>3</sub>OH substrates is represented by the following (Liu and Whitman, 2008):



Methane is also produced thermogenically in deep subsurface environments (Schoell, 1988). Thermogenic CH<sub>4</sub> is primarily generated in sedimentary basins due to the breakdown of hydrocarbons upon their exposure to high temperatures and pressures (Schoell, 1988). It has been shown to migrate upward from deep reservoirs, with major pathways along faults and fractures as well as lateral displacement and movement through permeable rock (Etiope and Klusman, 2002). Through these pathways, thermogenic CH<sub>4</sub> may eventually intrude groundwater, surface water, and soils (Van Stempvoort et al., 2005).

### 3.1.2 Methane in groundwater

Dissolved CH<sub>4</sub> in groundwater originates from upward migration of thermogenic CH<sub>4</sub> sources as well as from *in situ* biogenic production (Taylor et al., 2000; Vengosh et al., 2014). Concentrations in groundwater are found to be highly variable within and among regions of North America (Brantley et al., 2014). Across the Appalachian Basin of the eastern U.S., which contains the Marcellus Shale, groundwater dissolved

CH<sub>4</sub> concentrations range from 0–4.42 mM (0–71 mg/L), depending on location (Vidic et al., 2013). Similar variability is reported for groundwater in other regions of North America (Aravena and Wassenaar, 1993; Zhang et al., 1998). Dissolved CH<sub>4</sub> in groundwater raises environmental and public health concerns since groundwater is widely used for household and agricultural needs across the U.S. (Vidic et al., 2013). Occurrence of CH<sub>4</sub> at concentrations above 0.623 mM (10 mg/L) in domestic and drinking water sources is an asphyxiation and explosion hazard (Revesz et al., 2010). More than 40 million U.S. citizens obtain drinking water from private wells fed by shallow groundwater (Vidic et al., 2013), and in Garrett County, MD, the area of interest for this thesis and an area of potential fracking development, 90% of citizens use private well water (Eshleman, 2013). Given the water quality risks associated with CH<sub>4</sub>, the U.S. Department of the Interior advises caution and an investigation if well water reaches dissolved CH<sub>4</sub> concentrations of 0.623 mM (10 mg/L), and immediate action is necessary if concentrations reach 1.76 mM (28 mg/L) (Vidic et al., 2013).

Variability of groundwater CH<sub>4</sub> may be due to the irregularity of underlying geology. For example, cross-formational fractures and faults, which are prevalent in some areas (Sharma et al., 2014), facilitate upward flow of CH<sub>4</sub> to aquifers driven by the buoyancy of gas-phase CH<sub>4</sub> (Etiope and Klusman, 2002; Sharma et al., 2014). In several regions of North America, including the Michigan Basin (Long et al., 1988; Weaver et al., 1995), Appalachian Basin (Schedl et al., 1992), and the Williston Basin in Manitoba, Canada (Grasby and Betcher, 2002), evidence of cross-formational

migration of fluids has been found, and it is theorized that such cross-formational networks also facilitate upward migration of CH<sub>4</sub> (Llewellyn, 2014).

Cross-formational fluid migration has been shown to connect the Marcellus Shale, a Devonian formation of 1,200–2,600 m depths, to shallow groundwater (Warner et al., 2012). It is indicated that this hydraulic connectivity may promote upward CH<sub>4</sub> migration, particularly in the presence of fracking activity (Warner et al., 2012). Some have contested this, however, theorizing that, with low permeability of the Marcellus Shale and overlying formations, the upward migration of shale CH<sub>4</sub> is only possible over geologic time scales and is not of concern with regard to fracking development (Flewelling and Sharma, 2014; Flewelling et al., 2013).

### 3.1.3 Methane in surface waters

In freshwater rivers and streams, CH<sub>4</sub> is derived from *in situ* microbial production, transport from methanogenesis in riparian areas, and transport from groundwater through bedrock flow paths (Jones and Mulholland, 1998b). In a forested Appalachian stream, Jones and Mulholland (1998b) found inputs from riparian zones to be the predominant CH<sub>4</sub> source; however, relative inputs of the stream CH<sub>4</sub> sources vary within and among streams due to irregularity of factors such as hydrologic flow paths, organic matter storage in the catchment, and the availability of oxygen in riparian zones (Jones and Mulholland, 1998b). Consequently, in stream networks where CH<sub>4</sub> has been measured, concentrations vary over space and time. Jones et al (1998a) showed that in summer, CH<sub>4</sub> concentrations were positively related to soil organic matter storage for streams in southern Appalachian catchments.

In hemiboreal streams, Wallin et al. (2014) attributed measurements of high CH<sub>4</sub> to locations of riparian peat or standing waters at low flow where CH<sub>4</sub> production is prolific.

Methane in terrestrial surface waters has particularly important implications with regard to CH<sub>4</sub> emissions to the atmosphere (Etiope and Klusman, 2002; Jones and Mulholland, 1998b). It has been suggested that CH<sub>4</sub> emissions from surface waters may offset as much as 25% of the estimated terrestrial greenhouse gas sink (Bastviken et al., 2011), based on a compilation of CH<sub>4</sub> concentration measurements in freshwater systems. Although river systems were included in this estimate, they were represented by fewer data sets than were lakes and reservoirs, and in general, data on CH<sub>4</sub> concentrations and evasion from streams are less prevalent. Recent studies also show that the areal extent of headwater streams has been underestimated by previous inventories, and stream CH<sub>4</sub> emission estimates based on existing data may be too low (Benstead and Leigh, 2012; Downing et al., 2012). Estimates of CH<sub>4</sub> emissions from streams are therefore not widespread or comprehensive (Wallin et al., 2014). To better inform terrestrial CH<sub>4</sub> emission estimates, it is important to understand natural CH<sub>4</sub> occurrence and variability in stream systems. Toward this objective, monitoring of CH<sub>4</sub> concentrations in MD streams is carried out in the current study, and measurements of stable carbon isotope composition are also made to elucidate sources of CH<sub>4</sub>.

### 3.1.4 The isotopic composition of carbon in dissolved CH<sub>4</sub>

For determining the origin of CH<sub>4</sub> in various aquatic and geologic environments, analysis of carbon isotopic composition is useful because the carbon isotope ratio of CH<sub>4</sub> varies depending on whether it is formed biogenically or thermogenically (Schoell, 1980). The carbon isotopic composition of a substance is expressed relative to that of a standard reference material using delta notation ( $\delta^{13}\text{C}$ ), which is defined as:

$$\delta^{13}\text{C} = \left[ \left( R_{\text{Sample}} / R_{\text{Standard}} \right) - 1 \right] \times 1000 \quad (3.4)$$

where R represents the  $^{13}\text{C}/^{12}\text{C}$  abundance ratio of the sample or standard reference material, and  $\delta^{13}\text{C}$  values are reported in units of per mil (‰) (Fry, 2006). Pee Dee Belemnite (PDB) is a carbonate which has a relatively high  $^{13}\text{C}/^{12}\text{C}$  ratio and is used as the international standard reference material with  $\delta^{13}\text{C} = 0$ , per definition (Eq. 3.4). Natural samples with a lower abundance of  $^{13}\text{C}$  compared to PDB have negative  $\delta^{13}\text{C}$  values, with increasing  $^{13}\text{C}$  depletion corresponding to increasingly negative  $\delta^{13}\text{C}$  values and *vice versa* (Craig, 1957). When referring to CH<sub>4</sub>, the C isotopic composition is denoted by  $\delta^{13}\text{C}\text{-CH}_4$ .

Considering biogenic CH<sub>4</sub> production, precursor C used in the process (i.e. organic matter) initially has  $\delta^{13}\text{C}$  values between  $-32\text{‰}$  and  $-22\text{‰}$  (Whiticar, 1996). In the methanogenic process, microbes preferentially utilize precursor compounds containing  $^{12}\text{C}$  to produce  $^{12}\text{CH}_4$  (Whiticar, 1996). This fractionation process results in CH<sub>4</sub> that is characteristically depleted with respect to the heavy isotope and has  $\delta^{13}\text{C}\text{-CH}_4$  values  $< -50\text{‰}$  (Hornibrook et al., 2000a; Whiticar, 1996). Contrary to this isotopically depleted CH<sub>4</sub>, there is little fractionation that occurs when CH<sub>4</sub> is

formed from thermogenic processes, and thermogenic CH<sub>4</sub> is therefore less depleted in <sup>13</sup>C than biogenic CH<sub>4</sub> (Schoell, 1980). Thermogenic CH<sub>4</sub>, including that produced in the Marcellus Shale, is characterized by values of δ<sup>13</sup>C-CH<sub>4</sub> > -50‰ (Hakala, 2014; Schoell, 1980). Values of δ<sup>13</sup>C-CH<sub>4</sub> between -64‰ and -50‰ may represent a mixture of thermogenic and biogenic CH<sub>4</sub> (Schoell, 1980).

### 3.1.5 Methane behavior in relation to fracking

Methane contamination has recently been explored in regions of fracking activity in view of the potential for CH<sub>4</sub> flow between deep formations, groundwater, and surface water. In regions of the Marcellus Shale, analysis of well water CH<sub>4</sub> has been carried out in areas near active fracking wells (within 1 km) and in areas outside of the fracking areas (Jackson et al., 2013a; Osborn et al., 2011). The authors found that average well water CH<sub>4</sub> concentrations within active fracking areas were significantly higher than those away from fracking. It was also found that shallow groundwater near fracking wells with higher CH<sub>4</sub> concentrations showed higher values of δ<sup>13</sup>C-CH<sub>4</sub> than groundwater away from wells, suggesting a greater prevalence of thermogenic CH<sub>4</sub>. In contrast, a similar study in the Fayetteville Shale region found no difference between groundwater CH<sub>4</sub> concentrations within and outside of active fracking areas (Warner et al., 2013b).

Such studies comparing dissolved CH<sub>4</sub> of active and inactive fracking areas are contested, though, since CH<sub>4</sub> may be found in groundwater irrespective of fracking activity (Molofsky et al., 2013; Saba and Orzechowski, 2011). Baseline groundwater analyses of >1,700 wells in Pennsylvania (PA) regions where fracking has not

occurred found dissolved CH<sub>4</sub> in 78% of water wells (Molofsky et al., 2013). Moreover, in several non-fracking regions of PA and New York (NY), concentrations of CH<sub>4</sub> are relatively high, between 0.623–4.42 mM (10–71 mg/L) (Kappel and Nystrom, 2012; Moore and Buckwalter, 1996; Sloto, 2013), in the range of groundwater concentrations measured by Osborn et al. (2011). As pre-drilling groundwater CH<sub>4</sub> data was not available in the study areas investigated by Osborn et al. (2011) and Jackson et al. (2013a), it is difficult to affirm that CH<sub>4</sub> concentrations in these areas are elevated due to fracking.

To further investigate the relationship between fracking activity and CH<sub>4</sub> concentrations of natural waters, particularly since baseline concentration measurements were not available in studies to date, stable C isotope analysis has been used. In several analyses of groundwater wells throughout PA,  $\delta^{13}\text{C-CH}_4$  values ranged between -50‰ to -30‰, consistent with thermogenic CH<sub>4</sub> from either Upper Devonian or Middle Devonian (Marcellus) formations (Jackson et al., 2013a; Molofsky et al., 2013; Osborn et al., 2011). Although Upper Devonian CH<sub>4</sub> in groundwater has been linked to upward migration over geologic time in some regions (Vengosh et al., 2014), its migration may be associated with fracking in certain cases. It was found that some groundwater wells in PA located <1 km from fracking wells were elevated in dissolved CH<sub>4</sub> and showed Upper Devonian isotopic signatures. These water samples also showed proportions of C<sub>2</sub>H<sub>6</sub> and <sup>4</sup>He that are inconsistent with migration over geologic time (Darrah et al., 2014).

Alternative to migration of Upper Devonian CH<sub>4</sub>, some groundwater  $\delta^{13}\text{C-CH}_4$  measurements overlying the Marcellus Shale suggest the presence of deeper

Marcellus Shale CH<sub>4</sub>, showing values between -45‰ and -30‰ characteristic of this reservoir (Hakala, 2014; Sharma et al., 2014). In one subset of groundwater wells in PA within 1 km of fracking wells, gas analysis showed δ<sup>13</sup>C-CH<sub>4</sub> values within the range of -45‰ and -30‰ and also showed C<sub>2</sub>H<sub>6</sub> isotopic signatures characteristic of Marcellus Shale gas (Jackson et al., 2013a).

The diagram of a fracking well in Fig. 3.1 shows proposed CH<sub>4</sub> flowpaths linked to fracking that may allow thermogenic CH<sub>4</sub> to intrude groundwater and eventually surface waters. Arrow A in this figure indicates leakage through poorly joined casing near groundwater reservoirs, a pathway which has been suggested as an explanation for findings of characteristic Marcellus Shale CH<sub>4</sub> in groundwater, as in PA (Darrah et al., 2014). Arrow B indicates migration of Upper Devonian CH<sub>4</sub> facilitated by leaky well annuli, consistent with findings of Upper Devonian CH<sub>4</sub> in groundwater in proximity to fracking (Darrah et al., 2014; Vengosh et al., 2014). Well annuli, the spaces between well casing layers, are typically filled with cement, although seal failures or cement permeability can occur, allowing Upper Devonian CH<sub>4</sub> to be transported to shallow groundwater (Brantley et al., 2014; Darrah et al., 2014). Geochemical and isotopic evidence for CH<sub>4</sub> transport via annuli has been found in regions of conventional gas drilling in North America (Harrison, 1983; Rowe and Muehlenbachs, 1999). Another potential mode of CH<sub>4</sub> contamination is migration from the deep shale formation through newly initiated fractures, represented by Arrow D, although this mechanism is thought to be of low likelihood because of the thickness (1–2 km) of overlying formations (Osborn et al., 2011). Fracking may also

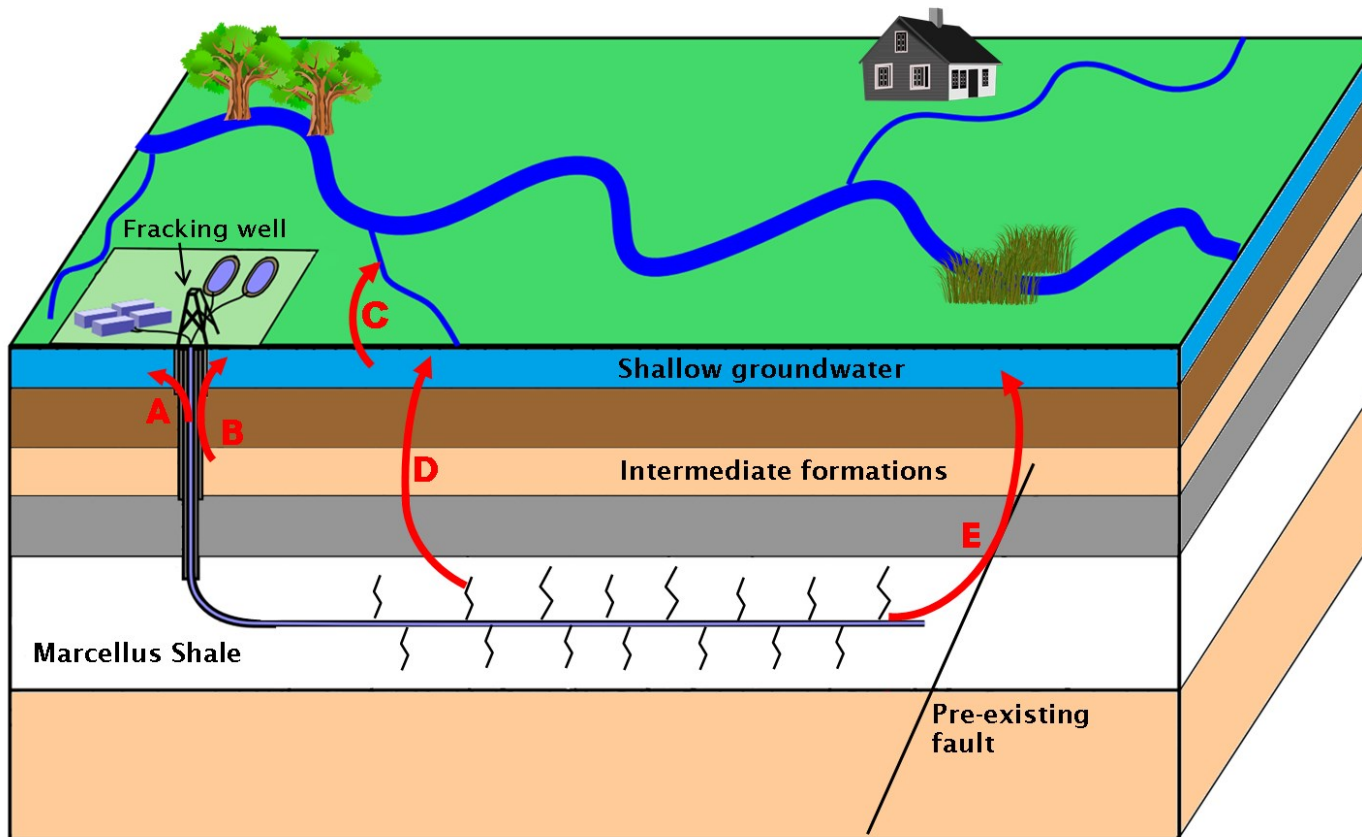


**Figure 3.1** Diagram showing a fracking well drilled into the Marcellus Shale, with red arrows indicating mechanisms for  $\text{CH}_4$  contamination of water. Arrow A represents leakage of Marcellus Shale  $\text{CH}_4$  through failed wellbore casing and B represents transport of intermediate formation  $\text{CH}_4$  through annuli. Arrow C represents transport of  $\text{CH}_4$  from shallow groundwater to streams. Arrow D represents a potential pathway of Marcellus Shale  $\text{CH}_4$  from depth and E represents  $\text{CH}_4$  migration from depth facilitated by pre-existing faults.

stimulate upward CH<sub>4</sub> migration along pre-existing fault systems which are prevalent in many regions of the Marcellus Shale (Osborn et al., 2011). This pathway is represented by Arrow E in Fig. 3.1. Arrow C in Fig. 3.1 represents flowpaths by which CH<sub>4</sub> is transported from groundwater to streams (Heilweil et al., 2013), such that each of the indicated pathways facilitating groundwater contamination may ultimately cause stream contamination. With the known flow of CH<sub>4</sub> between groundwater and surface waters, monitoring of stream CH<sub>4</sub>, as is carried out in this study, is important since shifts in stream concentrations may indicate groundwater as well as surface water contamination following fracking activity.

Notably, two major modes of CH<sub>4</sub> contamination associated with fracking—transport through annuli (Arrow B) and leakage through failed casings (Arrow A)—are caused by defective well structures. Such structural problems have been documented at a rate of 1–2% for fracking wells in PA (Considine et al., 2012), although an even greater rate of 3.4% was indicated from a survey by the PA Department of Environmental Protection (DEP) (Vidic et al., 2013). Construction rates of fracking wells are high in the Marcellus Shale region, with 60,000 wells projected to be built in the next 30 years (Entrekin et al., 2011), so the problem of substandard well construction offers many opportunities for CH<sub>4</sub> migration and contamination of natural waters.

### 3.1.6 Monitoring baseline dissolved CH<sub>4</sub> in western and southern MD streams

Given the connectivity of deep CH<sub>4</sub> reservoirs with groundwater and surface water as depicted in Fig. 3.1, as well as the documented structural challenges of wells,

there are many opportunities for CH<sub>4</sub> contamination associated with fracking. This contamination may be conflated, however, with *in situ* production of CH<sub>4</sub> in groundwater and streams. It is therefore necessary to determine the natural distribution of surface and groundwater CH<sub>4</sub> in areas surrounding fracking operations and to determine predominant CH<sub>4</sub> sources. In the current study, I pursue this by monitoring baseline stream CH<sub>4</sub> concentrations and C isotope compositions in rural catchments slated for fracking development.

The first goal of this work was to determine temporal and spatial variability of stream CH<sub>4</sub> concentrations overlying the Marcellus Shale. This allowed for establishment of baseline CH<sub>4</sub> concentrations in western MD. Determining variability in CH<sub>4</sub> concentrations also allowed for assessment of the viability of stream CH<sub>4</sub> as an indicator of fracking contamination. In assessing temporal and spatial variability of stream CH<sub>4</sub>, concentrations were also measured in MD's coastal plain region, allowing comparisons on a larger spatial scale.

It has been shown in some laboratory and field studies that methanogenic activity, which can occur in soils and sediments surrounding streams (Jones and Mulholland, 1998b), is elevated at higher temperature (Kelly and Chynoweth, 1981; Zeikus and Winfrey, 1976). I therefore hypothesized that, temporally, CH<sub>4</sub> concentrations would be greatest in summer and lowest in winter. Inherent in this projection is the hypothesis that CH<sub>4</sub> in western MD streams is primarily biogenic, which was reasoned based on previous works finding methanogenesis to be a predominant CH<sub>4</sub> source in freshwater systems (Jones et al., 1995; Jones and Mulholland, 1998a).

Previous research has also shown that methanogenesis occurring in anoxic riparian sediments and stream bottom sediments is a major source of stream CH<sub>4</sub> (Jones and Mulholland, 1998b), and this led to the hypothesis that stream CH<sub>4</sub> concentrations vary spatially based on the observed environmental setting of the stream. Forested stream sites were expected to be lowest in CH<sub>4</sub> since bottom sediments are typically coarse with little organic matter, and water flow at these sites is relatively fast. Sites near anthropogenic influences, such as roadways and agricultural or residential areas, were expected to be higher in CH<sub>4</sub> than forested sites since these streams likely receive higher amounts of allochthonous organic matter and nutrients which stimulate in-stream methanogenesis (Sanders et al., 2007). Sites in wetland-type settings were expected to be highest in CH<sub>4</sub> due to an abundance of organic matter which facilitates high productivity and anoxic conditions in sediments adjacent to and within the streams. Also, wetland sites have relatively slow streamflow allowing lower rates of CH<sub>4</sub> evasion and more widespread development of anoxia (Jones et al., 1995; Wallin et al., 2014). Although the stream sites in this study are spatially divided amongst five major catchments, it was expected that stream CH<sub>4</sub> concentrations are more closely tied to the immediate landscape surrounding the site rather than larger spatial divisions such as catchment, particularly as land use and landscapes are heterogeneous within catchment areas (Appler, 2010). Considering large-scale variability across physiographic regions of MD, it was hypothesized that dissolved CH<sub>4</sub> in coastal plain freshwater streams is primarily biogenic, as in western MD, although it was expected that concentrations in this region of MD are higher than those in western MD due to features of the coastal plain

streams. Streams in this region are characterized by finer sediments, with lower stream gradients which allow greater rates of sediment deposition (Paul, 2002; Roth, 1999); these characteristics then stimulate greater rates of methanogenesis relative to streams of western MD.

To assess temporal variability, with the hypothesis of increased CH<sub>4</sub> concentrations in summer and lower concentrations in winter, concentration measurements were taken across a period of 1 year in western MD, and stream samples were collected every 4–8 weeks. To evaluate spatial variability of dissolved CH<sub>4</sub>, concentrations were regularly monitored in 25 streams throughout western MD and the coastal plain region of Calvert County, with all streams characterized by either a forested, wetland, or anthropogenically influenced setting. Stream CH<sub>4</sub> concentrations measured in both western MD and Calvert County were compared with concentrations reported for other North American headwater streams which do not overlie shale formations.

The second major goal of this portion of the study was to verify the source of stream CH<sub>4</sub>, either biogenic or thermogenic, in both western MD and Calvert County, with the use of carbon isotopic analysis of CH<sub>4</sub>. Measurements of carbon isotopic composition of CH<sub>4</sub> may distinguish biogenic and thermogenic CH<sub>4</sub> in streams, and they may also demonstrate baseline  $\delta^{13}\text{C-CH}_4$  values in these settings. This is of particular importance in a region before the onset of fracking since fracking contamination may stimulate increased flow of thermogenic CH<sub>4</sub> to streams.

Stream CH<sub>4</sub> in both MD regions was hypothesized to be primarily biogenic based on previous studies of CH<sub>4</sub> in freshwater systems (Jones et al., 1995; Sansone

et al., 1999). To test this hypothesis, a subset of samples from the western MD and Calvert County regions was analyzed for C isotopic composition. Isotopic analysis was carried out for sites YOUG105D and YOUG106D, which were assessed across all seasons, and for Aug–Oct samples which were measured across all sites the region. As CH<sub>4</sub> was presumed to be primarily biogenic, δ<sup>13</sup>C-CH<sub>4</sub> values were expected to be between –110‰ and –50‰ (Whiticar, 1996).

Monitoring of both CH<sub>4</sub> concentrations and C isotopic compositions across spatial and temporal ranges in this study increases understanding of natural behaviors of CH<sub>4</sub> in streams which connect to both groundwater flow paths and major downstream river systems (Roth, 1999). This will enable detection of shifts in concentrations and C isotopic compositions of CH<sub>4</sub> should CH<sub>4</sub> migration or contamination occur in the future.

### 3.2 Materials and methods

#### 3.2.1 Field sampling methods

Water samples were collected from streams near potential fracking wells in Garrett and Allegany Counties in western MD. All samples were collected during base flow, which was defined as normal flow conditions for each season, not during high-flow conditions or following storm events. Sampling occurred in the five catchment areas delineated on the map in Fig. 2.1: Casselman River, Georges Creek, Savage River, Potomac River Upper North Branch, and Youghiogheny River. Groundwater from the Savage River Pumping Station (SRPS) and water from the Frostburg Water Treatment Plant (which blends SRPS water with intake from Piney

Creek Reservoir within the Casselman River catchment) were also monitored. As described for the metals analyses in Chapter 2, samples for CH<sub>4</sub> were collected in three separate sets: two in western MD and one in southern MD. The western MD sites are shown on the map in Fig 2.1. The first set includes eight sites in Garrett and Allegany Counties that were sampled monthly during the period Sep 2012–Feb 2013. The second set includes fourteen sites in Garrett County that were sampled every 6–8 weeks during the period Apr 2013–Apr 2014. Also within this set are five sites sampled biannually, once in winter and once in summer, between Apr 2013–Apr 2014 (PRUN301D, SAVA302D, YOUG201D, YOUG301D, and YOUG302D). Samples in this set were collected with assistance from the Maryland Department of Natural Resources (DNR), who obtained landowner permission for site access, where necessary. The third set includes seven sites in Calvert County which were sampled in June and July of 2014. Sites are found within the West Chesapeake Bay and the Patuxent River Lower catchments. The seven stream sites sampled in Calvert County are shown on the map in Fig 2.2. In both western MD and Calvert County sample sets, streams were found in environments that I designated as either forested, wetland, or anthropogenically influenced, where anthropogenically influenced sites were adjacent to features such as major roads, residential areas, lawns, or industrial activities.

Before each field trip, 8 M KOH solution (Sigma-Aldrich) for sample preservation was made in the lab at CBL and allowed to equilibrate with air for one day. Within 24 hours of sampling, 10-mL syringes were filled with CH<sub>4</sub>-free air ('zero air'; Airgas) slightly past the 10-mL mark and closed with a 3-way stopcock.

These syringes were used to add headspace to the CH<sub>4</sub> sample bottles in the field. One syringe was prepared for each sample bottle, with some spares, in addition to another ten to be used as blanks. The blank syringes were brought to the field sites and back with the other equipment, remaining securely closed throughout, and subsequently analyzed for CH<sub>4</sub> content. In a preliminary test, syringes were exposed to field conditions and showed negligible syringe intrusion of atmospheric CH<sub>4</sub> during 60 hours of exposure.

For collection of CH<sub>4</sub> samples in the field, 125-mL glass serum bottles (Wheaton) were first carefully rinsed with stream water three times. The vial was then submerged and filled to the rim with no headspace, avoiding bubbling while filling to prevent entrainment of ambient air in the sample. The sample was preserved by adding 0.5 mL of 8 M KOH solution into the bottom of the sample bottle while letting excess sample overflow the top. Next, a 1-cm thick black butyl rubber stopper (Geo-Microbial Technologies) pierced with a steel needle attached to a 3-mL syringe was inserted firmly into the top of the sample bottle, taking care not to introduce an air bubble. Excess sample was simultaneously expelled into the syringe, which was subsequently removed and drained into a waste container. Finally, an aluminum cap was crimped over the stopper to secure it and make a gas-tight seal. Triplicate samples were collected at each site.

After collection of samples at each site, a 10-mL headspace of zero air was added to each bottle at ambient pressure (1 atm) for equilibration with the water sample and subsequent analysis of CH<sub>4</sub> content. This addition prevented bottles from breaking due to thermal expansion during transport. To ensure the injection of exactly 10 mL,

each syringe was first tested for leaks by applying pressure to the plunger with the stopcock closed. The stopcock was then opened, and the plunger pushed in to the 10-mL mark, using the excess zero air to flush the needle before inserting it into the bottle through the stopper. Another steel needle was inserted through the stopper to drain excess sample into the waste container while the headspace was injected. After removing the syringe and second needle, sample bottles were stored upside down in a cooler during transport from the field to minimize contact of the headspace with the stopper.

To assess the small-scale spatial variability in CH<sub>4</sub> concentrations at a single site, five samples were collected within a 50 m reach upstream and downstream of CASS101D, in Sep 2013. Triplicate samples were taken at CASS101D, as well as 10 m and 20 m upstream, and 20 m and 30 m downstream.

For Calvert County sites, in view of their proximity to the Chesapeake Bay, the salinity of all water samples was tested using a refractometer and found to be <1 everywhere, indicating the absence of any seawater influence.

### 3.2.2 Analysis of CH<sub>4</sub> partial pressure in the headspace

Field samples were returned to the lab for analysis of dissolved CH<sub>4</sub>. An additional 10 mL of zero air was added to each bottle, without displacing sample, increasing the headspace pressure to 2 atm and enabling subsequent removal of headspace gas for analysis. The bottles were vigorously shaken for 2 minutes to re-equilibrate the headspace with the water. For analysis of CH<sub>4</sub> partial pressure in the headspace by gas chromatography (GC), 8 mL of headspace gas were extracted

into an empty syringe through a steel needle at ambient pressure (1 atm). Before extraction the plunger was pumped 10 times to ensure good equilibration between the headspace and the syringe. Contents of the syringe were analyzed on an SRI 8610C GC, equipped with a HayeSep D column (1.83 m, 3.2 mm ID) and flame ionization detector (FID). The limit of detection,  $L_D$ , for  $\text{CH}_4$  analysis by GC-FID was 0.85 nM, calculated as:

$$L_D = 3.3\sigma_1 \quad (3.5)$$

where  $\sigma_1$  is the standard deviation (nM) of the low concentration standard using the GC-FID analysis (Magen et al., 2014). The relative precision of the instrument from repeated measurements of a  $\text{CH}_4$  standard gas was found to be 4.5%.

### 3.2.3 Theory

According to Henry's Law, the partial pressure of  $\text{CH}_4$  in equilibrium with the solution is proportional to the amount of  $\text{CH}_4$  dissolved in the solution, so the  $\text{CH}_4$  concentration in the water sample (mol/L) may be determined by measuring the  $\text{CH}_4$  partial pressure in the headspace (atm) with a gas chromatograph (GC). This partial pressure,  $F_{\text{CH}_4\text{HS}}$  (ppmv), is determined from the area of the  $\text{CH}_4$  peak in the gas chromatogram by comparison with a gas standard of known  $\text{CH}_4$  partial pressure. The ideal gas law is used to convert  $F_{\text{CH}_4\text{HS}}$  into the number of moles of  $\text{CH}_4$  in the headspace,  $n_{\text{CH}_4\text{HS}}$ , as follows:

$$n_{\text{CH}_4\text{HS}} = \frac{F_{\text{CH}_4\text{HS}} \times P_{\text{HS}} \times V_{\text{HS}}}{R(273.15 + T)} \quad (3.6)$$

where  $T$  is temperature ( $^{\circ}\text{C}$ ),  $R$  is the ideal gas constant ( $0.08206 \text{ L}\cdot\text{atm}\cdot\text{K}^{-1}\cdot\text{mol}^{-1}$ ),  $V_{HS}$  is the headspace volume, and  $P_{HS}$  is the headspace pressure (2 atm).

The number of moles of  $\text{CH}_4$  remaining in the water sample after headspace equilibration,  $n_{\text{CH}_4\text{w}}$ , is calculated from the Bunsen coefficient,  $\beta$ , for  $\text{CH}_4$  at known temperature, pressure, and salinity (Yamamoto et al., 1976):

$$n_{\text{CH}_4\text{w}} = \beta \frac{F_{\text{CH}_4\text{HS}} \times P_{\text{HS}} \times V_{\text{w}}}{R(273.15 + T)} \quad (3.7)$$

where  $V_{\text{w}}$  is the sample volume (L).

The moles of  $\text{CH}_4$  in the water,  $n_{\text{CH}_4\text{w}}$ , may then be added to the moles of  $\text{CH}_4$  in the headspace,  $n_{\text{CH}_4\text{HS}}$ , in order to determine the total moles of  $\text{CH}_4$  in the water sample  $n_{\text{CH}_4}$  at the time of sample collection. This is divided by the sample volume,  $V_{\text{w}}$ , to calculate the concentration of  $\text{CH}_4$  dissolved in the water,  $[\text{CH}_4]$ :

$$[\text{CH}_4] = \frac{n_{\text{CH}_4}}{V_{\text{w}}} \times 10^9 \quad (3.8)$$

where the factor  $10^9$  yields units of nmol/L (nM).

Two of the triplicate samples taken at each time and site were analyzed for  $\text{CH}_4$  and the concentrations were averaged. The relative spread of sample duplicates was  $\leq 8\%$  for most measurements.

### 3.2.4 Calculation of stream $\text{CH}_4$ saturation

The saturation of stream waters with  $\text{CH}_4$  was determined as the saturation ratio  $S$  based on the dissolved  $\text{CH}_4$  concentrations. For each sample,  $S$  was determined from the equation:

$$S = \frac{[CH_4]}{[CH_4]_{Eq}} \quad (3.9)$$

where  $[CH_4]$  is the measured  $CH_4$  concentration (nM) of the sample, and  $[CH_4]_{Eq}$  is the stream concentration (nM) of  $CH_4$  in equilibrium with the atmosphere. Stream  $CH_4$  concentrations in equilibrium with the atmosphere were determined using the Bunsen coefficient,  $\beta$ , for  $CH_4$  in water temperature  $10^\circ C$ , 1 atm pressure, and salinity 0 (Yamamoto et al., 1976), according to the following equation:

$$n_{CH_4, Eq} = \frac{\beta \cdot C_{Atm}}{R(273.15 + T)} \cdot 1000 \quad (3.10)$$

where  $C_{atm}$  is the atmospheric  $CH_4$  concentration, estimated to be 1.89 ppm (Blasing, 2014),  $T$  is the stream temperature ( $^\circ C$ ), and  $R$  is the ideal gas constant ( $0.08206 \text{ L}\cdot\text{atm}\cdot\text{K}^{-1}\cdot\text{mol}^{-1}$ ). Western MD streams were calculated using  $T=10^\circ C$ , the average stream temperature across all sampling dates, and in Calvert County stream temperature was estimated as  $25^\circ C$  for the calculation.

### 3.2.5 Analysis of $\delta^{13}C\text{-}CH_4$

After  $CH_4$  concentration analysis, a subset of samples was analyzed for  $\delta^{13}C\text{-}CH_4$  in the isotope ratio mass spectrometry (IRMS) laboratory of Dr. Jeff Chanton at Florida State University, Department of Earth, Ocean, and Atmospheric Science. A total of 33 samples were analyzed for  $\delta^{13}C\text{-}CH_4$ , all of which were  $>34 \text{ nM}$  in  $CH_4$  concentration, which is sufficiently high for IRMS analysis. Two sites, YOUG105D and YOUG106D, which show consistently high  $CH_4$  concentrations relative to other sites, were analyzed for  $\delta^{13}C\text{-}CH_4$  across all six time points for assessment of

temporal variability of  $\delta^{13}\text{C-CH}_4$  (12 samples). As most sites reach the maximum  $\text{CH}_4$  concentration in summer and fall, samples from summer and fall time points of 15 other sites were also analyzed for  $\delta^{13}\text{C-CH}_4$  (21 additional samples). This allowed for determining spatial variability of  $\delta^{13}\text{C-CH}_4$  within the region.

In the samples analyzed for carbon isotopic composition, 10 mL zero air was again added to each sample vial to allow the removal of headspace gas for  $\delta^{13}\text{C-CH}_4$  analysis. For water samples of  $\text{CH}_4$  concentration  $<1690$  nM, ( $<100$  ppmv  $\text{CH}_4$  in the headspace after the final zero-air addition), headspace gas was first injected into a preparative chromatographic column (stainless steel, 20 cm length, 1/8-inch OD, 1.5 mm ID; 80-100 mesh Hayesep D) cooled to  $-118^\circ\text{C}$  to retain  $\text{CH}_4$  and  $\text{CO}_2$  and remove  $\text{N}_2$ ,  $\text{O}_2$ , and Ar. After warming the preparation column, sample gas was transferred by He carrier gas to the analytical column, a porous-layer open tubular (PLOT) column (PoraPLOT Q, 25 m length, 0.32 mm ID; 10  $\mu\text{m}$  particle layer) for gas separation. The gas stream flowed to a reactor containing NiO for combustion of  $\text{CH}_4$  to  $\text{CO}_2$ , and effluent from the combustion was dried in a semi-permeable Nafion® membrane tube. Capillary tubing introduced effluent from the Nafion® tube to the IRMS. For samples with  $\text{CH}_4$  concentrations  $>1690$  nM, the preparative column was not required, and the first 2 m of the PLOT column were cooled temporarily for trapping of  $\text{CH}_4$  and  $\text{CO}_2$  before separation (Merritt et al., 1995).

Ion currents were measured for  $\text{CO}_2$  species at  $m/z$  44, 45, and 46, with  $m/z$  44 representing the abundance of  $^{12}\text{CO}_2$  and  $m/z$  46 representing  $^{12}\text{C}^{18}\text{O}^{16}\text{O}$ . The known relative abundance of  $^{17}\text{O}$  to  $^{18}\text{O}$  was used to determine contributions of  $^{13}\text{C}^{16}\text{O}_2$  and  $^{12}\text{C}^{16}\text{O}^{17}\text{O}$  to  $m/z$  45. Relative abundance of  $^{13}\text{C}$  in the  $\text{CH}_4$  sample was compared to

relative  $^{13}\text{C}$  abundance in the standard material Pee Dee Belemnite (PDB) and was expressed in  $\delta$  notation as defined in Equation (3.4), where  $R_{\text{Standard}}$ , the known  $^{13}\text{C}/^{12}\text{C}$  ratio of the PDB standard material, is equal to  $1.124 \times 10^{-2}$  (Craig, 1957). Values of  $\delta^{13}\text{C}\text{-CH}_4$  are reported in units of per mil (‰).

Reported values of  $\delta^{13}\text{C}\text{-CH}_4$  are the mean of sample duplicates. Relative analytical precision based on repeated IRMS measurements of a standard was 0.3‰. The relative spread of sample duplicates was  $\leq 2\%$  for most  $\delta^{13}\text{C}\text{-CH}_4$  measurements.

### 3.3 Results

The results of measured  $\text{CH}_4$  concentrations in all western MD sampled streams are shown in Appendix B, Table B1. Concentrations range from 1.4 nM to 5,100 nM and show both spatial and temporal variability. Results are discussed below within the context of the hypotheses posed in the introduction.

#### 3.3.1 Temporal Variability

Western MD streams of both the Sep 2012–Feb 2013 and the Apr 2013–Apr 2014 sets are variable with time (Table B1). Eight representative sites illustrate this in Figure 3.2, with four of relatively high concentration (Fig. 3.2, panels A and C) and four of relatively low concentration (Fig. 3.2, panel B and D) among western MD streams. Panels A and B of Fig. 3.2 show sites of the Sep 2012–Feb 2013 sampling set. Of samples collected from Tributary G8,  $\text{CH}_4$  concentrations reach as high as 5,100 nM in September and as low as 100 nM in February (Fig. 3.2, panel A). The highest concentration reached in the Reservoir is 4,000 nM in Oct (Fig. 3.2, panel A).

Among low concentration sites of this sample set (Sep 2012–Feb 2013), SRPS was found to reach a maximum concentration of 42 nM in November, with a minimum concentration of 6 nM, as measured in January (Fig. 3.2, panel B). In Tributary B7, the maximum concentration (142 nM) also occurs in November, although the minimum, 66 nM, was measured in September. Samples were not collected in the summer months at these sites. For the Apr 2013–Apr 2014 sample set, represented in Fig 3.2 panels C and D, all seasons were included in the sampling campaign. In panel C the highest concentrations for YOUG105D were found in October (3,820 nM), yet in June for YOUG106D (2,820 nM, Fig. 3.2, panel C). Concentrations were nearly an order of magnitude lower in the Casselman (CASS) catchment but showed similar patterns over time (Fig. 3.2, panel D). Concentrations in CASS101D were highest in June (373 nM) and lowest in December and April when concentrations were between 29–40 nM. Similarly, CASS103D shows highest concentrations in June (453 nM) and lowest in April (85 nM) (Fig. 3.2, panel D).

In Calvert County, all sites vary in concentration between June and July, apart from GRAY02 and PARK01 which are stable between the two months (Fig. 3.3). Most sites show an increase in CH<sub>4</sub>, with concentrations increasing by 25–515% between June and July. Site THOM02 shows a decrease in CH<sub>4</sub> concentration by 22% between June and July (Fig. 3.3, Table B3).

### 3.3.2 Spatial variability

Spatial variability was assessed by determining average CH<sub>4</sub> concentrations

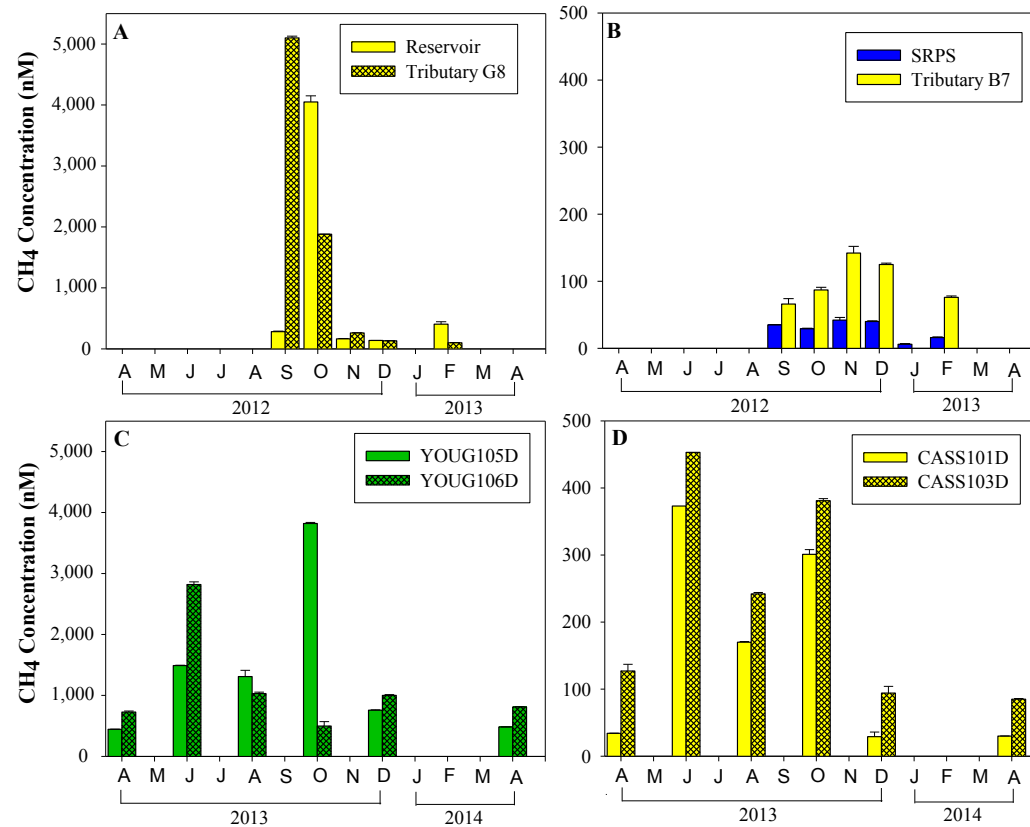


**Figure 3.2** Temporal variability in western MD stream CH<sub>4</sub> concentrations (nM) across 1 year. Top panels (A and B) show sites from the 2012–2013 set, with high CH<sub>4</sub> concentration sites shown in A and low concentration sites in B. Bottom panels (C and D) show sites from the 2013–2014 set, with high concentration sites shown in C and intermediate concentration sites in D. SRPS indicates the Savage River Pumping Station. Note that the scale in panels B and D is an order of magnitude lower than in A and C. Bar color indicates site catchment, with yellow indicating Casselman River, blue Savage River, and green Youghiogheny River. Error bars indicate half of the difference between the sample duplicates, <8% of the concentration value in most cases.

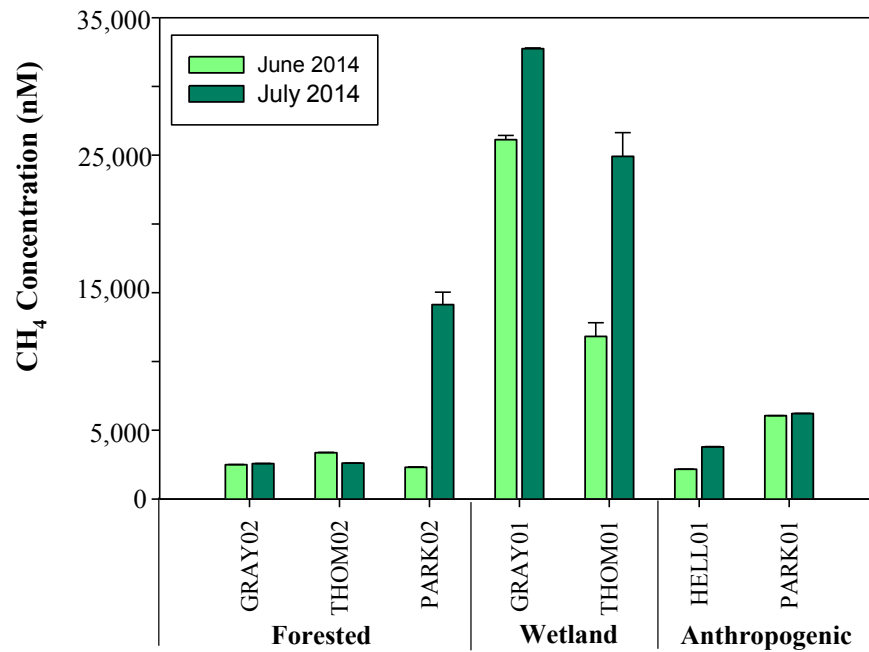


**Figure 3.3.** Methane concentrations (nM) in Calvert County from June and July 2014 measurements, grouped by stream setting (forested, wetland, or anthropogenically influenced).

among streams of the three different environmental settings: forested, wetland, and anthropogenically influenced. Averages were statistically compared to each other (Kruskal-Wallis test) and it was found that concentrations in wetland and anthropogenically influenced sites are not significantly different ( $p > 0.05$ ), but both of these environmental settings were found to be significantly greater than CH<sub>4</sub> concentrations at forested sites ( $p < 0.05$ ). Among all wetland sites, concentrations range from 55–5,100 nM and among anthropogenically influenced sites from 4–4,047 nM. For all measurements at forested sites the concentration range is 4–373 nM. Spatial variability both within and among these stream settings is demonstrated in Fig. 3.4, which shows Aug/Sep concentrations in western MD.

While CH<sub>4</sub> concentrations varied over all the sites visited, there was also small-scale variability within a 50-m stream reach where longitudinal measurements were made (Table B4, Fig. 3.5). In September 2013, CH<sub>4</sub> concentrations were 170 nM at the center location, indicated as 0 m in Fig. 3.5. Twenty meters downstream, values reached  $274 \pm 40$  nM and 10 m further downstream decreased again to 179 nM. Upstream, concentrations are slightly lower but do not vary between the +10 m and +20 m points, with concentrations of  $125 \pm 2$  nM and  $124 \pm 1$  nM, respectively. The average value of these 5 points in the stream reach is  $174 \pm 60$  nM with a relative standard deviation of 34%. This average value is well within the range of concentrations occurring at this site over the 1-year study period, between 30–301 nM (Table B1).

Methane concentrations in coastal plain streams of Calvert County, when compared with those in western MD, show that large-scale spatial variability is also observed. Concentrations are elevated relative to western MD and range between 2,100–33,000 nM (Table B3, Fig. 3.3). As in western MD, Calvert County CH<sub>4</sub> concentrations vary across different environmental settings, as observed for July 2014 measurements which are shown in Fig. 3.4. On average the CH<sub>4</sub> concentration in wetland sites is  $23,904 \pm 8,760$  nM and that in anthropogenically influenced sites is  $4,559 \pm 1,940$  nM. The average concentration in forested sites is  $4,581 \pm 4,696$  nM. Although concentrations differ across the settings, concentration differences between the three setting types in Calvert County are not significant ( $p > 0.05$ ).

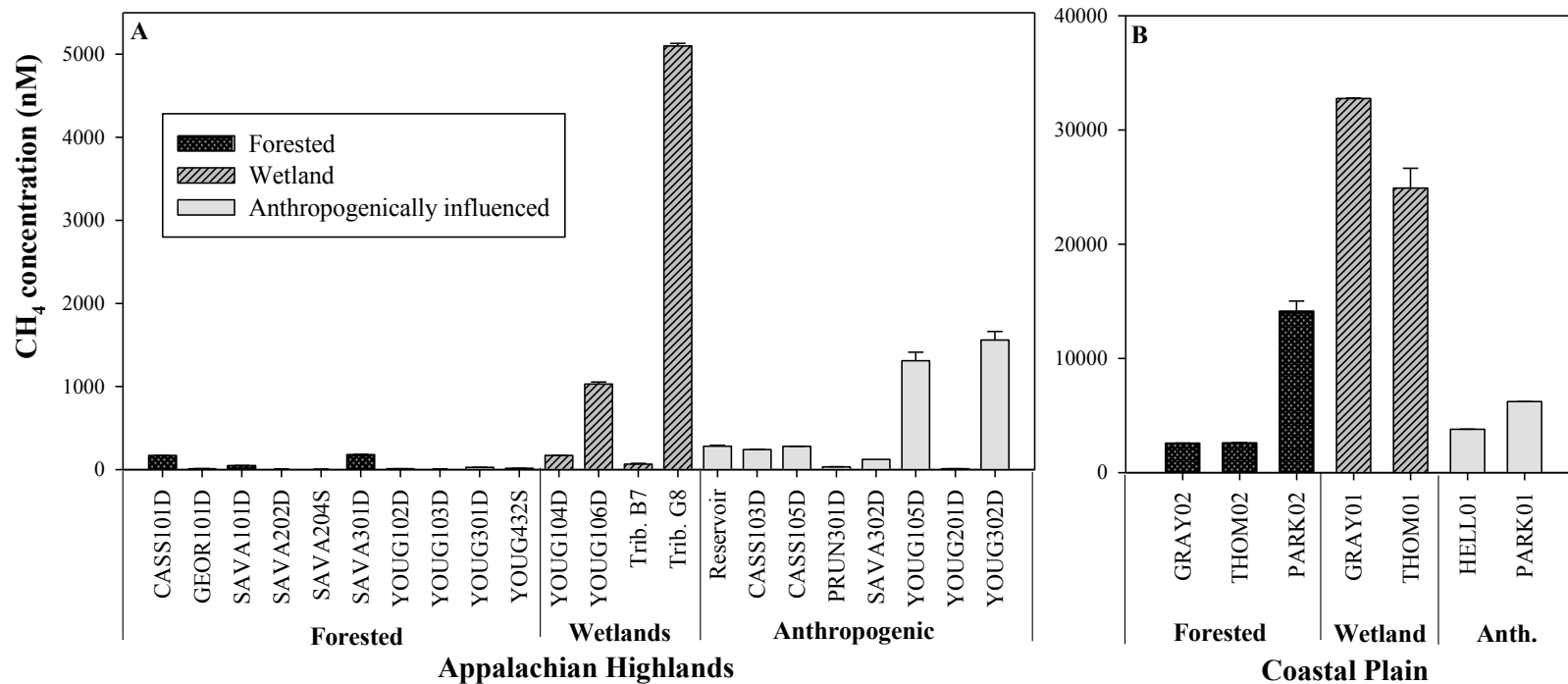


**Figure 3.4** Spatial distribution of CH<sub>4</sub> concentrations (nM) according to site setting, with sites characterized as forested, wetland, or anthropogenically influenced. Concentrations measured in Aug/Sep sampling in western MD (of both the 2012–2013 and 2013–2014 sets) are shown in (A) and those measured in July in Calvert County shown in (B). Concentrations shown in B are the same as those shown in Fig. 3.3 for July 2014. Note the order of magnitude higher concentrations in (B) which shows Calvert County measurements relative to (A) which shows those of western MD. Error bars indicate half of the difference between duplicate samples, <8% of the concentration values for most measurements.

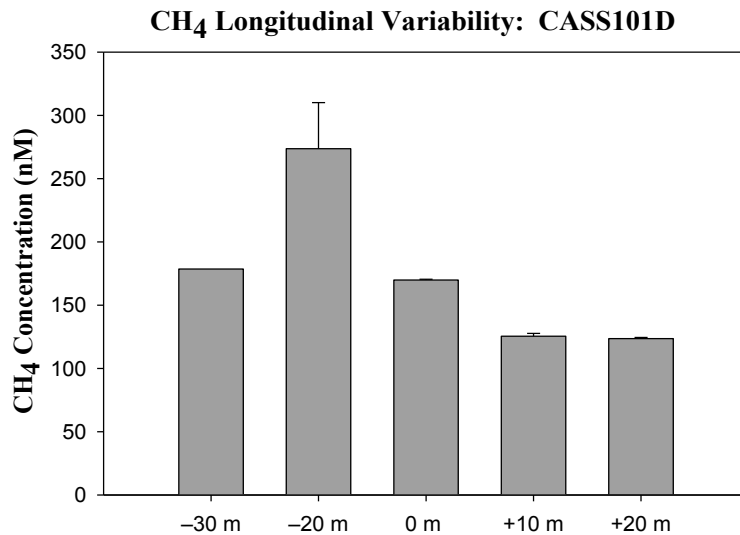


**Figure 3.5** Longitudinal variability in dissolved CH<sub>4</sub> (nM) along the CASS101D stream reach in Sep 2013. Sampling occurred at CASS101D (0 m), 2 upstream locations (+10 m, +20 m), and 2 downstream locations (-20 m, -30 m). Error bars indicate half of the difference between duplicate samples.

Relatively high variability in dissolved CH<sub>4</sub> is observed among streams within each of the three settings. The highest range in concentrations across both June and July is observed for wetland sites, with concentrations ranging from 11,820–32,748 nM. Anthropogenically influenced sites in Calvert County range between 2,168–6,220 nM and forested sites between 2,307–14,138 nM over the two months. Concentrations of each of the three settings in Calvert County are significantly greater than those of these stream settings in western MD ( $p < 0.05$ ).

### 3.3.3 Carbon isotopic composition of CH<sub>4</sub>

Across the Sep 2012–Feb 2013 and Apr 2013–Apr 2014 sampling sets,  $\delta^{13}\text{C-CH}_4$  values range from  $-60\text{‰}$  to  $-44.3\text{‰}$ , with  $>80\%$  of values distributed between  $-60\text{‰}$  and  $-50\text{‰}$  (Table B2).

Due to the extensive nature of this dataset, the isotope time series is visualized by examining 2 sites (YOUG105D and YOUG106D) which were analyzed with highest temporal resolution for  $\delta^{13}\text{C-CH}_4$ . The YOUG106D  $\delta^{13}\text{C-CH}_4$  value was  $-54\text{‰}$  in April 2012 (Fig. 3.6). This increased to  $-44\text{‰}$  by October and then quickly decreased to  $-58\text{‰}$  in December 2013 and April 2014 (Figure 3.6, Table B2). Values for YOUG105D showed less fluctuation and ranged between  $-59\text{‰}$  and  $-52\text{‰}$  over the same time period.

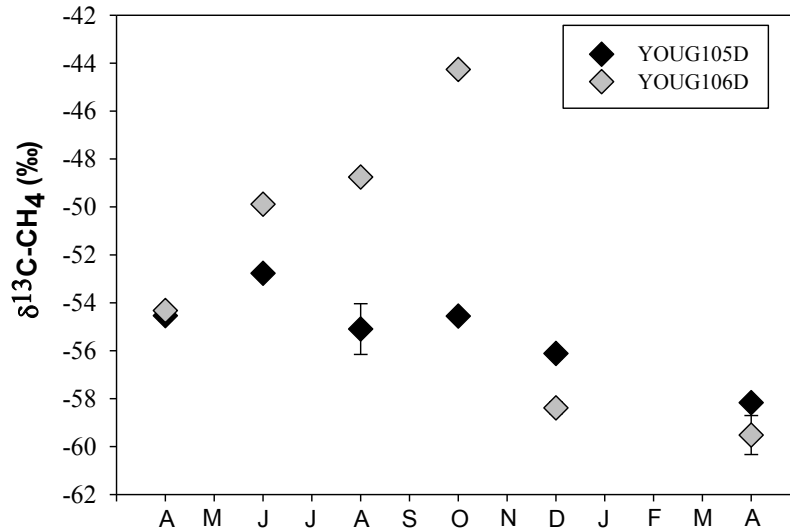


**Figure 3.6** Measurements of  $\delta^{13}\text{C-CH}_4$  values (‰) for sites YOUG105D and YOUG106D across time (Apr 2013–Apr 2014).

Spatial variability in  $\delta^{13}\text{C-CH}_4$  is comparable to temporal variability. At one time point (e.g. Oct 2013; Fig. 3.7),  $\delta^{13}\text{C-CH}_4$  values span the range of  $-60\text{‰}$  to  $-44.3\text{‰}$ , while at other time points (e.g. Apr 2013, Table B2),  $\delta^{13}\text{C-CH}_4$  values across the region range by only  $5\text{‰}$ , with values between  $-52.1\text{‰}$  and  $-57.0\text{‰}$ . Although  $\text{CH}_4$  concentrations in this region were found to vary based on setting of the stream site,  $\delta^{13}\text{C-CH}_4$  values do not vary according to stream setting (Fig 3.7) (Kruskal-Wallis test,  $p>0.05$ ). Average  $\delta^{13}\text{C-CH}_4$  values in forested, wetland, and anthropogenically influenced settings are  $-54 \pm 4\text{‰}$ ,  $-52 \pm 5\text{‰}$ ,  $-54 \pm 2\text{‰}$ , respectively.

In Calvert County, spatial variability of  $\delta^{13}\text{C-CH}_4$  was assessed based on environmental settings of streams as in western MD. In forested, wetland, and anthropogenically influenced sites, average  $\delta^{13}\text{C-CH}_4$  values in this region are  $-53 \pm 1\text{‰}$ ,  $-44 \pm 2\text{‰}$ , and  $-55 \pm 2\text{‰}$ , respectively. Although wetland sites show the highest values, differences in average  $\delta^{13}\text{C-CH}_4$  values of the three settings are not significant (Kruskal-Wallis test,  $p>0.05$ ). Measurements from the three settings in Calvert County do not differ significantly from those of any western MD stream settings ( $p>0.05$ ). For the stream site PARK02, measurements of  $\delta^{13}\text{C-CH}_4$  were made in both June and July, and the two values were in agreement within the standard deviation of the measurements (Table B3).

Overall, in Calvert County streams  $\delta^{13}\text{C-CH}_4$  values range between  $-56.7\text{‰}$  and  $-43\text{‰}$  (Table B3), within the range of values observed in western MD streams ( $-60\text{‰}$  to  $-44.3\text{‰}$ ), despite the significantly elevated  $\text{CH}_4$  concentrations in Calvert County

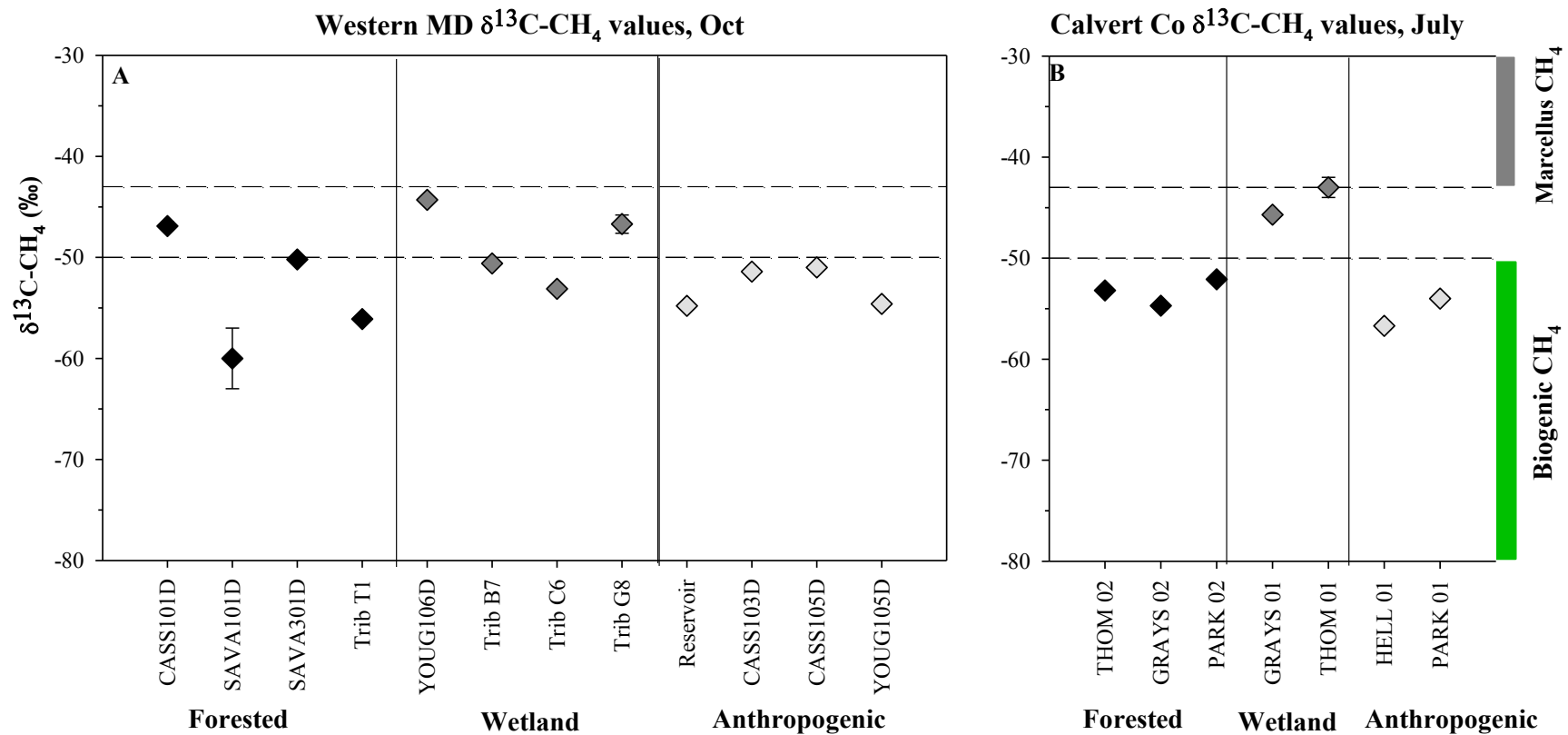


**Figure 3.7**  $\delta^{13}\text{C-CH}_4$  values (‰) in Oct samples in western MD streams (A) and July samples in Calvert County streams (B), separated by stream setting (forested, wetland, or anthropogenically influenced). The range of  $\delta^{13}\text{C-CH}_4$  values characteristic of biogenic  $\text{CH}_4$ ,  $-110\text{‰}$  to  $-50\text{‰}$  (Whiticar, 1996), is indicated by the green bar. The range characteristic of Marcellus Shale  $\text{CH}_4$ , from  $-43\text{‰}$  to  $-27\text{‰}$  (Hakala, 2014), is indicated by the gray bar.

relative to western MD. As in western MD, the majority of values are distributed between  $-60\text{‰}$  and  $-50\text{‰}$ .

### 3.4 Discussion

Dissolved  $\text{CH}_4$  in streams shows considerable spatial and temporal variability in the Marcellus Shale region of MD, within both the 2012–2013 and 2013–2014 sampling sets. Although variability was observed,  $\text{CH}_4$  concentration ranges (from 1.4–5,100 nM) are consistent with those reported for other North American temperate streams of relatively undisturbed catchments. In a long-term study in western Oregon streams, De Angelis and Lilley (1987) report spatial variability across stream environments, with  $\text{CH}_4$  concentrations ranging between 5–1,800 nM. In the northeastern U.S., naturally occurring dissolved  $\text{CH}_4$  was found at concentrations between 580–2,440 nM in predominantly forested or mixed forested and agricultural catchments (Sansone et al., 1999). De Angelis and Lilley (1993) found  $\text{CH}_4$  concentrations in the Upper Hudson River to range between 50–950 nM. Consistent  $\text{CH}_4$  oversaturation with respect to the atmosphere was found in streams of western Oregon as well as in those of the northeastern U.S. (De Angelis and Lilley, 1987; De Angelis and Scranton, 1993; Sansone et al., 1999). Similar to the previous studies, all western MD streams were found to be at saturation or oversaturated with  $\text{CH}_4$  with respect to the atmosphere, with saturation ratios  $S$  ranging from 1–1,075. All streams, therefore, provide a  $\text{CH}_4$  flux to the atmosphere.

Western MD streams, ranging from 0–5,100 nM with 92% of measurements  $<1,000$  nM, show a low concentration range relative to groundwater  $\text{CH}_4$

measurements in the northeastern U.S. Analyses from PA, West Virginia, MD, and NY show groundwater CH<sub>4</sub> concentrations ranging from 0–4,400,000 nM, with 80% of measurements between 0–311,720 nM (Brantley et al., 2014; Vidic et al., 2013). Western MD stream CH<sub>4</sub> is also very low in comparison to U.S. caution concentrations and action concentrations for CH<sub>4</sub> in drinking water, 0.623 mM (10 mg/L) and 1.76 mM (28 mg/L), respectively (Vidic et al., 2013).

#### 3.4.1 Temporal variability of stream CH<sub>4</sub>

Temporally, concentrations ranged by as much 5,000 nM at a single site (Table B1). All sites show lowest concentrations in winter and reach maximum concentrations in summer or fall (Fig. 3.2), consistent with my hypothesis that concentrations would be highest when temperature and microbial activity are highest. Previous works similarly report seasonal shifts in dissolved CH<sub>4</sub>, with elevated concentrations in warm months which is attributed to biogenic CH<sub>4</sub> sources in anoxic bottom sediments and riparian soils near streams (De Angelis and Scranton, 1993; Fedorov et al., 2003; Jones et al., 1995). In lab experiments, anaerobic microbial CH<sub>4</sub> production in peat was found to correlate with ambient temperature (Dunfield et al., 1993). Freshwater sediment incubation experiments have also shown a positive relation between temperature and rates of CH<sub>4</sub> production (Kelly and Chynoweth, 1981; Zeikus and Winfrey, 1976).

In the current field study, however, CH<sub>4</sub> concentrations showed no direct correlation to water temperature (Fig. 3.8), which may be due to other factors affecting CH<sub>4</sub> concentrations. Methanotrophy, a microbial CH<sub>4</sub> consumption process,

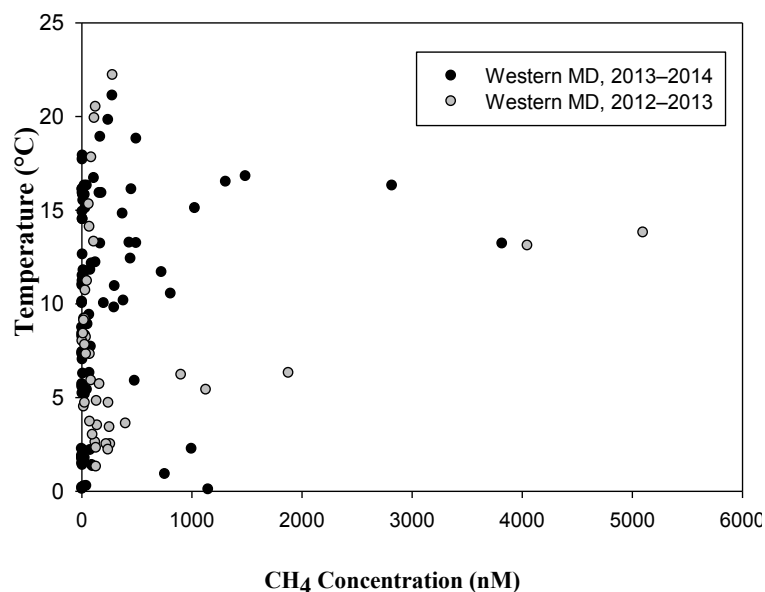


**Figure 3.8** Plot of CH<sub>4</sub> concentration (nM) vs. water temperature (°C) for the 2012–2013 and 2013–2014 western MD sampling sets.

may be one such factor as it responds differently to temperature than methanogenesis (Bastviken et al., 2008; Segers, 1998) hence, with both processes occurring simultaneously in streams, a correlation between CH<sub>4</sub> concentration and temperature may not be observed. Inputs of leaf litter and organic debris also affect temporal variability in CH<sub>4</sub> and may be another reason that a direct correlation between temperature and CH<sub>4</sub> concentration is not observed. Leaf litter and organic debris in stream areas provide a labile carbon source in streambed and bank sediments, accelerating microbial CH<sub>4</sub> production (Jones and Mulholland, 1998a). It has been shown that CH<sub>4</sub> flux from freshwater lakes is positively related to organic matter input rates (Kelly and Chynoweth, 1981). Research in an agricultural stream catchment similarly indicated a positive link between the abundance of allochthonous organic matter inputs and stream CH<sub>4</sub> production (Sanders et al., 2007). The

connection between organic matter deposits and CH<sub>4</sub> production likely accounts for relatively high CH<sub>4</sub> concentrations observed in late summer and fall when leaf litter and other plant debris has accumulated in and alongside streams. Findings of elevated dissolved CH<sub>4</sub> in both summer and fall are consistent with temporal patterns observed in a study of hemiboreal streams which showed highest CH<sub>4</sub> concentrations in summer and fall periods (Wallin et al., 2014).

The temporal concentration patterns in this study support the hypothesis of biogenic production as the primary stream CH<sub>4</sub> source. Biogenic production patterns are further supported by C isotopic measurements of CH<sub>4</sub> in western MD. Values of  $\delta^{13}\text{C-CH}_4$  are between  $-60\text{‰}$  and  $-44.3\text{‰}$  in western MD streams (Table B2, Fig. 3.7), which are predominantly in the predicted range ( $-110\text{‰}$  and  $-50\text{‰}$ ) for a biogenic stream CH<sub>4</sub> source. The  $\delta^{13}\text{C-CH}_4$  range in western MD suggests that biogenic CH<sub>4</sub> may be produced primarily by acetate fermentation, a CH<sub>4</sub> production process which occurs in freshwater and is known to give  $\delta^{13}\text{C-CH}_4$  values between  $-65\text{‰}$  and  $-50\text{‰}$  (Hornibrook et al., 2000a; Whiticar et al., 1986).

### 3.4.2 Spatial variability of stream CH<sub>4</sub>

Stream CH<sub>4</sub> concentrations are highly variable across western MD. Spatial variability appears to be driven largely by stream setting, as was hypothesized, with streams categorized as either forested, wetland, or anthropogenically influenced. Wetland and anthropogenically influenced streams were significantly elevated in CH<sub>4</sub> relative to forested streams. Similarly, a principle component analysis (PCA) based on CH<sub>4</sub> concentration, temperature, and flow shows that anthropogenic and wetland

sites cluster more closely in the diagram, with forested sites grouped separately (Fig. 3.9), indicating that stream concentrations, temperature, and flow were more similar in the anthropogenic and wetland sites.

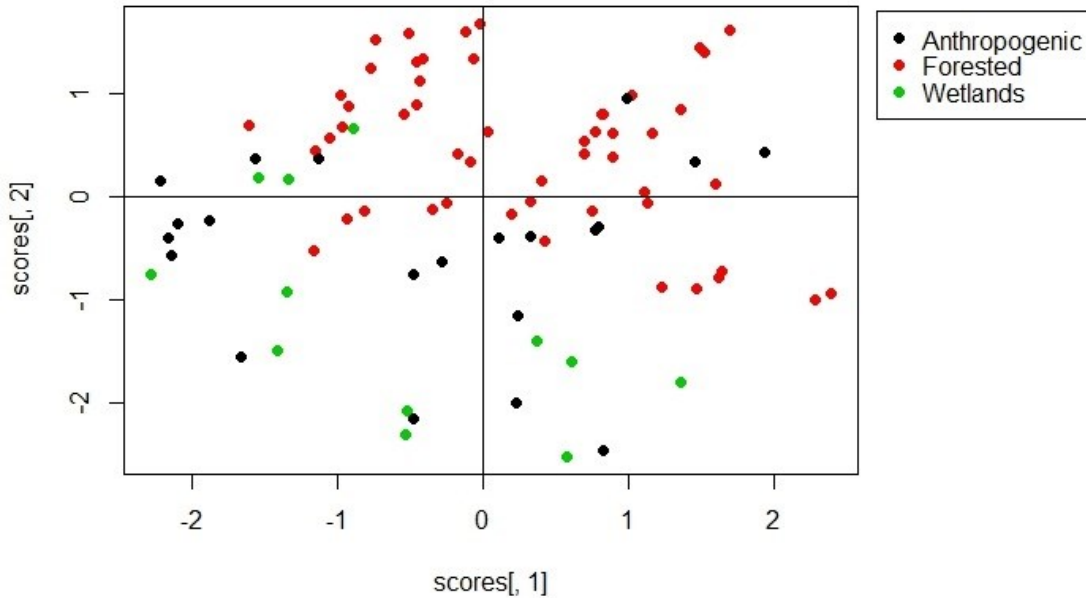


**Figure 3.9** Diagram of Principle Component Analysis (PCA) based on variables CH<sub>4</sub> concentration, temperature, and streamflow for western MD samples. Color separates samples by environmental setting.

The relation of CH<sub>4</sub> concentration to stream setting is reasonable since it has been found that streams typically receive a large portion of dissolved CH<sub>4</sub> from the riparian zone through runoff and lateral diffusion (Jones and Mulholland, 1998b). In wetland settings in western MD, streams are found in lowland areas with significant plant matter and inundated soils. These conditions promote anoxia and methanogenesis in the zones surrounding streams and likely contribute to high CH<sub>4</sub> concentrations. Also, in the wetland settings, stream beds have more fine-grained sediments with a predominance of organic matter, promoting in-stream

methanogenesis (Jones and Mulholland, 1998a). Further, streams of this type have relatively slow flow, contributing to lower rates of CH<sub>4</sub> evasion relative to streams with higher flow. Streamflow rates were not found to be directly related to CH<sub>4</sub> concentration, however, (Fig 3.10), implying that a combination of stream characteristics influence concentrations.

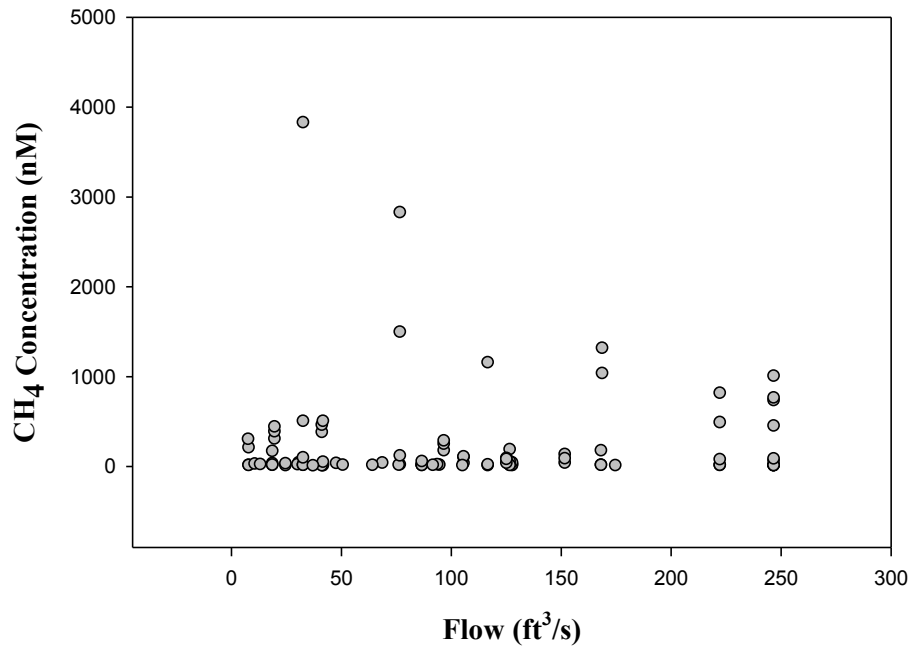


**Figure 3.10** Plot of CH<sub>4</sub> concentration (nM) vs. streamflow for the 2013–2014 western MD sampling set. Streamflow values (ft<sup>3</sup>/s) obtained from each sampling trip were taken from the USGS gauge nearest to each site.

Streams influenced by adjacent anthropogenic activities including major roads, residential or recreational developments, and coal extraction facilities show relatively high CH<sub>4</sub> concentrations which were in general comparable to those at wetland sites (Fig. 3.4). These anthropogenic influences are expected to be associated with an excess of sediment and nutrients. Roads and highways are major sources of sediments and nutrients to runoff (Forman and Alexander, 1998), as are residential

areas (Waschbusch et al., 1993), which are found near some western MD stream sites. One anthropogenically influenced site (CASS103D) is adjacent to a golf course, which likely generates runoff with high levels of nutrients from grass fertilization. Another site (YOUG105D) is just downstream of existing oil and coal facilities, which may provide effluent with high amounts of sediment. In each of the anthropogenically influenced settings, excess sediments and nutrients may be delivered to stream riparian areas, where high rates of respiration and methanogenesis may occur, supporting an abundance of stream dissolved CH<sub>4</sub> (Jones and Mulholland, 1998b). High amounts of sediment and nutrients may also be delivered directly to streams, supporting relatively high rates of respiration and methanogenesis in the stream bed (Sanders et al., 2007).

Agriculture has been found to contribute to the occurrence of greenhouse gases CH<sub>4</sub>, CO<sub>2</sub>, and N<sub>2</sub>O in streams (Jacinthe et al., 2012); however, the percentage of upstream agricultural land use for western MD sites, as reported by MD DNR (StreamHealth, 2014), was not found to correlate with dissolved CH<sub>4</sub> concentrations (Fig 3.11). Areas of agricultural land cover are found throughout the western MD study region (Appler, 2010), and the stream chemistry effects of this land use may be moderated by localized stream settings and lateral flow to streams from the riparian zone, where CH<sub>4</sub> concentrations in these flowpaths are closely tied to riparian organic matter deposition and the availability of electron acceptors (Werner et al., 2012).

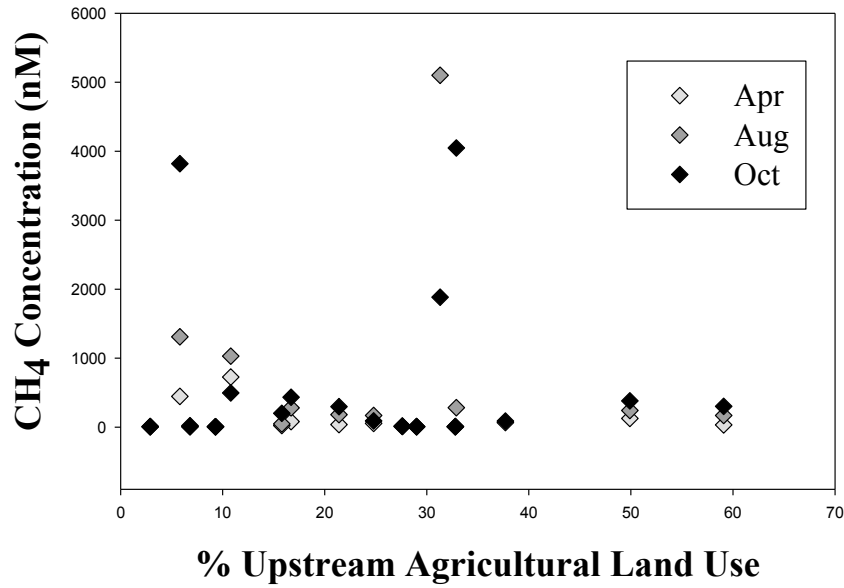


**Figure 3.11** Plot of CH<sub>4</sub> concentration vs. Upstream Agricultural Land Use (%) for each site. April, August, and October samples are plotted, with each month including samples of the Sep 2012–Feb 2013 and the Apr 2013–Apr 2014 sample sets.

Stream sites in forested settings, which show significantly low dissolved CH<sub>4</sub> relative to wetland and anthropogenic sites, are typically well buffered by the forest from excessive sediment and nutrient inputs which contribute to methanogenesis at anthropogenic sites. Also, forested sites are characterized by primarily rocky substrate in and around the stream bed which are not conducive to organic matter deposition or methanogenesis (Jones and Mulholland, 1998a). Further, most stream sites in forested settings are fast flowing, with some turbulence due to rocky substrates. Methane at these sites is therefore removed at greater rates by evasion to the atmosphere (Anthony et al., 2012; Wallin et al., 2014), contributing to low concentrations.

Although CH<sub>4</sub> concentrations vary spatially according to stream setting, some variability is observed among sites of the same setting (Fig. 3.4). This may be in part caused by groundwater contributions of CH<sub>4</sub> to streams, as these contributions vary on both large and small scales in stream networks (Jones and Mulholland, 1998b; Werner et al., 2012). Also, the methanotrophic process of CH<sub>4</sub> oxidation, a major CH<sub>4</sub> sink in freshwater systems, affects CH<sub>4</sub> concentrations (De Angelis and Scranton, 1993). Microbial oxidation is found to vary with several water chemistry parameters, including nutrient concentrations and fine particle size (De Angelis and Scranton, 1993), and this may allow greater variability in CH<sub>4</sub> concentrations even among sites of the same setting type in western MD.

Another source of concentration variability for sites within the same setting type is coarseness inherent in designating site settings. Some characteristics of wetland sites, such as relatively slow flow, for example, are found in certain forested and anthropogenically influenced sites, causing higher variability across sites in these settings. Similarly, some forest cover may be found nearby wetland and anthropogenically influenced sites, affecting the extent to which these sites are buffered from adjacent environments. Taking the average concentration for each stream setting also introduces high variability since the average combines all CH<sub>4</sub> measurements, incorporating temporal shifts in concentrations.

Yet another source of variability across sites is the small-scale variability within a longitudinal stream section which was shown in this study. The longitudinal measurements at five points surrounding site CASS101D shows a range of 150 nM within a 50-m stream reach, with four points between 120–180 nM CH<sub>4</sub> and one point

(–20 m in the stream reach) of elevated CH<sub>4</sub> concentration, 274 nM. This along-stream variability in concentration with localized points of particularly high CH<sub>4</sub> is in agreement with “patchiness” in stream CH<sub>4</sub> which has been observed in some streams (Jones et al., 1995; Wallin et al., 2014). *In situ* microbial CH<sub>4</sub> production and microbial production in riparian zones are irregular along a stream reach, producing this small-scale concentration variability (Jones and Mulholland, 1998b). Groundwater inputs of CH<sub>4</sub> are also a factor as these vary on the stream reach scale (Jones and Mulholland, 1998b). Variability inherent in sampling and GC analysis may affect some variability observed in the stream reach, as the relative precision of the sampling and analysis is up to 8% for stream samples based on analyses of sample duplicates. While small-scale variability on the stream reach scale is thought to contribute to spatial variability observed in western MD streams, larger-scale factors such as the stream morphology and surrounding organic matter deposition generate regional spatial variability which is up to two orders of magnitude greater than small-scale variability.

Considering large-scale spatial variability across physiographic provinces of MD, CH<sub>4</sub> concentrations show extreme variability. Stream CH<sub>4</sub> is highly elevated in coastal plains of Calvert County relative to western MD, with Calvert County waters ranging between 2,100–33,000 nM (Table B3). Stream concentrations of each of the three environmental settings sampled in Calvert County—forested, wetland, and anthropogenically influenced—were found to be significantly greater in concentration than those of western MD (Fig. 3.4). All streams in Calvert County are oversaturated

with CH<sub>4</sub> with respect to the atmosphere, with S ranging from 940–13,400, so each provides a CH<sub>4</sub> flux to the atmosphere.

Several factors may contribute to differences in CH<sub>4</sub> concentrations between western MD and Calvert County. The first is that there are substantial differences in human development among the two regions, with greater population density and developed land in Calvert County relative to the western MD study area (U.S. Census Bureau, 2010). With greater urban and suburban development, higher nutrient loads in runoff allow greater microbial activity and depletion of electron acceptors in drainage areas (Jones et al., 1995). This eventually favors methanogenesis in and along streams (Jones et al., 1995) and may be a factor across stream settings of the region.

Another reason for observed elevated CH<sub>4</sub> concentrations in Calvert County relative to western MD may be the lower stream gradients in the Calvert County coastal plain. This allows slower hydrologic exchange with the riparian zone and subsurface and allows greater deposition of fine particles (Battin et al., 2008). These geophysical features may facilitate anoxic conditions within and around most streams in this region, contributing to high CH<sub>4</sub> concentrations observed in Calvert County (Jones and Mulholland, 1998a). Most western MD streams, in contrast, are within a high stream gradient environment (Eshleman, 2013), where more rapid exchange with subsurface flow can occur, minimizing opportunities for anoxia (Jones and Mulholland, 1998a) and yielding comparatively low CH<sub>4</sub> concentrations. Particles in the headwater streams are typically coarser and more permeable, which enhances exchange with subsurface flow and reduces the extent of anoxia and methanogenesis

within the streambed (Battin et al., 2008; Jones and Mulholland, 1998a). In a northeastern U.S. stream system, Bresney et al (2015) found lower-gradient sites had significantly higher concentrations of CH<sub>4</sub> than higher-gradient sites.

Finally, higher stream CH<sub>4</sub> concentrations in Calvert County may be related to the warmer climate of the coastal plain region compared to the Appalachian region in western MD. The longer growing season and shorter dormant season of this climate likely fosters greater CH<sub>4</sub> productivity and higher concentrations in streams. For hemiboreal streams studied across Sweden, Wallin et al. (2014) reported a positive relation between mean ambient air temperature and stream CH<sub>4</sub> concentration, suggesting that stream CH<sub>4</sub> concentrations are related to regional climate.

Within the Calvert County region, average stream concentrations of environmental settings are not significantly different from each other, yet high variability in concentrations is observed across the region as well as among sites of the same setting. As in western MD, the concentration variability among sites may be associated in part with microbial oxidation of CH<sub>4</sub>, which may vary spatially based on various stream water characteristics including temperature and nutrient levels (De Angelis and Scranton, 1993). Also, as with western MD study streams, designation of stream setting is somewhat coarse, with characteristics of setting types overlapping in some cases. For example, the site PARK02 is designated a forested site as it is surrounded by significant tree cover, although it has certain characteristics of wetland sites such as inundated soils surrounding the stream and relatively slow flow.

Although differences were not significant across settings, sites in the wetland settings (GRAY01 and THOM01) show a high average concentration relative to other

Calvert County settings, attributable to slow flow and substantial aquatic plant coverage at these sites. High rates of organic matter deposition and an abundance of inundated anoxic sediments likely facilitate high rates of CH<sub>4</sub> production in these systems (Hornibrook et al., 2000b; Ortiz-Llorente and Alvarez-Cobelas, 2012). Methane concentrations at these sites, in the range of 11,820–32,750 nM (Table B3), are consistent with concentrations measured in North American boreal wetlands, where CH<sub>4</sub> concentrations ranged between <1 μM and 23 μM, depending on season (Hamilton et al., 1994). At the wetland sites in both June and July, ebullition was observed in the surface waters, which was assumed to contain CH<sub>4</sub>. Ebullition of CH<sub>4</sub> is observed in many wetland systems. It occurs when sediment porewater is oversaturated in CH<sub>4</sub>, with porewater concentrations >1.75 mM (Wilson, 2014). In systems where ebullition occurs, it constitutes a major CH<sub>4</sub> emission source to the atmosphere, particularly during warm seasons (Hornibrook et al., 2000b).

### 3.4.3 Carbon Isotope Measurements

Values of δ<sup>13</sup>C-CH<sub>4</sub> in western MD, between –60‰ and –44.3‰, are consistent with a biogenic CH<sub>4</sub> source, as mentioned, and are suggestive of the acetate fermentation pathway characterized by the δ<sup>13</sup>C-CH<sub>4</sub> range of –65‰ to –50‰ (Hornibrook et al., 2000a). A biogenic CH<sub>4</sub> source to streams is compatible with observations of high CH<sub>4</sub> concentrations in summer and in areas of abundant organic matter. Further, western MD δ<sup>13</sup>C-CH<sub>4</sub> stream values were compared with δ<sup>13</sup>C-CH<sub>4</sub> values of the Marcellus Shale and overlying formations (–43‰ to –27‰) (Hakala, 2014), and western MD values were found to be significantly lower than this range

representing deep formations ( $p < 0.05$ ). This indicates that such thermogenic reservoirs are not the primary  $\text{CH}_4$  source in western MD streams.

Although in western MD  $\delta^{13}\text{C-CH}_4$  values and concentration patterns suggest microbial methanogenesis is the primary stream  $\text{CH}_4$  source, there is variability of  $\delta^{13}\text{C-CH}_4$  values with some values above the range expected for biogenic  $\text{CH}_4$  ( $-110\text{‰}$  to  $-50\text{‰}$ ). Higher values, though, are not associated with a specific season or site environment ( $p > 0.05$ ) (Figs. 3.6–3.7). This  $\delta^{13}\text{C-CH}_4$  range with no clear relation to specific environments or seasons may be associated with multiple factors influencing  $\delta^{13}\text{C-CH}_4$  of biogenic  $\text{CH}_4$  in the freshwater environment, as discussed below.

One factor which likely affects  $\delta^{13}\text{C-CH}_4$  and may preclude clear spatial or temporal patterns is the contribution of another methanogenic pathway,  $\text{CO}_2$  reduction, in addition to acetate fermentation. It is expected that acetate fermentation is the primary methanogenic pathway at the study sites since this pathway is known to be predominant in freshwater; however,  $\text{CO}_2$  reduction is thought to also contribute to some extent in most settings (Hornibrook et al., 2000a). Methane produced through  $\text{CO}_2$  reduction is of lower  $\delta^{13}\text{C-CH}_4$  values ( $-110\text{‰}$  to  $-60\text{‰}$ ) than that produced by acetate fermentation ( $-65\text{‰}$  to  $-50\text{‰}$ ) (Whiticar et al., 1986), so areas with greater contributions from  $\text{CO}_2$  reduction pathways would likely have lower  $\delta^{13}\text{C-CH}_4$  values in the biogenic  $\text{CH}_4$  pool. Although contributions from the acetate fermentation vs.  $\text{CO}_2$  reduction may vary based on the availability of labile organic matter, with acetate fermentation particularly dominant in areas with more organic matter (Hornibrook et al., 2000a), no spatial differences in  $\delta^{13}\text{C-CH}_4$  based on stream setting

were found ( $p > 0.05$ ). This may be related to alteration of the methanogenic isotopic signals by another factor, methanotrophy.

Methanotrophic oxidation of  $\text{CH}_4$  is a factor that likely affects stream  $\text{CH}_4$  and causes positive shifts in  $\delta^{13}\text{C}-\text{CH}_4$  values. The microbial oxidation of  $\text{CH}_4$  fractionates  $\delta^{13}\text{C}-\text{CH}_4$  since microbes preferentially utilize  $^{12}\text{CH}_4$ , leading to an increase in  $\delta^{13}\text{C}-\text{CH}_4$  (Whiticar, 1999). As a result, biogenic  $\text{CH}_4$ —whether formed by  $\text{CO}_2$  reduction or acetate fermentation—shows more positive  $\delta^{13}\text{C}-\text{CH}_4$  values which may be above expected ranges (Whiticar, 1999). Methanotrophy is known to be a significant sink of dissolved  $\text{CH}_4$  in aquatic systems (Hornibrook et al., 2000a). It occurs in both aerobic and anaerobic environments, although aerobic methanotrophy is more common in freshwater settings (Whiticar, 1999). In streams, methanotrophy is estimated to consume between 2% and 21% of  $\text{CH}_4$  inputs (Jones and Mulholland, 1998b). Laboratory studies indicate that, during aerobic methanotrophy,  $\text{CH}_4$  may be fractionated between 4–30‰ (Whiticar, 1999). This indicates that  $\text{CH}_4$  of a strongly biogenic isotopic signature, with  $\delta^{13}\text{C}-\text{CH}_4$  ranging between  $-110$ ‰ and  $-50$ ‰, may be offset in  $\delta^{13}\text{C}-\text{CH}_4$  following methanotrophy, leading to values in the range observed here,  $-60$ ‰ to  $-44.3$ ‰. Rates of methanotrophy are known to vary with sediment and nutrient characteristics as well as temperature (De Angelis and Scranton, 1993). A clear methanotrophic effect on  $\delta^{13}\text{C}-\text{CH}_4$  values is not observable, though, in the current study when comparing values across site environments (Fig. 3.7). This is likely due to isotopic shifts from methanotrophy overlying variability of  $\delta^{13}\text{C}-\text{CH}_4$  associated with the two different methanogenic pathways. Additionally, neither the extent of methanogenic acetate

fermentation and CO<sub>2</sub> reduction, nor the extent of methanotrophy was apparent from temporal trends in  $\delta^{13}\text{C-CH}_4$  (Fig. 3.6). The co-occurrence of these processes affecting dissolved CH<sub>4</sub> may preclude the differentiation of the isotopic effects of the individual processes in a bimonthly time series.

Previous measurements of C isotopic composition of freshwater CH<sub>4</sub> in North America have shown similar ranges in  $\delta^{13}\text{C-CH}_4$  that were likewise attributed to concurrent methanogenic and methanotrophic processes. In measurements of  $\delta^{13}\text{C-CH}_4$  across a variety of freshwater rivers in the U.S., Sansone et al. (1999) showed a range of  $-58\text{‰}$  to  $-36\text{‰}$ , similar to the range found in western MD and Calvert County streams. Sansone et al. argue that CH<sub>4</sub> in the observed systems is biogenic and that it is affected by microbial oxidation. Across multiple temperate North American wetlands, porewater  $\delta^{13}\text{C-CH}_4$  values were reported to fall between  $-75.9\text{‰}$  and  $-46.0\text{‰}$ , similar to the  $\delta^{13}\text{C-CH}_4$  range in western MD streams (Hornibrook et al., 2000a). Using isotopic characterization of porewater CH<sub>4</sub> and CO<sub>2</sub>, Hornibrook et al. showed that the reported range of wetland  $\delta^{13}\text{C-CH}_4$  values is associated with the combination of CO<sub>2</sub> reduction and acetate fermentation pathways in biogenic CH<sub>4</sub> production. Similarly, a combination of these pathways may contribute to CH<sub>4</sub> pools in western MD, although with relatively low values ( $-75.9\text{‰}$  to  $-61\text{‰}$ ) occurring in wetlands, there may be greater influence of CO<sub>2</sub> reduction in these environments than in western MD streams.

In Calvert County streams,  $\delta^{13}\text{C-CH}_4$  values range from  $-56.7\text{‰}$  to  $-43\text{‰}$ , in agreement with values of western MD streams and those previously reported for North American streams and wetlands (Hornibrook et al., 2000a; Sansone et al.,

1999). Measurements of  $\delta^{13}\text{C}\text{-CH}_4$  in Calvert County may be most informative, since  $\text{CH}_4$  in Calvert County is known to be biogenic due to the lack of deep groundwater sources of thermogenic  $\text{CH}_4$ . Calvert County July measurements of  $\delta^{13}\text{C}\text{-CH}_4$  versus concentration show a positive relationship (Fig. 3.12, white points,  $R^2 = 0.82$ ), and this suggests that in this region methanotrophy, which increases  $\delta^{13}\text{C}\text{-CH}_4$  values, is a predominant factor affecting dissolved  $\text{CH}_4$ . In a coastal plain river system in NY, De Angelis and Lilley (1993) show an inverse relationship between  $\text{CH}_4$  oxidation rate and  $\text{CH}_4$  concentration, with  $\text{CH}_4$  oxidation acting as a key control on riverine dissolved  $\text{CH}_4$  concentrations. Western MD measurements of  $\delta^{13}\text{C}\text{-CH}_4$  vs. concentration in Fig. 3.12 (gray and black points) show no relationship, which may indicate that  $\delta^{13}\text{C}\text{-CH}_4$  values in this region are affected by greater variability of methanogenic pathways (acetate fermentation and  $\text{CO}_2$  reduction) compared to Calvert County waters, precluding an observable trend from methanotrophic fractionation.

Fractionating processes, largely methanotrophy, are thus found to act upon biogenic  $\text{CH}_4$  in Calvert County, which may further support a biogenic  $\text{CH}_4$  source in western MD. Western MD stream  $\text{CH}_4$ , which shows a  $\delta^{13}\text{C}\text{-CH}_4$  range similar to that of Calvert County with some high values above the biogenic  $\delta^{13}\text{C}\text{-CH}_4$  range (Fig. 3.7), may also be predominantly biogenic, and stream values in the  $-50\text{‰}$  to  $-40\text{‰}$  range in western MD are likely attributable to fractionation from  $\text{CH}_4$  oxidation.



deviation from the baseline values. To more clearly distinguish biogenic and thermogenic CH<sub>4</sub> in streams, measurements of both  $\delta^{13}\text{C-CH}_4$  and  $\delta^2\text{H-CH}_4$  should be made. These two parameters together may better define particular types of microbial and thermogenic CH<sub>4</sub> which are affected by unique fractionation paths, with visualization in a  $\delta^{13}\text{C}$  vs.  $\delta^2\text{H}$  plot (Whiticar, 1999). In addition, C isotopic measurements of C<sub>2</sub>H<sub>6</sub> may be useful for comparison with stream  $\delta^{13}\text{C-CH}_4$  values since C<sub>2</sub>H<sub>6</sub> produced in the Marcellus Shale is characteristically less enriched in <sup>13</sup>C relative to CH<sub>4</sub>, such that  $\delta^{13}\text{C-CH}_4 - \delta^{13}\text{C-C}_2\text{H}_6 > 1$  (Jackson et al., 2013a). Although C<sub>2</sub>H<sub>6</sub> may not be detected in streams under baseline conditions, it could present as a result of fracking-related gas migration. With C<sub>2</sub>H<sub>6</sub> detection in streams, C isotopic analysis of both CH<sub>4</sub> and C<sub>2</sub>H<sub>6</sub> could be carried out to differentiate Marcellus Shale gases, of the isotopic trend  $\delta^{13}\text{C-CH}_4 - \delta^{13}\text{C-C}_2\text{H}_6 > 1$ , from Upper Devonian gases which have C<sub>2</sub>H<sub>6</sub> that is more enriched in <sup>13</sup>C than CH<sub>4</sub> ( $\delta^{13}\text{C-CH}_4 - \delta^{13}\text{C-C}_2\text{H}_6 < 1$ ) (Jackson et al., 2013a).

#### 3.4.4 Monitoring Implications and Conclusions

Through the monitoring of stream CH<sub>4</sub> concentrations, I found that dissolved CH<sub>4</sub> concentrations vary significantly throughout space and time within and among two distinct MD regions, with concentrations between 1–5,100 nM in western MD and between 2,100–33,000 nM in Calvert County. Temporally, highest concentrations were found in summer and fall for all sites. Spatial variability showed overall higher concentrations in wetland and anthropogenically influenced sites and lower concentrations at forested sites, although variability was also observed among

sites of the same setting type. This may be in part attributable to longitudinal variability in CH<sub>4</sub>, as stream reaches may show a concentration range of as much as 150 nM. This variability is also likely attributable to the somewhat coarse site environment distinctions, with some sites having characteristics of multiple types of environments. In future studies, concentration variability across different stream environments may be better assessed with inclusion of more monitoring streams of wetland and anthropogenically influenced environments. Temporally, more frequent sampling may better resolve the high variability of stream CH<sub>4</sub> concentrations. In this work, monthly monitoring showed higher resolution of concentration variability than bimonthly monitoring (Fig. 3.2, panels A and B vs. panels C and D), and biweekly monitoring may capture even better the temporal concentration variability. Still, sampling for CH<sub>4</sub> analysis is an involved process requiring replicate sampling and field addition of preservative and headspace, so increasing the frequency of sampling across space and across time may be burdensome. A monthly sampling frequency with the stream sites assessed in this work may then be optimal for capturing variability in CH<sub>4</sub> concentrations.

To better understand sources of concentration variability, future studies of stream CH<sub>4</sub> should incorporate measurements of stream nutrient levels and dissolved organic carbon (DOC) since these are likely linked to *in situ* biogenic methanogenesis, particularly in view of observed elevated CH<sub>4</sub> concentrations at wetland and anthropogenically influenced sites.

Although all western MD and Calvert County streams are saturated or oversaturated with CH<sub>4</sub> with respect to the atmosphere, stream concentrations are

very low relative to groundwater concentration ranges (0–4.42 mM) and also low relative to harmful well water concentrations ( $>0.623$  mM) (Vidic et al., 2013). Still, presence of CH<sub>4</sub> above baseline stream concentrations in the future will be of concern as this may indicate contamination related to fracking. The variability observed in streams indicates that outlying CH<sub>4</sub> concentration values which may occur will be site- and season-specific. In forested sites in winter and spring, CH<sub>4</sub> concentrations may range from 1–250 nM. In summer, forested sites show concentrations of 5–400 nM. In fall, these sites may range from 5–1,200 nM. Greater ranges are found in anthropogenically influenced environments, with concentrations expected between 5–1,200 nM in winter and spring and concentrations ranging between 5–4,050 nM in summer and fall. At wetland sites, CH<sub>4</sub> concentrations are found to range between 50–1,000 nM in winter and spring, and in summer and fall, wetland sites may range between 50–5,100 nM. A perturbation in stream CH<sub>4</sub> related to future fracking activity may be identifiable from CH<sub>4</sub> measurements above the ranges expected for specific sites and seasons. High CH<sub>4</sub> concentrations indicating surface water contamination would also likely be indicative of CH<sub>4</sub> contamination of groundwater from fracking wells and may indicate subsequent fracking fluid contamination by way of the same migration pathway (Heilweil et al., 2013; Jackson et al., 2013a).

With understanding of baseline ranges, the CH<sub>4</sub> concentration data set may be best used for identifying long term increases in stream CH<sub>4</sub>, which may occur with fracking-related CH<sub>4</sub> contamination (Vengosh et al., 2014). A trend of increasing CH<sub>4</sub> concentrations across all seasons, even if small, may be indicative of CH<sub>4</sub> migration which could develop or intensify over well life times (Vengosh et al.,

2014). Also, observation of concentration shifts in groups or clusters of sites may be indicative of CH<sub>4</sub> migration and contamination in certain locations. Long term interannual CH<sub>4</sub> monitoring across western MD region would allow observation of trends overlying natural variability of stream concentrations.

Although CH<sub>4</sub> concentrations vary considerably within and among the two MD regions, C isotope composition of CH<sub>4</sub> is relatively invariable, ranging between -60‰ and -43‰. Measurements of carbon isotopic composition do not clearly distinguish a biogenic or thermogenic CH<sub>4</sub> source, although they may be indicative of biogenic CH<sub>4</sub> formed largely by acetate fermentation, particularly as biogenic CH<sub>4</sub> is consistent with concentration increases in summer and in productive areas. Because multiple processes influence δ<sup>13</sup>C-CH<sub>4</sub> in streams, δ<sup>13</sup>C-CH<sub>4</sub> values alone are not useful for confirming the CH<sub>4</sub> sources. Measurements of δ<sup>13</sup>C-CH<sub>4</sub> which are constrained by corresponding δ<sup>2</sup>H-CH<sub>4</sub> measurements may allow distinct CH<sub>4</sub> types to be differentiated in streams (Whiticar, 1999).

Knowledge of natural CH<sub>4</sub> concentrations in streams, as characterized in this study, is important prior to fracking, particularly in view of the high variability of concentrations within and among stream catchments. Additionally, δ<sup>13</sup>C-CH<sub>4</sub> measurements indicate values typical of western MD streams. These CH<sub>4</sub> analyses also expand our overall understanding of CH<sub>4</sub> biogeochemistry in headwater streams. Temporally and spatially resolved monitoring of CH<sub>4</sub>, as was carried out in this study, will allow easier recognition of potential changes in CH<sub>4</sub> occurrence in streams and may help mitigate fracking impacts to these stream systems.

## Chapter 4: Conclusions

This study suggests that baseline monitoring of stream water is essential for a region slated for fracking. Background measurements of constituents associated with fracking contamination indicate the applicability of some of these constituents as tracers of contamination. Such baseline measurements also show the naturally occurring concentrations and ranges that are expected in streams not affected by fracking contamination. This allows identification of atypical concentrations which may represent stream contamination.

### 4.1 Use of $Sr^{2+}$ , $Ba^{2+}$ , and major ions as fracking fluid tracers

Stream concentrations of  $Sr^{2+}$  and  $Ba^{2+}$  are variable across space and time in western MD and Calvert County. All concentrations are low compared to fracking fluids, which are enriched by factors of 25,000–50,000 relative to streams (Barbot et al., 2013; Warner et al., 2013a). Upon occurrence of fracking fluid contamination events, which should be initially detected through continuous monitoring of conductivity, stream measurements of  $Sr^{2+}$  and  $Ba^{2+}$  can be carried out, whereby concentrations exceeding normal variability may signal the presence of fracking fluids in stream waters.

Values of  $\log([Ba]/[Sr])$  will also be useful as a tracer for fracking fluids. Most western MD sites show relatively constant  $\log([Ba]/[Sr])$  values across time, yet these are expected to shift in the presence of fracking fluids due to addition of  $Ba^{2+}$  and  $SO_4^{2-}$  with subsequent  $BaSO_4$  oversaturation. This will cause a significant increase in

$\text{Sr}^{2+}$  relative to  $\text{Ba}^{2+}$  in cases of fracking fluid contamination, resulting in a substantial decrease of  $\log([\text{Ba}]/[\text{Sr}])$  from typical values at the affected site.

Baseline measurements of  $\text{Sr}^{2+}$  and  $\text{Ba}^{2+}$ , and  $\log([\text{Ba}]/[\text{Sr}])$  in a region slated for fracking are necessary in order to use these constituents as tracers so that normal spatial and temporal variability may be assessed. Monthly monitoring of  $\text{Sr}^{2+}$  and  $\text{Ba}^{2+}$  concentrations appears to be an advantageous frequency for resolving patterns in the metal concentrations and is logistically feasible. This monitoring frequency also allows capturing of the temporal variability of  $\log([\text{Ba}]/[\text{Sr}])$  in streams. These constituents should be monitored just downstream of well pads where streams are most susceptible to fracking fluid contamination and where signals of fluid contamination would be most readily detected.

Regular monitoring of  $\text{Sr}^{2+}$  and  $\text{Ba}^{2+}$  will also be useful for observation of longer interannual trends in concentrations since there is potential with fracking for upward migration of shale fluids, and this phenomenon may occur over multi-year time scales (Vengosh et al., 2014). Further, sustained casing pressures may increase the potential for fluid leakage with well age (Vengosh et al., 2014). Monitoring of long-term trends in stream  $\text{Sr}^{2+}$  and  $\text{Ba}^{2+}$  across western MD allows surveillance of longer time scale fluid intrusion of streams which may be induced with fracking.

The isotopic composition of Sr may be a valuable tracer for fracking fluids in streams. Ratios of  $^{87}\text{Sr}/^{86}\text{Sr}$  in fracking fluids from the Marcellus Shale are distinct from ratios of groundwater and surface water in the region and are also distinct from ratios in overlying formation fluids (Chapman et al., 2012). Analysis of Sr isotopic

composition is more difficult and costly, however, making regular Sr isotopic measurements currently impractical for tracing fracking fluids.

Baseline measurements of major ion concentrations,  $\text{Na}^+$ ,  $\text{K}^+$ ,  $\text{Mg}^{2+}$ ,  $\text{Ca}^{2+}$ ,  $\text{Cl}^-$ , and  $\text{SO}_4^{2-}$ , were elevated in streams relative to  $\text{Sr}^{2+}$  and  $\text{Ba}^{2+}$ , as expected. Most major ion species show high variability, likely related to the variability of geologic and anthropogenic sources of these ions across the region. These findings confirm that stream sampling for major ion analyses is not useful for tracing fracking fluids. It was found through exploratory measurements in 2012 that the  $\text{Br}^-$  ion may be optimal for indicating fracking fluid contamination of streams. In a subset of 2012 western MD samples,  $\text{Br}^-$  was found to be below detection limit in stream waters. With enrichment of  $\text{Br}^-$  in fracking fluids, a detection of this species in streams could thus signal the presence of fracking fluids. Continuous monitoring of  $\text{Br}^-$  for at least 1 year, as was done for  $\text{Sr}^{2+}$ ,  $\text{Ba}^{2+}$ , and major ions, should be carried out to fully characterize baseline stream levels of  $\text{Br}^-$ , with monthly monitoring recommended to assess potential temporal variability.

#### 4.2 Use of dissolved $\text{CH}_4$ for tracing fracking contamination

Stream dissolved  $\text{CH}_4$ , another potential indicator of fracking contamination, was found to be significantly variable throughout space and time in both western and southern MD. Temporally, highest concentrations are observed in summer and fall at all sites. Spatially, wetland and anthropogenically influenced sites are on average elevated in concentration relative to forested sites. With this variability, atypical  $\text{CH}_4$  concentrations which may indicate contamination will vary based on site and season.

Although monitoring of stream CH<sub>4</sub> in this study was mainly carried out on a bimonthly basis, with monthly monitoring occurring for a shorter period (Sep 2012–Feb 2013), the observed high temporal variability in concentrations suggests that monthly measurements of CH<sub>4</sub> may better capture the characteristic baseline. Monthly concentration measurements more clearly show the temporal variability and ranges in CH<sub>4</sub> (Fig. 3.2 panels A and B). Throughout the region prior to fracking, dissolved CH<sub>4</sub> should be monitored in streams of different environmental settings, as was done in this study, since concentrations are highly variable between settings. As with Sr<sup>2+</sup> and Ba<sup>2+</sup> measurements, monitoring of dissolved CH<sub>4</sub> should occur in close proximity to well pads. Upon fracking development, increased stream CH<sub>4</sub> concentrations may indicate contamination of nearby groundwater reservoirs in addition to surface water contamination (Heilweil et al., 2013).

The observed variability in dissolved CH<sub>4</sub> suggests that monitoring its concentrations may be most useful over longer, perhaps interannual, time frames. Two important means of stimulated CH<sub>4</sub> flow—upward migration through annuli and leakage through well casings—may increase in potential over the life time of the well (Brufatto et al., 2003; Jackson et al., 2013a), so monitoring of long-term trends (on the order of years to decades) throughout western MD may be a beneficial use of CH<sub>4</sub> concentration data. It is particularly important to detect CH<sub>4</sub> migration related to well casing leaks since these may be followed some time later by brine or fracking fluid migration through the same contaminant pathway (Jackson et al., 2013a).

To determine whether stream CH<sub>4</sub> is primarily biogenic or thermogenic, measurements of C isotope composition were made. The range of δ<sup>13</sup>C-CH<sub>4</sub> values

(−60‰ to −43‰) across both western MD and Calvert County are not indicative of thermogenic CH<sub>4</sub> but are predominantly in agreement with biogenic CH<sub>4</sub> production by acetate fermentation (Whiticar, 1999). Biogenic production of CH<sub>4</sub> is consistent with the concentration patterns observed, where the highest concentrations occur in summer and fall and in areas of high organic matter abundance.

Nonetheless, δ<sup>13</sup>C-CH<sub>4</sub> values in the range measured here do not rule out the presence of thermogenic CH<sub>4</sub> in western MD streams. With multiple processes potentially affecting δ<sup>13</sup>C-CH<sub>4</sub>, measurements of δ<sup>13</sup>C-CH<sub>4</sub> alone are not able to differentiate biogenic and thermogenic CH<sub>4</sub> in stream settings. Values of δ<sup>13</sup>C-CH<sub>4</sub> may be more informative if used in combination with measurements of δ<sup>2</sup>H-CH<sub>4</sub>. Together, these two measurements allow identification of specific types of biogenic as well as thermogenic CH<sub>4</sub> in a 2-dimensional diagram of δ<sup>13</sup>C-CH<sub>4</sub> vs. δ<sup>2</sup>H-CH<sub>4</sub> (Whiticar, 1999).

#### 4.3 Further implications for fracking regions

For each of the tracer constituents of interest for stream water quality—Sr<sup>2+</sup>, Ba<sup>2+</sup>, Br<sup>−</sup>, and dissolved CH<sub>4</sub>—monitoring must be carried out before, during and after fracking activity such that potential changes in stream chemistry may be observed. This monitoring should thus be implemented as a Best Management Practice (BMP) for fracking in MD and other regions anticipating fracking development. Although not feasible within logistical constraints of the current study, monitoring of stream baselines should preferably be carried out for at least two years for all stream sites, as indicated in the Recommended Best Management Practices for

Marcellus Shale Gas Development in MD (Eshleman, 2013), such that interannual variability may be observed for stream constituents. It will be possible to continue baseline monitoring of streams in western MD as the statewide ban of fracking permitting was recently extended through October 2017 (Hicks, 2015).

Once well pads have been constructed, it may be beneficial to add new monitoring sites upstream from well pads in order to assess unaffected stream reaches. Measurements from such sites may be compared to those of sites downstream of well pads, as has been recommended by MD Department of Natural Resources (MD DNR). This will help to control for natural shifts in  $\text{Sr}^{2+}$ ,  $\text{Ba}^{2+}$ , and  $\text{CH}_4$  related to environmental factors other than fracking, which will be beneficial since natural variability in these constituents is considerable.

Baseline measurements in  $\text{Sr}^{2+}$ ,  $\text{Ba}^{2+}$ ,  $\text{CH}_4$ , and potentially  $\text{Br}^-$  will be important reference data for comparison with measurements collected during and after fracking in the region, allowing recognition of contamination from fracking fluids or mobilized  $\text{CH}_4$ . Recognition of such contamination is key to preserving stream quality. Recognition of fracking contamination may also indicate the effectiveness of other implemented BMPs, such as fluid containment practices or site setbacks, which are required distances separating well pads from vulnerable areas (Eshleman, 2013). Further, recognition of stream contamination informs fracking management in other regions of the U.S. and world and indicates the primary hazards to stream waters. Fracking will continue to spread in the U.S. and also globally, as only 11% of shale gas outside of North America has been recovered (Entrekin et al., 2011). Assessment

of stream impacts in MD through monitoring of stream water chemistry may thus influence the future development of fracking worldwide.

## Appendices

### **Appendix A**

Data tables of metal and major ion concentrations

**Table A1.** Stream concentrations of Na<sup>+</sup>, K<sup>+</sup>, Mg<sup>2+</sup>, and Ca<sup>2+</sup> (μM), Sr<sup>2+</sup> and Ba<sup>2+</sup> (nM), Cl<sup>-</sup>, SO<sub>4</sub><sup>2-</sup>, NO<sub>3</sub><sup>-</sup>, HCO<sub>3</sub><sup>-</sup>, and DOC (μM), and pH. Values of HCO<sub>3</sub><sup>-</sup> were approximated from charge balance, unless marked by \* which indicates HCO<sub>3</sub><sup>-</sup> measured by Gran Titration.

Sample	Na <sup>+</sup>	K <sup>+</sup>	Mg <sup>2+</sup>	Ca <sup>2+</sup>	Sr <sup>2+</sup>	Ba <sup>2+</sup>	Cl <sup>-</sup>	SO <sub>4</sub> <sup>2-</sup>	NO <sub>3</sub>	DOC	HCO <sub>3</sub> <sup>-</sup>	pH
<b>WTP Intake</b>												
Feb '12	658	32.2	125	326	437	454	923	79.9	88.1		421	
Mar '12	639	32.2	121	303	411	438	885	85.9	86.2		376	
Apr '12	582	30.9	121	331	428	429	812	76.9	73.2		478	
May '12	590	31.2	122	323	436	435	824	75.1	61.9		476	
June '12	620	30.7	129	354	476	450	881	70.5	42.0		554	
July '12	671	34.2	135	325	496	411	900	68.2			590	
Aug '12	670	35.1	141	343	525	402	895	63.3			652	
Sept '12	732	39.2	145	324	547	424	934	60.6			655	7.09
Oct '12	740	43.6	149	341	562	407	966	57.4			683	6.97
Nov '12	764	52.6	147	344	553	403	999	69.9			659	
Dec '12	674	47.3	147	377	540	437	941	82.4			662	6.88
Jan '13	693	49.5	143	337	509	445	954	88.1			571	6.88
Feb '13	1180	40.0	139	351	511	519	1545	87.9			481	6.81
<b>WTP Finished</b>												
Feb '12	726	32.8	127	319	437	452	1071	88.3	87.8		317	
Mar '12	918	32.1	126	322	441	449	1103	95.7	85.9		467	
Apr '12	802	31.5	122	344	428	424	995	87.4	79.6		515	
May '12	818	32.2	124	336	443	434	1010	84.5	60.4		531	
June '12	819	29.4	126	360	472	459	1055	84.6	44.5		550	
July '12	850	33.0	133	335	507	421	1112	79.3			550	
Aug '12	902	33.9	140	359	541	419	1141	75.2			644	
Sept '12	962	37.8	147	336	566	432	1189	72.0			634	7.02
Oct '12	1012	43.1	150	346	602	414	1269	69.1			639	6.84
Nov '12	998	48.9	149	355	576	379	1231	74.9			673	
Dec '12	903	53.0	146	347	513	399	1135	96.1			614	6.81
Jan '13	912	49.6	144	338	501	415	1160	100			567	7.01
Feb '13	1322	42.2	136	334	488	492	1607	103			490	7.18

**Table A1 (cont.)**

Sample	Na <sup>+</sup>	K <sup>+</sup>	Mg <sup>2+</sup>	Ca <sup>2+</sup>	Sr <sup>2+</sup>	Ba <sup>2+</sup>	Cl <sup>-</sup>	SO <sub>4</sub> <sup>2-</sup>	NO <sub>3</sub> <sup>-</sup>	DOC	HCO <sub>3</sub> <sup>-</sup>	pH
<b>Reservoir</b>												
Feb '12	673	54.0	111	190	346	386	776	94.1	125		239	
Mar '12	690	41.0	106	185	349	374	789	93.6	120		225	
Apr '12	679	39.2	110	189	364	369	776	91.3	90.9		267	
May '12	591	36.8	109	190	378	370	681	87.6	51.5		318	
June '12	603	38.7	114	204	412	323	680	83.7	34.4		396	
July '12	641	37.8	123	219	479	325	732	79.4			472	
Aug '12	714	37.7	133	235	500	335	836	72.7			506	
Sept '12	809	43.4	143	253	550	384	945	65.8			569	7.53
Oct '12	830	50.5	147	264	570	449	980	61.7			599	7.33
Nov '12	880	64.3	143	260	542	423	1033	77.6			561	
Dec '12	785	61.3	139	246	492	403	926	97.6			494	7.04
Jan '13												
Feb '13	633	48.7	116	203	366	426	745	95.6			382	6.77
<b>SRPS</b>												
Feb '12	434	16.7	109	476	462	525	782	58.2	45.8		677	
Mar '12	471	16.1	106	432	454	551	780	75.1	51.6		581	
Apr '12	346	15.2	99.4	505	468	500	634	57.0	48.2		774	
May '12	298	15.9	105	547	493	499	630	46.4	43.9		851	
June '12	296	15.4	97.9	540	459	472	599	42.6	37.4		866	
July '12	255	16.0	105	559	478	466	600	36.7	36.9		889	
Aug '12	222	15.6	102	590	462	452	556	32.8			1001	
Sept '12	241	16.7	116	620	456	450	620	32.2			1045	7.06
Oct '12	229	18.0	115	634	465	454	600	32.5			1081	6.92
Nov '12	299	17.0	125	646	573	537	709	43.6			1061	
Dec '12	337	18.6	127	629	599	558	734	54.4			1025	6.67
Jan '13	515	17.1	153	638	658	676	1058	59.3			936	6.72
Feb '13	605	20.4	143	562	611	696	1115	69.7			782	6.65

**Table A1 (cont.)**

<b>Sample</b>	<b>Na<sup>+</sup></b>	<b>K<sup>+</sup></b>	<b>Mg<sup>2+</sup></b>	<b>Ca<sup>2+</sup></b>	<b>Sr<sup>2+</sup></b>	<b>Ba<sup>2+</sup></b>	<b>Cl<sup>-</sup></b>	<b>SO<sub>4</sub><sup>2-</sup></b>	<b>NO<sub>3</sub><sup>-</sup></b>	<b>DOC</b>	<b>HCO<sub>3</sub><sup>-</sup></b>	<b>pH</b>
<b>Tributary T1</b>												
Feb '12	113	65.5	143	242	350	193	176	101	215		355	
Mar '12	89.4	60.7	132	217	322	178	136	102	244		267	
Apr '12	85.9	50.8	131	222	321	168	94.4	88.5	93.7		478	
May '12	110	63.3	151	288	402	200	86.8	75.3	45.5		768	
June '12	125	77.5	195	369	551	226	93.9	59.4	40.2		1078	
July '12	187	129	254	503	706	332	161	37.0			1594	
Aug '12	223	141	288	578	820	331	194	27.8			1848	
Sept '12	185	147	271	509	724	418	138	17.3			1720	7
Oct '12	217	145	212	378	542	283	351	139			911	7.19
Nov '12	136	154	153	294	372	195	224	111			737	
Dec '12	113	104	151	250	342	180	179	100			640	6.97
Jan '13												
Feb '13	114	72.5	140	244	335	181	178	100			574	6.87
<b>Tributary C6</b>												
Feb '12	839	40.1	126	193	369		968	96.6	114		241	
Mar '12	314	33.8	103	154	285		381	96.4	119		168	
Apr '12	293	29.9	99.4	149	288		362	89.0	67.6		211	
May '12	317	31.1	94.2	155	314		348	85.7	49.0		278	
June '12	538	40.3	138	217	430		708	82.0	62.0		354	
July '12	651	68.4	178	295	609		858	67.2			673	
Aug '12	759	72.9	197	329	681		1081	53.8			695	
Sept '12	878	79.1	212	336	694		1299	49.4			654	
Oct '12	649	84.5	202	331	656		910	77.6			734	7.1
Nov '12	305	58.0	133	210	384		373	109			457	
Dec '12	246	42.4	118	177	329		288	99.3			392	7.26
Jan '13												
Feb '13	603	40.1	121	196	367		738	97.1			345	6.65

**Table A1 (cont.)**

Sample	Na <sup>+</sup>	K <sup>+</sup>	Mg <sup>2+</sup>	Ca <sup>2+</sup>	Sr <sup>2+</sup>	Ba <sup>2+</sup>	Cl <sup>-</sup>	SO <sub>4</sub> <sup>2-</sup>	NO <sub>3</sub> <sup>-</sup>	DOC	HCO <sub>3</sub> <sup>-</sup>	pH
<b>CASS101D</b>												
Apr '13	65.3	40.1	167	240	434	539	130	128			534	7.15
Jun '13	76.7	44.5	197	284	500	523	142	96.5			748	
Aug '13	81.3	52.3	236	345	614	623	199	101			895	
Oct '13	86.6	78.9	223	314	523	527	220	79.5			725*	
Dec '13	71.8	47.3	190	262	470	540	177	126			596	
Jan '14												
Apr '14	71.9	40.9	178	244	429	526	160	124		99.1	537	
<b>CASS103D</b>												
Apr '13	140	86.6	114	216	333	644	170	119			479	7.18
Jun '13	135	62.0	124	228	358	502	147	87.4			580	
Aug '13	143	88.2	121	239	372	484	163	79.9			627	
Oct '13	141	82.3	148	244	389	491	200	44.0			634*	
Dec '13	135	87.2	124	242	359	565	167	97.7			592	
Jan '14												
Apr '14	143	60.7	110	218	324	592	168	119		166	434	
<b>CASS105D</b>												
Apr '13	126	22.7	67.6	108	181	233	162	114			109	6.64
Jun '13	94.9	21.2	68.6	109	184	172	120	116			119	
Aug '13	104	24.6	73.0	122	201	103	130	84.2			221	
Oct '13	90.4	41.9	91.9	153	220	149	132	89.5			261*	
Dec '13	112	33.2	76.5	123	205	352	145	181			37.4	
Jan '14												
Apr '14	110	21.4	67.7	106	180	310	141	142		83.3	44.1	

**Table A1 (cont.)**

Sample	Na <sup>+</sup>	K <sup>+</sup>	Mg <sup>2+</sup>	Ca <sup>2+</sup>	Sr <sup>2+</sup>	Ba <sup>2+</sup>	Cl <sup>-</sup>	SO <sub>4</sub> <sup>2-</sup>	NO <sub>3</sub> <sup>-</sup>	DOC	HCO <sub>3</sub> <sup>-</sup>	pH
<b>SAVA101D</b>												
Apr '13	48.4	17.6	50.1	79.7	129	291	32.3	87.3			119	6.97
Jun '13	58.7	19.8	54.5	83.7	142	314	35.0	63.7			192	
Aug '13	50.6	17.1	48.5	76.1	130	262	38.8	66.1			146	
Oct '13	66.6	29.4	56.6	83.4	139	269	38.9	56.5			197*	
Dec '13	56.4	15.6	51.1	77.8	128	249	38.0	80.9			130	
Jan '14												
Apr '14	55.7	15.2	52.1	83.3	134	283	42.7	84.1		50.0	21.3	
<b>SAVA202D</b>												
Apr '13	88.6	22.1	65.6	112	212	313	110	107			143	7.22
Jun '13	109	26.6	82.8	177	309	428	102	93.3			367	
Aug '13	90.8	22.7	78.0	160	291	392	67.2	92.3			339	
Oct '13	104	33.8	98.0	224	378	478	84.6	77.7			523*	
Dec '13	93.9	19.9	67.8	141	241	290	88.2	94.7			254	
Jan '14												
Apr '14	97.8	22.2	65.5	116	219	308	97.5	107		52.5	12.8	
<b>SAVA204S</b>												
Apr '13	415	25.1	88.6	245	379	330	466	136			369	7.61
Jun '13	457	32.7	140	433	638	496	559	127			822	
Aug '13	375	31.4	127	375	569	452	410	129			742	
Oct '13	382	40.0	166	500	720	536	476	117			998*	
Dec '13	465	25.4	100	280	426	324	553	130			436	
Jan '14	396	24.4	108	307	443	345	471	141			497	
Apr '14	401	25.2	93.4	252	385	329	449	138		58.3	39.5	

**Table A1 (cont.)**

Sample	Na <sup>+</sup>	K <sup>+</sup>	Mg <sup>2+</sup>	Ca <sup>2+</sup>	Sr <sup>2+</sup>	Ba <sup>2+</sup>	Cl <sup>-</sup>	SO <sub>4</sub> <sup>2-</sup>	NO <sub>3</sub> <sup>-</sup>	DOC	HCO <sub>3</sub> <sup>-</sup>	pH
<b>SAVA301D</b>												
Apr '13	1034	26.2	95.9	192	329	333	1153	108			267	7.36
Jun '13	2241	38.0	164	361	609	499	2564	105			557	
Aug '13	1593	43.3	166	346	587	406	1889	100			571	
Oct '13	2097	76.0	255	495	874	606	2585	126			591*	
Dec '13	1549	30.4	125	252	439	361	1806	113			302	
Jan '14												
Apr '14	1370	28.1	109	209	378	334	1537	109		116	233	
<b>SAVA302D</b>												
Apr '13												
Jun '13												
Aug '13	1863	39.5	207	416	751	490	2396	136			482	
Oct '13												
Dec '13												
Jan '14	2235	31.6	194	390	639	513	2759	138			398	
Apr '14												
<b>GEOR101D</b>												
Apr '13	21.1	18.9	46.4	57.9	158	350	27.9	86.9			46.8	6.07
Jun '13	23.9	20.1	48.4	62.3	164	358	39.2	82.1			62.0	
Aug '13	22.2	14.8	45.0	60.5	157	348	28.2	79.8			60.2	
Oct '13	16.3	15.3	47.0	60.8	162	380	33.1	83.5			38.5*	
Dec '13	21.3	14.0	50.0	55.4	153	314	30.8	85.3			44.8	
Jan '14												
Apr '14	21.4	17.8	47.1	59.3	158	332	35.5	85.6		69.1	38.3	

**Table A1 (cont.)**

Sample	Na <sup>+</sup>	K <sup>+</sup>	Mg <sup>2+</sup>	Ca <sup>2+</sup>	Sr <sup>2+</sup>	Ba <sup>2+</sup>	Cl <sup>-</sup>	SO <sub>4</sub> <sup>2-</sup>	NO <sub>3</sub> <sup>-</sup>	DOC	HCO <sub>3</sub> <sup>-</sup>	pH
<b>YOUG102D</b>												
Apr '13	97.4	38.5	413	649	708	285	126	758			619	7.58
Jun '13	116	55.0	555	964	1087	404	126	1012			1058	
Aug '13	97.7	54.6	602	997	1078	430	114	1174			888	
Oct '13	108	75.0	815	1313	1380	525	146	1576			1035*	
Dec '13	112	40.4	317	549	597	216	159	531			664	
Jan '14												
Apr '14	79.8	34.9	323	531	579	234	96.3	549		64.9	620	
<b>YOUG103D</b>												
Apr '13	79.7	33.4	306	528	626	270	103	536			609	7.60
Jun '13	102	47.2	411	776	1010	390	110	668			1078	
Aug '13	85.4	42.5	451	796	955	400	104	832			854	
Oct '13	99.6	62.8	597	1040	1260	476	128	1073			1078*	
Dec '13	91.1	34.8	250	465	553	214	128	402			623	
Jan '14												
Apr '14	68.2	28.3	253	456	536	232	82.2	410		69.1	604	
<b>YOUG104D</b>												
Apr '13	69.2	23.0	193	737	859	326	58.3	269			1355	7.62
Jun '13	102	32.9	263	1137	1261	469	60.4	312			2252	
Aug '13	86.1	34.0	257	1066	1241	474	65.7	302			2095	
Oct '13	99.8	39.3	274	1233	1300	495	87.5	336			2334*	
Dec '13	76.5	22.8	177	701	790	277	94.9	230			1299	
Jan '14												
Apr '14	64.3	20.3	178	677	757	273	63.5	239		55.8	1247	



**Table A1 (cont.)**

Sample	Na <sup>+</sup>	K <sup>+</sup>	Mg <sup>2+</sup>	Ca <sup>2+</sup>	Sr <sup>2+</sup>	Ba <sup>2+</sup>	Cl <sup>-</sup>	SO <sub>4</sub> <sup>2-</sup>	NO <sub>3</sub> <sup>-</sup>	DOC	HCO <sub>3</sub> <sup>-</sup>	pH
<b>YOUG301D</b>												
Apr '13												
Jun '13												
Aug '13	521	27.9	124	342	428	366	622	179			501	
Oct '13												
Dec '13												
Jan '14	758	23.1	117	307	399	310	897	166			401	
Apr '14												
<b>YOUG302D</b>												
Apr '13												
Jun '13												
Aug '13	428	64.0	132	357	687	397	493	59.2			859	
Oct '13												
Dec '13												
Jan '14	636	50.5	114	284	496	376	729	84.9			583	
Apr '14												
<b>YOUG432S</b>												
Apr '13	44.7	25.0	51.1	144	214	251	52.9	96.5			214	7.28
Jun '13	55.0	26.7	57.7	184	262	302	61.4	86.8			330	
Aug '13	45.9	24.8	55.9	172	252	274	57.1	91.1			287	
Oct '13	47.4	42.3	65.1	209	272	295	76.8	80.2			357*	
Dec '13	49.3	27.5	53.0	152	219	234	64.3	100			224	
Jan '14												
Apr '14	49.7	25.1	53.4	151	220	256	57.2	88.5		76.6	241	

**Table A1 (cont.)**

Sample	Na <sup>+</sup>	K <sup>+</sup>	Mg <sup>2+</sup>	Ca <sup>2+</sup>	Sr <sup>2+</sup>	Ba <sup>2+</sup>	Cl <sup>-</sup>	SO <sub>4</sub> <sup>2-</sup>	NO <sub>3</sub> <sup>-</sup>	DOC	HCO <sub>3</sub> <sup>-</sup>	pH
<b>PRUN301D</b>												
Apr '13												
Jun '13												
Aug '13	776	59.2	425	1203	3151	448	207	1545			794	
Oct '13												
Dec '13												
Jan '14	405	33.1	237	596	1450	258	168	653			631	
Apr '14												
<b>HELL01</b>												
June '14	1899	89.5	192	143	487	248	1821	134			569	
July '14	1847	98.6	165	132	443	287	1698	113			616	
<b>GRAY01</b>												
June '14	364	21.8	105	87.7	302	222	417	52.9			248	
July '14	514	20.4	105	87.5	292	211	498	36.3			350	
<b>GRAY02</b>												
June '14	524	32.9	106	85.6	275	287	643	73.7			150	
July '14	608	34.2	114	91.0	296	304	732	69.6			182	
<b>PARK01</b>												
June '14	1384	37.0	147	539	1280	178	1721	76.6			918	
July '14	1920	53.6	206	729	1749	202	2588	68.5			1119	
<b>PARK02</b>												
June '14	670	26.6	136	649	1516	142	765	63.6			1372	
July '14	976	39.9	754	196	1814	198	1078	51.8			1735	
<b>THOM01</b>												
June '14	267	18.6	57.5	57.9	190	116	147	46.1			277	
July '14	238	27.0	61.5	66.9	227	191	201	37.6			245	
<b>THOM02</b>												
June '14	195	30.6	49.9	22.1	190	109	163	63.4			79.2	
July '14	214	29.3	47.7	20.4	110	149	187	58.4			75.4	

## Appendix B

Data tables of CH<sub>4</sub> concentrations and  $\delta^{13}\text{C}$ -CH<sub>4</sub> measurements.

**Table B1.** Dissolved CH<sub>4</sub> concentrations (nM) in western MD streams from the Sep 2012–Feb 2013 sample set and the Apr 2013–Apr 2014 sample set. The meaning of site names is described in Chapter 2. Concentration values are taken as the mean of sample duplicates, and relative errors, determined as half the difference between duplicate samples, is <8% for most values. The designated site environment is given in the column labeled ‘Env.’ with ‘A’ indicating anthropogenically influenced sites, ‘F’ indicating forested sites, and ‘W’ indicating wetland sites.

Site	Env.	2012				2013						2014		
		Sep	Oct	Nov	Dec	Jan	Feb	Apr	Jun	Aug	Oct	Dec	Jan	Apr
WTP Intake		117	112	73		20	31							
WTP Finished		128	89	76	50	22	31							
Reservoir	A	282	4050	164	137		405							
SRPS		35	29	42	40	6	16							
Tributary B7	W	66	87	142	125		76							
Tributary G8	W	5100	1880	261	132		100							
Tributary C6	W		904	401	245		132							
Tributary T1	F		1130	254	225		242							
CASS101D	F							34	373	170	301	29		30
CASS103D	A							127	453	242	381	94		85
CASS105D	A							80	497	280	434	102		73
SAVA101D	F							23	27	48	202	13		13
SAVA202D	F							5.1	7.0	8.2	8.2	3		5.4
SAVA204S	F							4.9	9	6.5	6.3	1.4	4.2	5.5
SAVA301D	F							36	163	181	297	43		49
SAVA302D	A									122			25	
GEOR101D	F							4	28	10	21	3.0		4.7
YOUG102D	F							4.5	12	9.7	8.0	3.7		5.5
YOUG103D	F							4.5	8.6	7.8	8.2	4.8		6.7
YOUG104D	W							55	112	170	91	79		70
YOUG105D	A							445	1490	1310	3820	757		483
YOUG106D	W							727	2820	1030	497	1000		810
YOUG201D	A									9.5			4.5	
YOUG301D	F									26			13	
YOUG302D	A									1560			1150	
YOUG432S	F							9	35	15	17	8.2		7.8
PRUN301D	A									33			15	

**Table B2.** Values of  $\delta^{13}\text{C-CH}_4$  (‰) measured in western MD streams from the Sep 2012–Feb 2013 sample set as well as the Apr 2013–Apr 2014 sample set. Values were determined from the mean  $\delta^{13}\text{C-CH}_4$  measurement of sample duplicates, and the relative error, determined as half the difference between duplicate samples, was <2% for most samples.

Site	2012		2013					2014	
	Sep	Oct	Apr	Jun	Aug	Oct	Dec	Jan	Apr
Reservoir SRPS	-57.4	-54.8							
Tributary B7		-50.6							
Tributary G8		-46.7							
Tributary C6		-53.1							
Tributary T1		-56.1							
CASS101D			-54.8				-46.9		
CASS103D			-52.1				-51.4		
CASS105D			-57.0				-51.0		
SAVA101D							-60		
SAVA301D			-55.7				-50.2		
SAVA302D					-53				
YOUG104D			-55.2		-48.7				
YOUG105D			-54.5	-52.8	-55	-54.6	-56.1		-58.2
YOUG106D			-54.3	-49.9	-48.8	-44.3	-58.4		-59.5
YOUG302D					-54			-56.2	
YOUG432S				-56.5					

**Table B3.** Dissolved CH<sub>4</sub> concentrations (nM) and δ<sup>13</sup>C-CH<sub>4</sub> values (‰) in Calvert County streams in June and July of 2014. Site names were designated based on the stream in which sites were located, as defined in Chapter 2. Concentration values were determined from the mean of sample duplicates and showed relative error <8% for most measurements. δ<sup>13</sup>C-CH<sub>4</sub> values were taken from the mean of sample duplicates and relative errors were <2% for most samples.

Site	[CH <sub>4</sub> ] (nM)		δ <sup>13</sup> C-CH <sub>4</sub> (‰)	
	June '14	July '14	June '14	July '14
HELL01	2169	3793		-56.7
GRAY01	26130	32750		-45.7
GRAY02	2492	2576		-54.7
PARK01	6055	6219		-54.0
PARK02	2307	14140	-52.4	-52.1
THOM01	11820	24920		-43
THOM02	3363	2607		-53.2

**Table B4** Longitudinal gradient of dissolved CH<sub>4</sub> concentrations (nM) measured in Sep 2013. Duplicate samples were measured at the CASS101D site (0 m), as well as from locations downstream (-30 m and -20 m) and upstream (+10 m and +20 m). Errors were determined as half the difference between duplicate samples.

distance from site (m)	[CH <sub>4</sub> ] (nM)
-30	179
-20	274 ± 40
0	170 ± 1
+10	125 ± 2
+20	124 ± 1

## Bibliography

- Adair, S.K.P., B.R.; Monast, J.; Vengosh, A.; Jackson, R.B., 2012. Considering Shale Gas Extraction in North Carolina: Lessons from Other States, Duke Environmental Law and Policy Forum.
- Ahearn, D.S., Sheibley, R.W., Dahlgren, R.A., Keller, K.E., 2004. Temporal dynamics of stream water chemistry in the last free-flowing river draining the western Sierra Nevada, California. *J. Hydrol.* 295, 47-63.
- Allen, D.T., Torres, V.M., Thomas, J., Sullivan, D.W., Harrison, M., Hendler, A., Herndon, S.C., Kolb, C.E., Fraser, M.P., Hill, A.D., Lamb, B.K., Miskimins, J., Sawyer, R.F., Seinfeld, J.H., 2013. Measurements of methane emissions at natural gas production sites in the United States. *Proceedings of the National Academy of Sciences of the United States of America* 110, 17768-17773.
- Alvarez, R.A., Pacala, S.W., Winebrake, J.J., Chameides, W.L., Hamburg, S.P., 2012. Greater focus needed on methane leakage from natural gas infrastructure. *Proceedings of the National Academy of Sciences* 109, 6435-6440.
- Anning, D.W.F., M.E., 2014. Dissolved-solids sources, loads, yields, and concentrations in streams of the coterminous United States. U.S. Geological Survey, Reston, VA.
- Anthony, S.E., Prahl, F.G., Peterson, T.D., 2012. Methane dynamics in the Willamette River, Oregon. *Limnol. Oceanogr.* 57, 1517-1530.
- Appler, M., 2010. Garrett County Land Use/Land Cover, in: Planning, M.D.o. (Ed.), Baltimore, MD.
- Aravena, R., Wassenaar, L.I., 1993. Dissolved organic-carbon and methane in a regional confined aquifer, southern Ontario, Canada: Carbon-isotope evidence for associated subsurface sources. *Appl. Geochem.* 8, 483-493.
- Armor, J.N., 2014. Key questions, approaches, and challenges to energy today. *Catalysis Today* 236, 171-181.
- Arnaud, C.H., 2015. Figuring Out Fracking Wastewater. *Chemical and Engineering News* 93, 8-12.
- Barbot, E., Vidic, N.S., Gregory, K.B., Vidic, R.D., 2013. Spatial and Temporal Correlation of Water Quality Parameters of Produced Waters from Devonian-Age Shale following Hydraulic Fracturing. *Environ. Sci. Technol.* 47, 2562-2569.

- Bastviken, D., Cole, J.J., Pace, M.L., Van de Bogert, M.C., 2008. Fates of methane from different lake habitats: Connecting whole-lake budgets and CH<sub>4</sub> emissions. *Journal of Geophysical Research-Biogeosciences* 113.
- Bastviken, D., Tranvik, L.J., Downing, J.A., Crill, P.M., Enrich-Prast, A., 2011. Freshwater Methane Emissions Offset the Continental Carbon Sink. *Science* 331, 50-50.
- Battin, T.J., Kaplan, L.A., Findlay, S., Hopkinson, C.S., Marti, E., Packman, A.I., Newbold, J.D., Sabater, F., 2008. Biophysical controls on organic carbon fluxes in fluvial networks. *Nature Geoscience* 1, 95-100.
- Benstead, J.P., Leigh, D.S., 2012. An expanded role for river networks. *Nature Geoscience* 5, 678-679.
- Blasing, T.J., 2014. Recent Greenhouse Gas Concentrations. U.S. Department of Energy, Carbon Dioxide Information Analysis Center.
- Brantley, S.L., Yoxtheimer, D., Arjmand, S., Grieve, P., Vidic, R., Pollak, J., Llewellyn, G.T., Abad, J., Simon, C., 2014. Water resource impacts during unconventional shale gas development: The Pennsylvania experience. *Int. J. Coal Geol.* 126, 140-156.
- Bresney, S.R., Moseman-Valtierra, S., Snyder, N.P., 2015. Observations of Greenhouse Gases and Nitrate Concentrations in a Maine River and Fringing Wetland. *Northeast. Nat* 22, 120-143.
- Brezinski, D.K., Conkwright, R.D., 2013. Geologic Map of Garrett, Allegany, and Western Washington Counties in Maryland. Maryland Department of Natural Resources.
- Brufatto, C., Cochran, J., Conn, L., Power, D., El-Zeghaty, S.Z.A.A., Fraboulet, B., Griffin, T., James, S., Munk, T., Justus, F., 2003. From mud to cement—building gas wells. *Oilfield Review* 15, 62-76.
- Burnham, A., Han, J., Clark, C.E., Wang, M., Dunn, J.B., Palou-Rivera, I., 2012. Life-Cycle Greenhouse Gas Emissions of Shale Gas, Natural Gas, Coal, and Petroleum. *Environ. Sci. Technol.* 46, 619-627.
- Canedo-Arguelles, M., Kefford, B.J., Piscart, C., Prat, N., Schafer, R.B., Schulz, C.J., 2013. Salinisation of rivers: An urgent ecological issue. *Environmental Pollution* 173, 157-167.
- Carnevale, G., Godfrey, S.J., Pietsch, T.W., 2011. Stargazer (Teleostei, Uranoscopidae) cranial remains from the Miocene Calvert Cliffs, Maryland,

U.S.A. (St. Marys Formation, Chesapeake Group). *Journal of Vertebrate Paleontology* 31, 1200-1209.

- Carpenter, N.E., 2014. *Chemistry of sustainable energy*. Taylor and Francis Group, Boca Raton, FL.
- Caulton, D.R., Shepson, P.B., Santoro, R.L., Sparks, J.P., Howarth, R.W., Ingraffea, A.R., Cambaliza, M.O.L., Sweeney, C., Karion, A., Davis, K.J., Stirm, B.H., Montzka, S.A., Miller, B.R., 2014. Toward a better understanding and quantification of methane emissions from shale gas development. *Proceedings of the National Academy of Sciences of the United States of America* 111, 6237-6242.
- Chapman, E.C., Capo, R.C., Stewart, B.W., Kirby, C.S., Hammack, R.W., Schroeder, K.T., Edenborn, H.M., 2012. Geochemical and Strontium Isotope Characterization of Produced Waters from Marcellus Shale Natural Gas Extraction. *Environ. Sci. Technol.* 46, 3545-3553.
- Clark, C.E., Horner, R.M., Harto, C.B., 2013. Life Cycle Water Consumption for Shale Gas and Conventional Natural Gas. *Environ. Sci. Technol.* 47, 11829-11836.
- Considine, T., Watson, R., Considine, N., Martin, J., 2012. Environmental impacts during Marcellus shale gas drilling: Causes, impacts, and remedies. Report 2012-1 Shale Resources and Society Institute.
- Craig, H., 1957. Isotopic standards for carbon and oxygen and correction factors for mass-spectrometric analysis of carbon dioxide *Geochim. Cosmochim. Acta* 12, 133-149.
- Dale, A.T., Khanna, V., Vidic, R.D., Bilec, M.M., 2013. Process Based Life-Cycle Assessment of Natural Gas from the Marcellus Shale. *Environ. Sci. Technol.* 47, 5459-5466.
- Darrah, T.H., Vengosh, A., Jackson, R.B., Warner, N.R., Poreda, R.J., 2014. Noble gases identify the mechanisms of fugitive gas contamination in drinking-water wells overlying the Marcellus and Barnett Shales. *Proceedings of the National Academy of Sciences*.
- De Angelis, M.A., Lilley, M.D., 1987. Methane in surface waters of Oregon estuaries and rivers. *Limnol. Oceanogr.* 32, 716-722.
- De Angelis, M.A., Scranton, M.I., 1993. Fate of methane in the Hudson River and estuary. *Glob. Biogeochem. Cycle* 7, 509-523.

- Downing, J.A., Cole, J.J., Duarte, C.M., Middelburg, J.J., Melack, J.M., Prairie, Y.T., Kortelainen, P., Striegl, R.G., McDowell, W.H., Tranvik, L.J., 2012. Global abundance and size distribution of streams and rivers. *Inland Waters* 2, 229-236.
- Dresel, P.E., Rose, A.W., 2010. Chemistry and origin of oil and gas well brines in western Pennsylvania. Open-File Report OFOG 10, 01.00.
- Dunfield, P., Knowles, R., Dumont, R., Moore, T.R., 1993. Methane production and consumption in temperate and sub-arctic peat soils - Response to temperature and pH *Soil Biology & Biochemistry* 25, 321-326.
- Elias, R.W., Hirao, Y., Patterson, C.C., 1982. The circumvention of the natural biopurification of calcium along nutrient pathways by atmospheric inputs of industrial lead. *Geochim. Cosmochim. Acta* 46, 2561-2580.
- Entrekin, S., Evans-White, M., Johnson, B., Hagenbuch, E., 2011. Rapid expansion of natural gas development poses a threat to surface waters. *Frontiers in Ecology and the Environment* 9, 503-511.
- Eshleman, K.N., Elmore, A., 2013. Recommended Best Management Practices for Marcellus Shale Gas Development in Maryland. University of Maryland Center for Environmental Science, Frostburg, MD.
- Etiopie, G., Klusman, R.W., 2002. Geologic emissions of methane to the atmosphere. *Chemosphere* 49, 777-789.
- Fedorov, Y.A., Khoroshevskaya, V.O., Tambieva, N.S., 2003. Variations in methane concentrations in the water of the Don River and Taganrog Bay under the effect of natural factors. *Water Resources* 30, 81-85.
- Ferrar, K.J., Michanowicz, D.R., Christen, C.L., Mulcahy, N., Malone, S.L., Sharma, R.K., 2013. Assessment of Effluent Contaminants from Three Facilities Discharging Marcellus Shale Wastewater to Surface Waters in Pennsylvania. *Environ. Sci. Technol.* 47, 3472-3481.
- Fitzpatrick, M.L., Long, D.T., Pijanowski, B.C., 2007. Exploring the effects of urban and agricultural land use on surface water chemistry, across a regional watershed, using multivariate statistics. *Appl. Geochem.* 22, 1825-1840.
- Flewelling, S.A., Sharma, M., 2014. Constraints on Upward Migration of Hydraulic Fracturing Fluid and Brine. *Ground Water* 52, 9-19.
- Flewelling, S.A., Tymchak, M.P., Warpinski, N., 2013. Hydraulic fracture height limits and fault interactions in tight oil and gas formations. *Geophysical Research Letters* 40, 3602-3606.

- Fontenot, B.E., Hunt, L.R., Hildenbrand, Z.L., Carlton, D.D., Oka, H., Walton, J.L., Hopkins, D., Osorio, A., Bjorndal, B., Hu, Q.H.H., Schug, K.A., 2013. An Evaluation of Water Quality in Private Drinking Water Wells Near Natural Gas Extraction Sites in the Barnett Shale Formation. *Environ. Sci. Technol.* 47, 10032-10040.
- Forman, R.T.T., Alexander, L.E., 1998. Roads and Their Major Ecological Effects. *Annu. Rev. Ecol. Syst.* 29, 207-C202.
- Fry, B., 2006. *Stable Isotope Ecology*. Springer, New York.
- Godwin, K.S., Hafner, S.D., Buff, M.F., 2003. Long-term trends in sodium and chloride in the Mohawk River, New York: the effect of fifty years of road-salt application. *Environmental Pollution* 124, 273-281.
- Grasby, S.E., Betcher, R.N., 2002. Regional hydrogeochemistry of the carbonate rock aquifer, southern Manitoba. *Canadian Journal of Earth Sciences* 39, 1053-1063.
- Gregory, K.B., Vidic, R.D., Dzombak, D.A., 2011. Water Management Challenges Associated with the Production of Shale Gas by Hydraulic Fracturing. *Elements* 7, 181-186.
- Gross, S.A., Avens, H.J., Banducci, A.M., Sahlme, J., Panko, J.M., Tvermoes, B.E., 2013. Analysis of BTEX groundwater concentrations from surface spills associated with hydraulic fracturing operations. *Journal of the Air & Waste Management Association* 63, 424-432.
- Hakala, J.A., 2014. Use of stable isotopes to identify sources of methane in Appalachian Basin shallow groundwaters: a review. *Environmental Science-Processes & Impacts* 16, 2080-2086.
- Haluszczak, L.O., Rose, A.W., Kump, L.R., 2013. Geochemical evaluation of flowback brine from Marcellus gas wells in Pennsylvania, USA. *Appl. Geochem.* 28, 55-61.
- Hamilton, J.D., Kelly, C.A., Rudd, J.W.M., Hesslein, R.H., Roulet, N.T., 1994. Flux to the atmosphere of CH<sub>4</sub> and CO<sub>2</sub> from wetland ponds on the Hudson Bay lowlands (HBLs). *J. Geophys. Res.-Atmos.* 99, 1495-1510.
- Hammer, R., VanBriesen, J., Levine, L., 2012. In fracking's wake: new rules are needed to protect our health and environment from contaminated wastewater. *Natural Resources Defense Council* 11.

- Harkness, J.S., Dwyer, G.S., Warner, N.R., Parker, K.M., Mitch, W.A., Vengosh, A., 2015. Iodide, Bromide, and Ammonium in Hydraulic Fracturing and Oil and Gas Wastewaters: Environmental Implications. *Environ. Sci. Technol.*
- Harrison, S.S., 1983. Evaluating system for groundwater contamination hazards due to gas-well drilling on the glaciated Appalachian Plateau. *Ground Water* 21, 689-700.
- Hayes, T., 2009. Sampling and Analysis of Water Streams Associated with the Development of Marcellus Shale Gas. Marcellus Shale Coalition.
- He, C., Li, M., Liu, W.S., Barbot, E., Vidic, R.D., 2014. Kinetics and Equilibrium of Barium and Strontium Sulfate Formation in Marcellus Shale Flowback Water. *Journal of Environmental Engineering* 140.
- Heilweil, V.M., Stolp, B.J., Kimball, B.A., Susong, D.D., Marston, T.M., Gardner, P.M., 2013. A Stream-Based Methane Monitoring Approach for Evaluating Groundwater Impacts Associated with Unconventional Gas Development. *Ground Water* 51, 511-524.
- Hicks, J., 2015. Md. fracking moratorium to become law without Hogan's signature, *The Washington Post*.
- Hitzman, M.W., 2012. Induced Seismicity Potential in Energy Technologies, in: Council, N.R. (Ed.). *The National Academies Press*, Washington, D.C.
- Hockstad, L.W., M., 2013. Inventory of U.S. Greenhouse Gas Emissions and Sinks: 1990-2011, in: E.P.A., U.S. (Ed.), Washington, D.C. .
- Hoffmann, W., 2014. *The Economic Competitiveness of Renewable Energy*. Scrivener Publishing, Beverly, MA.
- Hogan, J.F., Blum, J.D., 2003. Tracing hydrologic flow paths in a small forested watershed using variations in  $(^{87}\text{Sr}/^{86}\text{Sr})$ ,  $\text{Ca} / \text{Sr}$  ,  $\text{Ba} / \text{Sr}$  and  $\delta \text{O-18}$ . *Water Resour. Res.* 39.
- Hornibrook, E.R.C., Longstaffe, F.J., Fyfe, W.S., 2000a. Evolution of stable carbon isotope compositions for methane and carbon dioxide in freshwater wetlands and other anaerobic environments. *Geochim. Cosmochim. Acta* 64, 1013-1027.
- Hornibrook, E.R.C., Longstaffe, F.J., Fyfe, W.S., 2000b. Factors influencing stable isotope ratios in  $\text{CH}_4$  and  $\text{CO}_2$  within subenvironments of freshwater wetlands: implications for delta-signatures of emissions (vol 36, pg 151, 2000). *Isotopes in Environmental and Health Studies* 36, U1-U1.

- Jacinthe, P.A., Filippelli, G.M., Tedesco, L.P., Raftis, R., 2012. Carbon storage and greenhouse gases emission from a fluvial reservoir in an agricultural landscape. *Catena* 94, 53-63.
- Jackson, R.B., Vengosh, A., Darrah, T.H., Warner, N.R., Down, A., Poreda, R.J., Osborn, S.G., Zhao, K.G., Karr, J.D., 2013a. Increased stray gas abundance in a subset of drinking water wells near Marcellus shale gas extraction. *Proceedings of the National Academy of Sciences of the United States of America* 110, 11250-11255.
- Jackson, R.E., Gorody, A.W., Mayer, B., Roy, J.W., Ryan, M.C., Van Stempvoort, D.R., 2013b. Groundwater Protection and Unconventional Gas Extraction: The Critical Need for Field-Based Hydrogeological Research. *Ground Water* 51, 488-510.
- Johnson, C.E., Driscoll, C.T., Siccama, T.G., Likens, G.E., 2000. Element fluxes and landscape position in a northern hardwood forest watershed ecosystem. *Ecosystems* 3, 159-184.
- Jones, J.B., Holmes, R.M., Fisher, S.G., Grimm, N.B., Greene, D.M., 1995. Methanogenesis in Arizona, USA dryland streams. *Biogeochemistry* 31, 155-173.
- Jones, J.B., Mulholland, P.J., 1998a. Influence of drainage basin topography and elevation on carbon dioxide and methane supersaturation of stream water. *Biogeochemistry* 40, 57-72.
- Jones, J.B., Mulholland, P.J., 1998b. Methane input and evasion in a hardwood forest stream: Effects of subsurface flow from shallow and deep pathways. *Limnol. Oceanogr.* 43, 1243-1250.
- Judson, S.K., M.E.; Leet, L.D., 1987. *Physical Geology*, 7th ed. Prentice-Hall, Inc., Englewood Cliffs, NJ.
- Kappel, W.M., Nystrom, E.A., 2012. Dissolved methane in New York groundwater, 1999–2011. US Geological Survey Open-File Report 1162.
- Kargbo, D.M., Wilhelm, R.G., Campbell, D.J., 2010. Natural Gas Plays in the Marcellus Shale: Challenges and Potential Opportunities. *Environ. Sci. Technol.* 44, 5679-5684.
- Kaushal, S.S., Groffman, P.M., Likens, G.E., Belt, K.T., Stack, W.P., Kelly, V.R., Band, L.E., Fisher, G.T., 2005. Increased salinization of fresh water in the northeastern United States. *Proceedings of the National Academy of Sciences of the United States of America* 102, 13517-13520.

- Kell, S., 2009. Modern Shale Gas Development in the United States; A Primer, in: Energy, U.S.D.o. (Ed.). Ground Water Protection Council, Oklahoma City, OK.
- Keller, E.A., 1982. Environmental Geology, 3rd ed. Bell & Howell Company, Columbus, OH.
- Kelly, C.A., Chynoweth, D.P., 1981. The Contributions of Temperature and of the Input of Organic Matter in Controlling Rates of Sediment Methanogenesis. *Limnol. Oceanogr.* 26, 891-897.
- Key World Energy Statistics, 2014. Organisation for Economic Co-operation and Development, Paris, France. Retrieved from: <http://www.iea.org/publications/freepublications/publication/keyworld2014.pdf>
- Kim, W.Y., 2013. Induced seismicity associated with fluid injection into a deep well in Youngstown, Ohio. *Journal of Geophysical Research-Solid Earth* 118, 3506-3518.
- Kolb, R.W., 2014. The Natural Gas Revolution. Pearson, Upper Saddle River, NJ.
- Kondash, A.J., Warner, N.R., Lahav, O., Vengosh, A., 2014. Radium and Barium Removal through Blending Hydraulic Fracturing Fluids with Acid Mine Drainage. *Environ. Sci. Technol.* 48, 1334-1342.
- Kravchenko, J., Darrah, T.H., Miller, R.K., Lysterly, H.K., Vengosh, A., 2014. A review of the health impacts of barium from natural and anthropogenic exposure. *Environmental Geochemistry and Health* 36, 797-814.
- Land, M., Ingri, J., Andersson, P.S., Ohlander, B., 2000. Ba/Sr, Ca/Sr and Sr-87/Sr-86 ratios in soil water and groundwater: implications for relative contributions to stream water discharge. *Appl. Geochem.* 15, 311-325.
- Lautz, L.K., Hoke, G.D., Lu, Z.L., Siegel, D.I., Christian, K., Kessler, J.D., Teale, N.G., 2014. Using Discriminant Analysis to Determine Sources of Salinity in Shallow Groundwater Prior to Hydraulic Fracturing. *Environ. Sci. Technol.* 48, 9061-9069.
- Lester, Y., Ferrer, I., Thurman, E.M., Sitterley, K.A., Korak, J.A., Aiken, G., Linden, K.G., 2015. Characterization of hydraulic fracturing flowback water in Colorado: Implications for water treatment. *Science of the Total Environment* 512, 637-644.
- Letcher, T.M., 2014. Future Energy: Improved, Sustainable and Clean Options for Our Planet, 2nd ed. Elsevier, London.

- Lewis, A., 2012. Wastewater Generation and Disposal from Natural Gas Wells in Pennsylvania, Nicholas School of the Environment. Duke University.
- Likens, G.E., Bormann, F.H., Johnson, N.M., Pierce, R.S., 1967. Calcium magnesium potassium and sodium budgets for a small forested ecosystem. *Ecology* 48, 772-&.
- Liu, Y.C., Whitman, W.B., 2008. Metabolic, phylogenetic, and ecological diversity of the methanogenic archaea, in: Wiegel, J., Maier, R.J., Adams, M.W.W. (Eds.), *Incredible Anaerobes: From Physiology to Genomics to Fuels*. Blackwell Publishing, Oxford, pp. 171-189.
- Llewellyn, G., 2014. Evidence and mechanisms for Appalachian Basin brine migration into shallow aquifers in NE Pennsylvania, USA. *Hydrogeol J*, 1-12.
- Long, D.T., Wilson, T.P., Takacs, M.J., Rezabek, D.H., 1988. Stable-isotope geochemistry of saline near-surface ground-water - East-central Michigan Basin. *Geological Society of America Bulletin* 100, 1568-1577.
- Magen, C., Lapham, L.L., Pohlman, J.W., Marshall, K., Bosman, S., Casso, M., Chanton, J.P., 2014. A simple headspace equilibration method for measuring dissolved methane. *Limnology and Oceanography-Methods* 12, 637-650.
- Mair, R., Bickle, M., Goodman, D., Koppelman, B., Roberts, J., Selley, R., Shipton, Z., Thomas, H., Walker, A., Woods, E., 2012. Shale gas extraction in the UK: a review of hydraulic fracturing.
- Malakoff, D., 2014. The gas surge. *Science* 344, 1464-1467.
- Marshak, S., 2005. *Earth: Portrait of a Planet*, 2 ed. W. W. Norton & Company.
- Martell, A.E., Smith, R.M., Motekaitis, R.J., 2004. NIST Critically Selected Stability Constants of Metal Complexes. Texas A&M University, NIST Standard Reference Database 46 Version 8.0.
- Maryland Dept of Planning, Land Use/Land Cover. 2010. Retrieved from: <http://www.mdp.state.md.us/PDF/OurWork/LandUse/County/Garrett.pdf>
- Mast, A., Turk, J.T., 1999. Environmental Characteristics and Water Quality of Hydrologic Benchmark Network Stations in the Eastern United States, 1963-95. US Geological Survey.
- McKenzie, L.M., Witter, R.Z., Newman, L.S., Adgate, J.L., 2012. Human health risk assessment of air emissions from development of unconventional natural gas resources. *Science of the Total Environment* 424, 79-87.

- Merritt, D.A., Hayes, J.M., Marias, D.J.D., 1995. Carbon isotopic analysis of atmospheric methane by isotope-ratio-monitoring gas-chromatography mass-spectrometry. *J. Geophys. Res.-Atmos.* 100, 1317-1326.
- Meyer, J.L., Strayer, D.L., Wallace, J.B., Eggert, S.L., Helfman, G.S., Leonard, N.E., 2007. The Contribution of Headwater Streams to Biodiversity in River Networks1. *JAWRA Journal of the American Water Resources Association* 43, 86-103.
- Miller, S.M., Wofsy, S.C., Michalak, A.M., Kort, E.A., Andrews, A.E., Biraud, S.C., Dlugokencky, E.J., Eluszkiewicz, J., Fischer, M.L., Janssens-Maenhout, G., Miller, B.R., Miller, J.B., Montzka, S.A., Nehrkorn, T., Sweeney, C., 2013. Anthropogenic emissions of methane in the United States. *Proceedings of the National Academy of Sciences of the United States of America* 110, 20018-20022.
- Molofsky, L.J., Connor, J.A., Wylie, A.S., Wagner, T., Farhat, S.K., 2013. Evaluation of Methane Sources in Groundwater in Northeastern Pennsylvania. *Ground Water* 51, 333-349.
- Moniz, E.J.J., H.D.; Meggs, A.J.M, 2011. *The Future of Natural Gas: An Interdisciplinary MIT Study.* MIT Energy Initiative.
- Moore, M.E., Buckwalter, T.F., 1996. Ground-water resources data for Warren County, Pennsylvania. US Geological Survey; Branch of Information Services [distributor].
- Negrel, P., Allegre, C.J., Dupre, B., Lewin, E., 1993. Erosion sources determined by inversion of major and trace-element ratios and strontium isotopic-ratios in river water - the Congo Basin case. *Earth and Planetary Science Letters* 120, 59-76.
- Nesbitt, H.W., Markovics, G., Price, R.C., 1980. Chemical processes affecting alkalis and alkaline-earths during continental weathering. *Geochim. Cosmochim. Acta* 44, 1659-1666.
- O'Malley, M., McDonough, J., 2011. Executive Order 01.01. 2011.11: The Marcellus Shale Safe Drilling Initiative.
- Oliver, B.G., Thurman, E.M., Malcolm, R.L., 1983. The contribution of humic substances to the acidity of colored natural waters. *Geochim. Cosmochim. Acta* 47, 2031-2035.
- Olmstead, S.M., Muehlenbachs, L.A., Shih, J.S., Chu, Z.Y., Krupnick, A.J., 2013. Shale gas development impacts on surface water quality in Pennsylvania.

Proceedings of the National Academy of Sciences of the United States of America 110, 4962-4967.

- Ortiz-Llorente, M.J., Alvarez-Cobelas, M., 2012. Comparison of biogenic methane emissions from unmanaged estuaries, lakes, oceans, rivers and wetlands. *Atmospheric Environment* 59, 328-337.
- Osborn, S.G., Vengosh, A., Warner, N.R., Jackson, R.B., 2011. Methane contamination of drinking water accompanying gas-well drilling and hydraulic fracturing. *Proceedings of the National Academy of Sciences of the United States of America* 108, 8172-8176.
- Parker, K.M., Zeng, T., Harkness, J., Vengosh, A., Mitch, W.A., 2014. Enhanced Formation of Disinfection Byproducts in Shale Gas Wastewater-Impacted Drinking Water Supplies. *Environ. Sci. Technol.* 48, 11161-11169.
- Patino, R., Dawson, D., VanLandeghem, M.M., 2014. Retrospective analysis of associations between water quality and toxic blooms of golden alga (*Prymnesium parvum*) in Texas reservoirs: Implications for understanding dispersal mechanisms and impacts of climate change. *Harmful Algae* 33, 1-11.
- Paul, M.J., Stribling, J.B., Klauda, R.J., Kazyak, P.F., Southerland, M.T., Roth, N.E., 2002. A Physical Habitat Index for Freshwater Wadeable Streams in Maryland. Maryland Department of Natural Resources, Annapolis, MD.
- Peek, S., Clementz, M.T., 2012. Sr/Ca and Ba/Ca variations in environmental and biological sources: A survey of marine and terrestrial systems. *Geochim. Cosmochim. Acta* 95, 36-52.
- Perlman, H., 2014. Saline water use in the United States, U.S. Geological Survey.
- Petron, G., Frost, G., Miller, B.R., Hirsch, A.I., Montzka, S.A., Karion, A., Trainer, M., Sweeney, C., Andrews, A.E., Miller, L., Kofler, J., Bar-Ilan, A., Dlugokencky, E.J., Patrick, L., Moore, C.T., Ryerson, T.B., Siso, C., Kolodzey, W., Lang, P.M., Conway, T., Novelli, P., Masarie, K., Hall, B., Guenther, D., Kitzis, D., Miller, J., Welsh, D., Wolfe, D., Neff, W., Tans, P., 2012. Hydrocarbon emissions characterization in the Colorado Front Range: A pilot study. *J. Geophys. Res.-Atmos.* 117.
- Pond, G.J., 2012. Biodiversity loss in Appalachian headwater streams (Kentucky, USA): Plecoptera and Trichoptera communities. *Hydrobiologia* 679, 97-117.
- Prieto, M., FernandezGonzalez, A., Putnis, A., FernandezDiaz, L., 1997. Nucleation, growth, and zoning phenomena in crystallizing (Ba,Sr)CO<sub>3</sub>, Ba(SO<sub>4</sub>,CrO<sub>4</sub>),

- (Ba,Sr)SO<sub>4</sub>, and (Cd,Ca)CO<sub>3</sub> solid solutions from aqueous solutions. *Geochim. Cosmochim. Acta* 61, 3383-3397.
- Rahm, B.G., Bates, J.T., Bertoia, L.R., Galford, A.E., Yoxtheimer, D.A., Riha, S.J., 2013. Wastewater management and Marcellus Shale gas development: Trends, drivers, and planning implications. *Journal of Environmental Management* 120, 105-113.
- Rai, S., Iqbal, M.Z., 2015. Using fluorescein and bromide tracers to investigate the role of baseflow in a small suburban watershed in Iowa, USA. *Hydrological Processes* 29, 173-186.
- Revesz, K.M., Breen, K.J., Baldassare, A.J., Burruss, R.C., 2010. Carbon and hydrogen isotopic evidence for the origin of combustible gases in water-supply wells in north-central Pennsylvania. *Appl. Geochem.* 25, 1845-1859.
- Rhodes, C., 2014. *Peak Oil is Not a Myth*. Royal Society of Chemistry, Reading, UK.
- Roth, N.E., Southerland, M.T., Mercurio, G., Chaillou, J.C., Kazyak, P.F., Stranko, S.S., Prochaska, A.P., Heimbuch, D.G., Seibel, J.C., , 1999. State of the Streams: 1995-1997 Maryland Biological Stream Survey Results. Maryland Department of Natural Resources, Annapolis, MD.
- Rowe, D., Muehlenbachs, K., 1999. Isotopic fingerprints of shallow gases in the Western Canadian sedimentary basin: tools for remediation of leaking heavy oil wells. *Organic Geochemistry* 30, 861-871.
- Saba, T., Orzechowski, M., 2011. Lack of data to support a relationship between methane contamination of drinking water wells and hydraulic fracturing. *Proceedings of the National Academy of Sciences of the United States of America* 108, E663-E663.
- Sanders, I.A., Heppell, C.M., Cotton, J.A., Wharton, G., Hildrew, A.G., Flowers, E.J., Trimmer, M., 2007. Emission of methane from chalk streams has potential implications for agricultural practices. *Freshw. Biol.* 52, 1176-1186.
- Sansone, F.J., Holmes, M.E., Popp, B.N., 1999. Methane stable isotopic ratios and concentrations as indicators of methane dynamics in estuaries. *Glob. Biogeochem. Cycle* 13, 463-473.
- Saville, J., Kashiwagi, M.T., Becker, A.J., Graves, P.H., 2014. A Multi-Year Update (2011–2014) to Maryland Biological Stream Survey's Sentinel Site Network.
- Schedl, A., McCabe, C., Montanez, I.P., Fullagar, P.D., Valley, J.W., 1992. Alleghenian regional diagenesis - A response to the migration of modified

metamorphic fluids derived from beneath the Blue Ridge-Piedmont Thrust Sheet. *J. Geol.* 100, 339-352.

Schobert, H.H., 2013. *Chemistry of Fossil Fuels and Biofuels*. Cambridge University Press, New York.

Schoell, M., 1980. The hydrogen and carbon isotopic composition of methane from natural gases of various origins *Geochim. Cosmochim. Acta* 44, 649-661.

Schoell, M., 1988. Multiple origins of methane in the earth. *Chem. Geol.* 71, 1-10.

Segers, R., 1998. Methane production and methane consumption: a review of processes underlying wetland methane fluxes. *Biogeochemistry* 41, 23-51.

Shaffer, D.L., Arias Chavez, L.H., Ben-Sasson, M., Romero-Vargas Castrillón, S., Yip, N.Y., Elimelech, M., 2013. Desalination and Reuse of High-Salinity Shale Gas Produced Water: Drivers, Technologies, and Future Directions. *Environ. Sci. Technol.* 47, 9569-9583.

Sharma, S., Mulder, M.L., Sack, A., Schroeder, K., Hammack, R., 2014. Isotope Approach to Assess Hydrologic Connections During Marcellus Shale Drilling. *Ground Water* 52, 424-433.

Skalak, K.J., Engle, M.A., Rowan, E.L., Jolly, G.D., Conko, K.M., Bentham, A.J., Kraemer, T.F., 2014. Surface disposal of produced waters in western and southwestern Pennsylvania: Potential for accumulation of alkali-earth elements in sediments. *Int. J. Coal Geol.* 126, 162-170.

Sloto, R.A., 2013. Baseline groundwater quality from 20 domestic wells in Sullivan County, Pennsylvania, 2012. US Department of the Interior, US Geological Survey.

Soeder, D.J., 2012. Advances in Natural Gas Technology, in: Al-Megren, H. (Ed.), *Shale Gas Development in the United States*. InTech, pp. 3-28.

Sovacool, B.K., 2014. Cornucopia or curse? Reviewing the costs and benefits of shale gas hydraulic fracturing (fracking). *Renew. Sust. Energ. Rev.* 37, 249-264.

Strahler, A.N., 1952. Hypsometric (Area-altitude) analysis of erosional topography. *Geological Society of America Bulletin* 63, 1117-&.

Stranko, S., Bourquin, R., Zimmerman, J., Kashiwagi, M., McGinty, M., Klauda, R., 2013. Do Road Salts Cause Environmental Impacts? Maryland Department of Natural Resources. Retrieved from:  
<http://www.dnr.state.md.us/streams/pdfs/RoadSalt2013.pdf>

- Suarez, A.A., 2012. The Expansion of Unconventional Production of Natural Gas (Tight Gas, Gas Shale and Coal Bed Methane), in: Al-Megren, H. (Ed.), *Advances in Natural Gas Technology*. InTech, pp. 123-146.
- Sugimura, Y., Suzuki, Y., 1988. A high-temperature catalytic-oxidation method for the determination of non-volatile dissolved organic carbon in seawater by direct injection of a liquid sample. *Marine Chemistry* 24, 105-131.
- Taylor, S.W., Lollar, B.S., Wassenaar, L.I., 2000. Bacteriogenic ethane in near-surface aquifers: Implications for leaking hydrocarbon well bores. *Environ. Sci. Technol.* 34, 4727-4732.
- Templeton, C.C., 1960. Solubility of Barium Sulfate in Sodium Chloride Solutions from 25° to 95° C. *Journal of Chemical & Engineering Data* 5, 514-516.
- Thompson, S.E., Basu, N.B., Lascurain, J., Aubeneau, A., Rao, P.S.C., 2011. Relative dominance of hydrologic versus biogeochemical factors on solute export across impact gradients. *Water Resour. Res.* 47.
- Timpano, A.J., Schoenholtz, S.H., Soucek, D.J., Zipper, C.E., 2015. Salinity as a Limiting Factor for Biological Condition in Mining-Influenced Central Appalachian Headwater Streams. *JAWRA Journal of the American Water Resources Association* 51, 240-250.
- Trexler, R., Solomon, C., Brislawn, C.J., Wright, J.R., Rosenberger, A., McClure, E.E., Grube, A.M., Peterson, M.P., Keddache, M., Mason, O.U., Hazen, T.C., Grant, C.J., Lamendella, R., 2014. Assessing impacts of unconventional natural gas extraction on microbial communities in headwater stream ecosystems in Northwestern Pennsylvania. *Frontiers in Microbiology* 5.
- Trimble, D.C., 2012. *Unconventional Oil and Gas Development: Key Environmental and Public Health Requirements*. Government Accountability Office, Washington, D.C.
- Turekian, K.K., Wedepohl, K.H., 1961. Distribution of the Elements in Some Major Units of the Earth's Crust. *Geol Soc America Bull Geological Society of America Bulletin* 72.
- U.S. Census Bureau, 2010, Maryland State Data Center. Retrieved from: <http://census.maryland.gov/>
- van der Elst, N.J., Savage, H.M., Keranen, K.M., Abers, G.A., 2013. Enhanced Remote Earthquake Triggering at Fluid-Injection Sites in the Midwestern United States. *Science* 341, 164-167.

- Van Stempvoort, D., Maathuis, H., Jaworski, E., Mayer, B., Rich, K., 2005. Oxidation of fugitive methane in ground water linked to bacterial sulfate reduction. *Ground Water* 43, 187-199.
- Vengosh, A., Jackson, R.B., Warner, N., Darrah, T.H., Kondash, A., 2014. A Critical Review of the Risks to Water Resources from Unconventional Shale Gas Development and Hydraulic Fracturing in the United States. *Environ. Sci. Technol.* 48, 8334-8348.
- Vidic, R.D., Brantley, S.L., Vandenbossche, J.M., Yoxtheimer, D., Abad, J.D., 2013. Impact of Shale Gas Development on Regional Water Quality. *Science* 340.
- Wallin, M.B., Lofgren, S., Erlandsson, M., Bishop, K., 2014. Representative regional sampling of carbon dioxide and methane concentrations in hemiboreal headwater streams reveal underestimates in less systematic approaches. *Glob. Biogeochem. Cycle* 28, 465-479.
- Warner, N.R., Christie, C.A., Jackson, R.B., Vengosh, A., 2013a. Impacts of Shale Gas Wastewater Disposal on Water Quality in Western Pennsylvania. *Environ. Sci. Technol.* 47, 11849-11857.
- Warner, N.R., Jackson, R.B., Darrah, T.H., Osborn, S.G., Down, A., Zhao, K.G., White, A., Vengosh, A., 2012. Geochemical evidence for possible natural migration of Marcellus Formation brine to shallow aquifers in Pennsylvania. *Proceedings of the National Academy of Sciences of the United States of America* 109, 11961-11966.
- Warner, N.R., Kresse, T.M., Hays, P.D., Down, A., Karr, J.D., Jackson, R.B., Vengosh, A., 2013b. Geochemical and isotopic variations in shallow groundwater in areas of the Fayetteville Shale development, north-central Arkansas. *Appl. Geochem.* 35, 207-220.
- Waschbusch, R.J., Selbig, W., Bannerman, R.T., 1993. Sources of phosphorus in stormwater and street dirt from two urban residential basins in Madison, Wisconsin, 1994-95, National Conference on Tools for Urban Water Resource Management and Protection proceedings, February 710, 2000, Chicago, IL. DIANE Publishing, p. 9.
- Watmough, S.A., 2014. Calcium, strontium and barium biogeochemistry in a forested catchment and insight into elemental discrimination. *Biogeochemistry* 118, 357-369.
- Waxman, H., Markey, E., DeGette, D., 2013. Chemicals Used in Hydraulic Fracturing. US House of Representatives Committee on Energy and Commerce Minority Staff.

- Weaver, T.R., Frape, S.K., Cherry, J.A., 1995. Recent cross-formational fluid-flow and mixing in the shallow Michigan Basin. *Geological Society of America Bulletin* 107, 697-707.
- Werner, S.F., Browne, B.A., Driscoll, C.T., 2012. Three-dimensional spatial patterns of trace gas concentrations in baseflow-dominated agricultural streams: implications for surface-ground water interactions and biogeochemistry. *Biogeochemistry* 107, 319-338.
- Whiticar, M.J., 1996. Stable isotope geochemistry of coals, humic kerogens and related natural gases. *Int. J. Coal Geol.* 32, 191-215.
- Whiticar, M.J., 1999. Carbon and hydrogen isotope systematics of bacterial formation and oxidation of methane. *Chem. Geol.* 161, 291-314.
- Whiticar, M.J., Faber, E., 1986. Methane oxidation in sediment and water column environments - isotopic evidence. *Organic Geochemistry* 10, 759-768.
- Whiticar, M.J., Faber, E., Schoell, M., 1986. Biogenic methane formation in marine and freshwater environments - CO<sub>2</sub> reduction vs acetate fermentation isotope evidence *Geochim. Cosmochim. Acta* 50, 693-709.
- Wilson, B., 2014. Geologic and baseline groundwater evidence for naturally occurring, shallowly sourced, thermogenic gas in northeastern Pennsylvania. *Aapg Bulletin* 98, 373-394.
- Wilson, J.M., VanBriesen, J.M., 2012. Oil and gas produced water management and surface drinking water sources in Pennsylvania. *Environmental Practice* 14, 288-300.
- Wright, P.R.M., P.B.; Mueller, D.K.; Clark, M.L., 2012. Groundwater-Quality and Quality-Control Data for Two Monitoring Wells near Pavillion, Wyoming, April and May 2012, Reston, VA.
- Yamamoto, S., Alcauskas, J.B., Crozier, T.E., 1976. Solubility of methane and distilled water and seawater. *Journal of Chemical and Engineering Data* 21, 78-80.
- Zeikus, J.G., Winfrey, M.R., 1976. Temperature limitation of methanogenesis in aquatic sediments. *Appl. Environ. Microbiol.* 31, 99-107.
- Zhang, C.L., Grossman, E.L., Ammerman, J.W., 1998. Factors influencing methane distribution in Texas ground water. *Ground Water* 36, 58-66.